

REVIEW ARTICLE

Chemical biology of inflammatory cytokine signaling

Takao Kataoka

Pro-inflammatory cytokines, such as tumor necrosis factor- α and interleukin-1, trigger the signal transduction pathway leading to the activation of the transcription factor, nuclear factor- κ B (NF- κ B). NF- κ B induces a large number of target genes involved in many biological processes, such as inflammation, immunity, cell survival, cell death and carcinogenesis. As therapeutic agents for inflammatory diseases and cancer, as well as bioprobes for the characterization of intracellular biological response and cell function, a large number of natural and synthetic small molecules have been identified to inhibit the activation of the NF- κ B signaling pathway. This review focuses on recent progress in the identification and biological properties of small molecules targeting the NF- κ B signaling pathway induced by pro-inflammatory cytokines.

The Journal of Antibiotics (2009) 62, 655–667; doi:10.1038/ja.2009.98; published online 16 October 2009

Keywords: cardenolide glycosides; epoxyquinoids; I κ B kinase inhibitors; protein synthesis inhibitors; sesquiterpene lactones

INTRODUCTION

Pro-inflammatory cytokines, such as tumor necrosis factor (TNF)- α and interleukin-1 (IL-1), trigger the activation of the transcription factor nuclear factor- κ B (NF- κ B), thereby inducing a variety of genes involved in inflammation, innate and adaptive immunity, cell survival and cell death, as well as cancer development and progression (Figure 1).^{1,2} The NF- κ B family of transcription factors has five members, p65 (RelA), RelB, c-Rel, p105/p50 (NF- κ B1) and p100/p52 (NF- κ B2), which share an N-terminal Rel homology domain responsible for DNA binding as well as homo- and hetero-dimerization, whereas a transcription activation domain is present only in p65, RelB and c-Rel (Figure 2a).^{3,4} Both NF- κ B hetero- and homo-dimers are able to bind to κ B sites located in target genes and regulate their transcriptional activation.^{3,4} In unstimulated cells, NF- κ B dimers, such as the p65/p50 heterodimer, are associated with the inhibitor of NF- κ B (I κ B) family proteins, such as I κ B α , and are present in the cytosol as an inactive complex in which I κ B α masks the nuclear localization sequence of p65 and prevents its nuclear translocation and subsequent DNA binding.^{3,4} The I κ B kinase (IKK) complex consists of two catalytic subunits, IKK α (IKK1) and IKK β (IKK2), and a regulatory subunit IKK γ (NEMO).^{5,6} In the canonical NF- κ B signaling pathway, IKK β has a major role in phosphorylating I κ B at two specific serine residues in the N-terminus (Figure 2b).^{7,8} Phosphorylated I κ B is recruited to the Skp1-Cullin1-F-box protein (SCF) ^{β TrCP} E3 ubiquitin ligase complex that catalyzes the polyubiquitination of I κ B.^{9,10} After polyubiquitinated I κ B is selectively degraded by 26S proteasome, the NF- κ B dimers become free and translocate to the nucleus, where they regulate the transcription of many target genes.^{3,4}

Tumor necrosis factor- α binds to two different receptors known as TNF receptor 1 (TNF-R1) and TNF receptor 2 (TNF-R2), and triggers a variety of intracellular signaling pathways, one of which leads to

NF- κ B activation (Figure 1).^{11,12} On TNF- α binding, TNF-R1 interacts with the adaptor protein TNF receptor-associated death domain (TRADD) to the cytoplasmic death domain, and this is followed by the recruitment of adaptor proteins receptor-interacting protein 1 (RIP1) and TNF receptor-associated factor 2 (TRAF2) to form complex I at the plasma membrane.¹³ In response to TNF- α stimulation, RIP1 is polyubiquitinated at a specific lysine residue (Lys-377) and subsequently recruits the TGF β -activated kinase (TAK1) complex and the IKK complex to its polyubiquitin chains.^{14–16} The activation of IKK requires phosphorylation of specific serine residues within the activation loop of the catalytic domain in IKK α and IKK β (Figure 2c).^{5,6} Two possible mechanisms are proposed: IKKs phosphorylate each other by trans-autophosphorylation and IKKs are phosphorylated by other upstream kinases, including TAK1.^{5,6}

After dissociation from the membrane-bound complex, TRADD and RIP1 interact with the adaptor protein Fas-associated death domain (FADD) and the initiator caspase-8 to form complex II in the cytosol, which mediates the homodimerization and subsequent self-processing of caspase-8 into its active tetramer (Figure 1).¹³ Active caspase-8 cleaves various substrates, such as effector caspases and the BH3-only protein Bid, to yield their active forms. Truncated Bid is translocated to mitochondria and induces the release of mitochondrial pro-apoptotic proteins, such as cytochrome *c*, into the cytosol. Cytochrome *c* collaborates with adaptor protein apoptotic protease-activating factor-1 (Apaf-1) to activate initiator caspase-9 in the apoptosome, allowing for the activation of effector caspases. Active effector caspases mediate the proteolytic cleavage of many cellular proteins and the execution of resultant apoptosis.

Cellular FADD-like IL-1 β -converting enzyme (FLICE)-inhibitory protein (c-FLIP) is an NF- κ B-inducible protein that modulates caspase-8 activation, and is a short-lived protein regulated posttranslationally

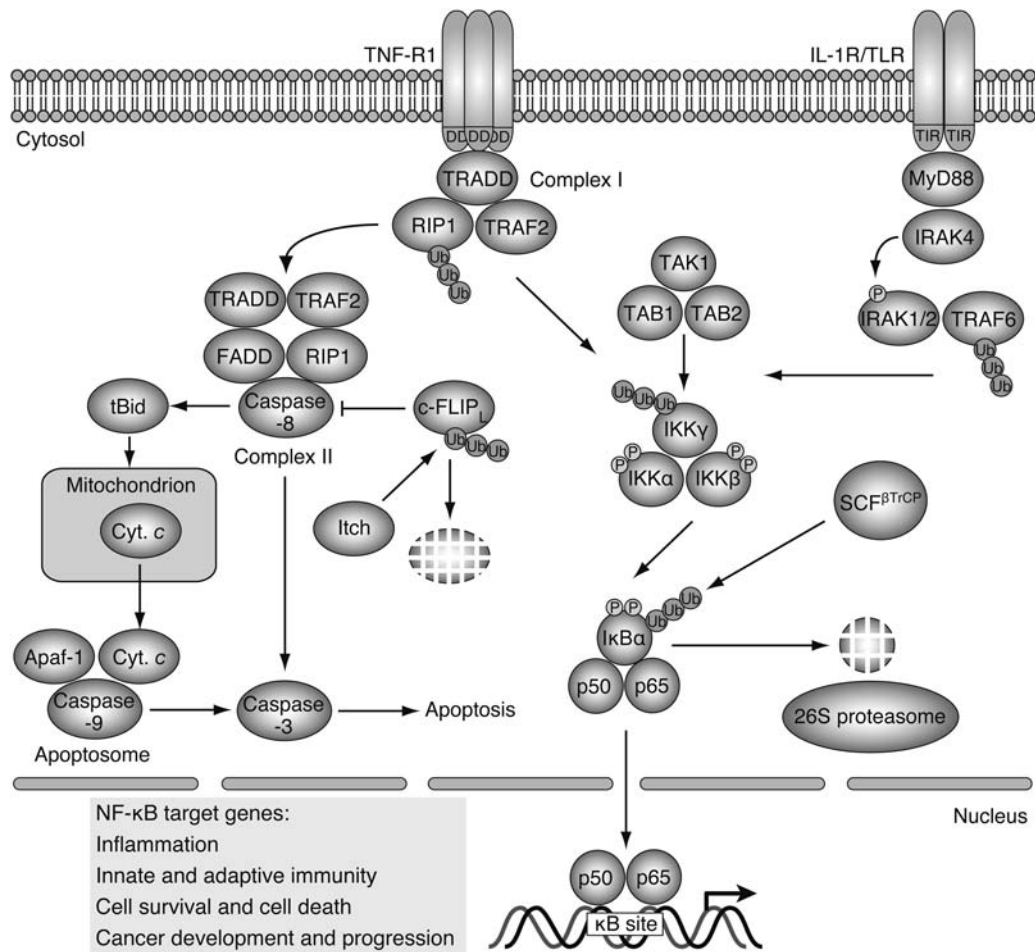


Figure 1 Inflammatory cytokine receptors and their intracellular signaling pathways. On tumor necrosis factor- α (TNF- α) stimulation, TNF receptor 1 (TNF-R1) recruits TNF receptor-associated death domain (TRADD) to its death domain (DD), and this is followed by the recruitment of receptor-interacting protein 1 (RIP1) and TNF receptor-associated factor 2 (TRAF2). RIP1 is then polyubiquitinated and subsequently recruits the TGF β -activated kinase (TAK1) complex and the inhibitor of NF- κ B (I κ B) kinase (IKK) complex to its polyubiquitin chain. Interleukin-1 receptor (IL-1R)/Toll-like receptor (TLR) recruits myeloid differentiation protein 88 (MyD88) to its Toll-IL-1 receptor (TIR) domain, which in turn recruits the IL-1 receptor-associated kinase (IRAK) family of proteins. IRAK4 phosphorylates IRAK1 and IRAK2, which promote the recruitment of TRAF6 and its polyubiquitination. Polyubiquitinated TRAF6 then recruits the IKK complex and the TAK1 complex to its polyubiquitin chains. IKK α and IKK β are activated by trans-autophosphorylation or other upstream kinases such as TAK1. The IKK complex phosphorylates N-terminal two serine residues of I κ B α . Phosphorylated I κ B α is polyubiquitinated by Skp1-Cullin1-F-box protein (SCF) ^{β TrCP} and selectively degraded by the 26S proteasome. The p50/p65 heterodimer becomes free and translocates to the nucleus, where it binds the κ B site and regulates various target genes. In the apoptosis signaling pathway, the complex I is released from the plasma membrane and then interacts with Fas-associated death domain (FADD) and caspase-8 to form complex II. Caspase-8 is activated by dimerization and subsequent self-processing into its active tetramer, which cleaves selective downstream substrates such as Bid and effector caspases. Bid is cleaved into its active form (tBid), which translocates to mitochondria and induces the release of pro-apoptotic proteins such as cytochrome c (Cyt. c) from mitochondria. Cyt. c collaborates with apoptotic protease-activating factor-1 (Apaf-1) to activate caspase-9 in the apoptosome. Active effector caspases, such as caspase-3, mediate the proteolytic cleavage of many cellular substrates, leading to apoptosis execution. TNF- α does not induce apoptosis in many types of cells by the nuclear factor- κ B (NF- κ B)-dependent upregulation of c-FLIP (cellular FADD-like IL-1 β -converting enzyme-inhibitory protein), which prevents the activation of caspase-8. c-FLIP_L, a long isoform of c-FLIP, is specifically ubiquitinated by Itch and rapidly degraded by the proteasome.

through the ubiquitin–proteasome pathway (Figure 1).^{17,18} The E3 ubiquitin ligase, Itch, specifically ubiquitinates a long isoform of c-FLIP (c-FLIP_L) and induces its proteasomal degradation.¹⁹ TNF- α does not induce apoptosis in many types of cells, largely because of its ability to induce NF- κ B activation, and thereby upregulate c-FLIP to levels sufficient to block apoptosis. Protein synthesis inhibitors block the translation of NF- κ B-inducible proteins, such as c-FLIP, and are thus often used to sensitize cells to undergo TNF- α -induced apoptosis.^{12,17}

Interleukin-1 can also induce NF- κ B activation. The IL-1 receptor (IL-1R) and Toll-like receptors (TLRs) possess a cytoplasmic Toll-IL-1 receptor (TIR) domain. On ligand binding, IL-1R and TLRs trigger

the recruitment of the adaptor protein myeloid differentiation protein 88 (MyD88), which in turn recruits the IL-1 receptor-associated kinase (IRAK) family members to their TIR domain (Figure 1).^{9,10,20} IRAK4 recruited to the receptor complex phosphorylates and activates IRAK1 and IRAK2, and these molecules in turn promote the recruitment of the RING-domain protein TRAF6 and its oligomer formation.^{9,10} TRAF6 oligomerization activates its ubiquitin ligase, leading to the polyubiquitination of target proteins, including TRAF6 itself.^{9,10} Polyubiquitinated TRAF6 recruits the IKK complex and the TAK1 complex to its polyubiquitin chains, leading to the activation of IKK.^{9,10}

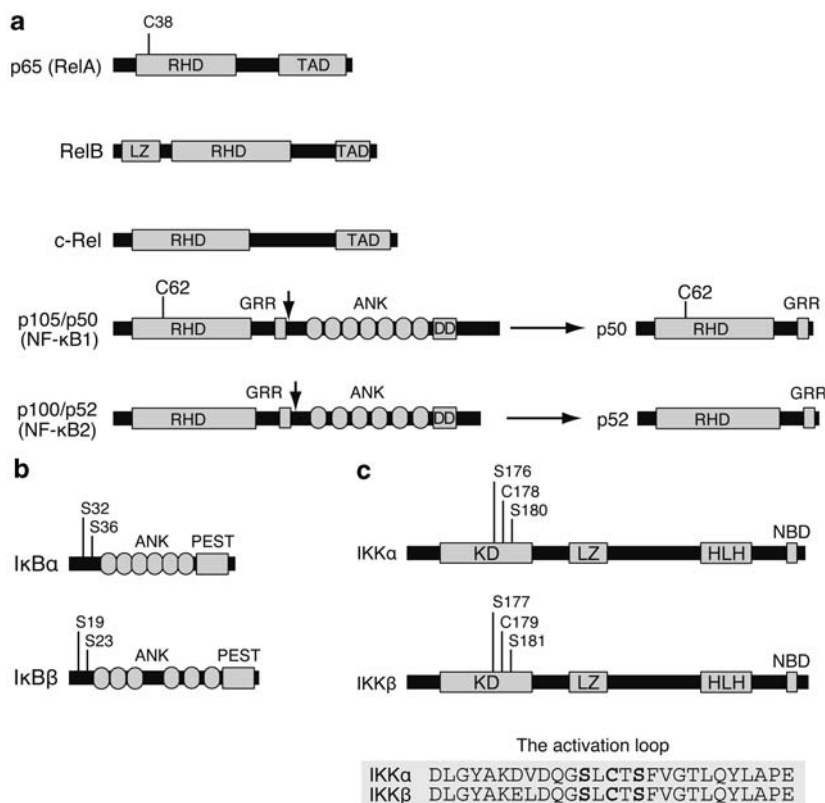


Figure 2 Nuclear factor- κ B (NF- κ B), inhibitor of NF- κ B (I κ B) and I κ B kinase (IKK) families of proteins. (a) Structures of NF- κ B family of proteins. The precursor proteins p105 and p100 are cleaved into p50 and p52 by the proteasome, as indicated by arrows. (b) Structures of I κ B α and I κ B β . N-terminal two serine residues phosphorylated by IKK are shown. (c) Structures of IKK α and IKK β . Two serine residues phosphorylated and a critical cysteine residue in the activation loop within the kinase domain are shown. ANK, ankyrin repeat; DD, death domain; GRR, glycine-rich region; HLH, helix-loop-helix domain; KD, kinase domain; LZ, leucine zipper domain; NBD, NEMO-binding domain; RHD, Rel homology domain; and TAD, transactivation domain.

It has recently become clear that the NF- κ B signaling pathway has a central role not only in inflammation but also in cancer development.^{1,2} NF- κ B inhibitors are most likely to be of great use as therapeutic agents for inflammatory diseases and cancer, and as bioprobes for the characterization of intracellular biological response and cell function. In the past decade, a number of structurally diverse small molecules have been identified that block the NF- κ B signaling pathway. This review describes recent progress in the identification and biological properties of natural and synthetic small molecules targeting the NF- κ B signaling pathway.

SYNTHETIC IKK INHIBITORS

The IKK complex of IKK α and IKK β directly phosphorylates I κ B α at the two N-terminal serine residues (Ser-32 and Ser-36) (Figure 2b).^{7,8} IKK β has a major role in I κ B α phosphorylation in the NF- κ B signaling pathway in response to pro-inflammatory cytokines and thus, its inhibition represents a potentially attractive way to treat inflammatory diseases. IKK-i²¹ (also known as IKK ϵ ²²) and TANK-binding kinase 1 (TBK1)/NF- κ B-inducing kinase/TRAF2-associated kinase are IKK-related kinases that are activated in response to various stimuli. The substrate specificity of IKK-i and TBK1 is distinct from that of IKK α and IKK β .²³ Small molecules that directly inhibit IKK α or IKK β have been developed by many research groups (Table 1). Specific IKK β inhibitors have been further employed to block NF- κ B activation in various cell types and animal models.

Many IKK β inhibitors have been designed and synthesized from lead compounds identified by high-throughput screening based on an

in vitro kinase assay. 5-Bromo-6-methoxy- β -carboline, a methylated natural product derivative, was initially obtained as a lead compound that non-specifically inhibits endogenous IKK and other kinases, and further chemical optimization has led to the identification of *N*-(6-chloro-9*H*- β -carbolin-8-yl)nicotinamide (PS-1145) as a selective IKK β inhibitor and *N*-(6-chloro-7-methoxy-9*H*- β -carbolin-8-yl)-2-methylnicotinamide (ML120B) as a more potent, reversible and ATP-competitive IKK β inhibitor.^{24–27} 4-Amino-2,3'-bithiophene-5-carboxamide (SC-514), an ATP-competitive IKK β inhibitor, has an IC₅₀ value > 10 μ M, but has little or no inhibitory effect on other kinases.²⁸ On the basis of the thiophenecarboxamide structure, more potent thiophenecarboxamide-type IKK β inhibitors, such as 2-((aminocarbonyl)amino)-5-(4-fluorophenyl)-3-thiophenecarboxamide (TPCA-1), as well as benzothieno(3,2-*b*)furan derivatives as novel IKK β inhibitors, have been developed independently by four individual groups.^{29–32} The identification of a 2-amino-3-cyano-4-aryl-6-(2-hydroxyphenyl)pyridine analog as a lead compound by high-throughput screening assay and subsequent chemical optimization have led to the identification of 2-amino-6-(2-(cyclopropylmethoxy)-6-hydroxyphenyl)-4-piperidin-4-yl nicotinonitrile (ACHP) as a potent and selective IKK β inhibitor.^{33–35} In the course of *in vitro* screening of a series of anilino-pyrimidine derivatives and ATP competitors for their inhibitory effects on a constitutively active version of IKK β in which two serine residues within the activation loop of the catalytic domain are replaced with glutamic acids, AS602868 was identified to be a potent, reversible and ATP-competitive IKK β inhibitor,^{36,37} and has been thus far used in various cell

Table 1 Profiles of synthetic IKK inhibitors

| Compound | IC_{50} (nM) | | | | Company | Reference |
|---|----------------|-------------|-----------|------------------|---------------------------------------|--|
| | IKK α | IKK β | IKK-i | IKK ^a | | |
| ACHP | 250 | 8.5 | > 20 000 | | Bayer Yakuin | Murata <i>et al.</i> ³⁴ ; Sanda <i>et al.</i> ³⁵ |
| AS602868 | 14 000 | 62 | | | Merck Serono | Frelin <i>et al.</i> ³⁶ ; Heckmann <i>et al.</i> ³⁷ |
| 2-Benzamido-pyrimidine (16) ^b | 200 | 40 | | 70 | Novartis | Waelchli <i>et al.</i> ⁴⁴ |
| BMS-345541 | 4000 | 300 | > 100 000 | | Bristol-Myers Squibb | Burke <i>et al.</i> ³⁸ ; Beaulieu <i>et al.</i> ³⁹ |
| IMD-0354 | | | | | Institute of Medical Molecular Design | Onai <i>et al.</i> ⁴¹ ; Tanaka <i>et al.</i> ⁴² |
| ML120B | > 100 000 | 45 | > 100 000 | 60 | Millennium Pharmaceuticals | Nagashima <i>et al.</i> ²⁶ ; Wen <i>et al.</i> ²⁷ |
| PF-184 | | 37 | | | Pfizer | Sommers <i>et al.</i> ⁵⁰ |
| PHA-408 | 14 100 | 40 | > 200 000 | | Pfizer | Mbalaviele <i>et al.</i> ⁴⁹ ; Sommers <i>et al.</i> ⁵⁰ |
| PS-1145 | | | | 100 | Millennium Pharmaceuticals | Hideshima <i>et al.</i> ²⁴ ; Castro <i>et al.</i> ²⁵ |
| S1627 | | | | 10 | Sanofi-aventis | Tegeer <i>et al.</i> ⁴³ |
| SC-514 | > 200 000 | 11 200 | > 200 000 | 6100 | Pfizer | Kishore <i>et al.</i> ²⁸ |
| TPCA-1 | 400 | 17.9 | | | GlaxoSmithKline | Podolin <i>et al.</i> ³¹ |

Abbreviations: ACHP, 2-amino-6-(2-(cyclopropylmethoxy)-6-hydroxyphenyl)-4-piperidin-4-yl nicotinonitrile; BMS-345541, 4-(2'-aminoethyl)amino-1,8-dimethylimidazo(1,2-*a*)quinoxaline; IKK, inhibitor of nuclear factor- κ B kinase; IMD-0354, *N*-(3,5-bis-trifluoromethyl-phenyl)-5-chloro-2-hydroxybenzamide; ML120B, *N*-(6-chloro-7-methoxy-9*H*- β -carbolin-8-yl)-2-methylnicotinamide; PF-184, 8-(2-(3,4-bis(hydroxymethyl)-3,4-dimethylpyrrolidin-1-yl)-5-chloroisonicotinamido)-1-(4-fluorophenyl)-4,5-dihydro-1*H*-benzo[*g*]indazole-3-carboxamide; PHA-408, 8-(5-chloro-2-(4-methylpiperazin-1-yl)isonicotinamido)-1-(4-fluorophenyl)-4,5-dihydro-1*H*-benzo[*g*]indazole-3-carboxamide; PS-1145, *N*-(6-chloro-9*H*- β -carbolin-8-yl)nicotinamide; SC-514, 4-amino-2,3'-bithiophene-5-carboxamide; TPCA-1, 2-((aminocarbonyl)amino)-5-(4-fluorophenyl)-3-thiophenecarboxamide.

^aIKK complex purified from cells was used in the *in vitro* kinase assay.

^bThe compound number in the reference is given in bold.

types and animal models. In addition to the ATP-competitive types of IKK β inhibitors described above, 4-(2'-aminoethyl)amino-1,8-dimethylimidazo(1,2-*a*)quinoxaline (BMS-345541) was identified as a highly selective IKK β inhibitor that binds to an allosteric binding site, by means of an *in vitro* kinase assay.³⁸ Further structure–activity relationship studies of BMS-345541 as a structural lead have recently revealed that its tetracycline analogs and imidazo(1,2-*a*)thieno(3,2-*e*)pyrazines are more potent IKK β inhibitors.^{39,40} As a different approach to the development of IKK β inhibitors, the molecular structure of *N*-(3,5-bis-trifluoromethyl-phenyl)-5-chloro-2-hydroxybenzamide (IMD-0354) was designed by analyzing the binding mode of aspirin to IKK β after the construction of the three-dimensional structure of a kinase domain of IKK β by homology modeling with protein kinase A as a template, and the estimation of the structure of active IKK β by referring to a model of IKK regulation.^{41,42} The phase I clinical trial of topical formulation of IMD-0354 for treatment of atopic dermatitis has been successfully completed. Other synthetic IKK inhibitors, including S1627,⁴³ 2-benzamido-pyrimidines,⁴⁴ 2-amino-3,5-diarylbenzamides,^{45,46} 6-aryl-7-alkoxyisoquinolines,⁴⁷ 4-phenyl-7-azaindoles,⁴⁸ PHA-408^{49,50} and PF-184,⁵⁰ have been reported.

THIOL-REACTIVE IKK INHIBITORS

IKK α and IKK β contain serine residues within the activation loop of the catalytic domain (Ser-176 and Ser-180 in IKK α , and Ser-177 and Ser-181 in IKK β), and their phosphorylation is required to induce kinase activity (Figure 2c).^{51,52} IKK α and IKK β also contain cysteine at positions 178 and 179 within their activation loop, respectively (Figure 2c).^{53,54} Indeed, it has been shown that Cys-179 of IKK β is critical for enzyme activation by promoting the phosphorylation of serines in the activation loop.⁵⁵ The IKK β mutant in which Cys-179 is replaced with alanine exhibited reduced kinase activity in response to physiological stimuli, whereas it exerted enzymatic activity at levels similar to wild-type IKK β when co-expressed with mitogen-activated protein (MAP) kinase kinase kinase, such as NF- κ B-inducing kinase.^{53–55} The difference in sensitivity between wild-type IKK β

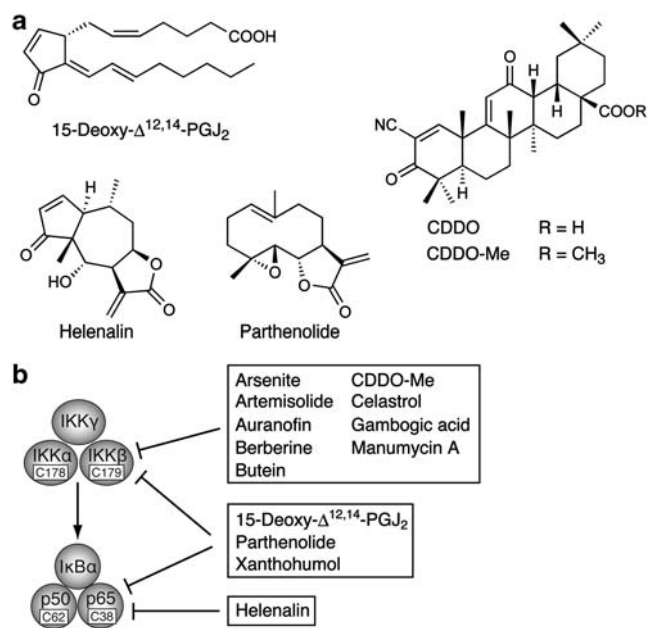


Figure 3 Structures and molecular targets of natural and synthetic compounds containing α,β -unsaturated carbonyl moieties. (a) Structures. (b) Target proteins in the nuclear factor- κ B (NF- κ B) signaling pathway are shown.

and its mutant IKK β (C179A) in cell culture or in their purified forms clearly revealed that a large number of small molecules directly inhibit IKK β activity by the modification of Cys-179.

Prostaglandin J₂ (PGJ₂) and its metabolites, such as 15-deoxy- $\Delta^{12,14}$ -PGJ₂ (Figure 3a), are naturally occurring metabolites of prostaglandin D₂. 15-Deoxy- $\Delta^{12,14}$ -PGJ₂ inhibits the NF- κ B signaling pathway by inhibiting IKK β activity.^{54,56} Synthetic triterpenoids, 2-cyano-3,12-dioxooleana-1,9-dien-28-oic acid methyl ester (CDDO-Me), as shown in Figure 3a) and 1-(2-cyano-3,12-dioxooleana-1,9-dien-28-oyl)imidazole (CDDO-Im), also block NF- κ B activation

through the direct inhibition of IKK β .^{57,58} The C179A mutation confers IKK β resistance to 15-deoxy- $\Delta^{12,14}$ -PGJ₂, CDDO-Me and CDDO-Im.^{54,57,58} This is consistent with the fact that 15-deoxy- $\Delta^{12,14}$ -PGJ₂, CDDO-Me and CDDO-Im contain an α,β -unsaturated carbonyl moiety that is known to form reversible adducts with reactive thiol groups. In the NF- κ B signaling pathway, it seems that Cys-179 of IKK β is highly reactive and thus targeted by many other compounds, including arsenite,⁵³ auranofin,⁵⁹ manumycin A,⁶⁰ celastrol,⁶¹ butein,⁶² berberine,⁶³ xanthohumol⁶⁴ and gambogic acid (Figure 3b).⁶⁵

SESQUITERPENE LACTONES AND RELATED COMPOUNDS

Sesquiterpene lactones are a large group of secondary metabolites of many medicinal plants. Sesquiterpene lactones often possess α,β -unsaturated carbonyl moieties, such as α -methylene- γ -lactones. These functional groups are known to react with cysteine thiol groups in the Michael-type addition.⁶⁶ It has been reported that many sesquiterpene lactones exert anti-inflammatory activity by preventing NF- κ B activation. Helenalin (Figure 3a), a sesquiterpene lactone that possesses an α -methylene- γ -lactone moiety, was initially isolated from flower head extract and found to inhibit NF- κ B activation in response to various stimuli.⁶⁷ It has been shown that helenalin does not inhibit I κ B degradation or NF- κ B nuclear translocation, but rather the DNA-binding activity of NF- κ B in the NF- κ B signaling pathway.⁶⁸ Helenalin inhibits the NF- κ B-binding activity of wild-type p65, but not that of its mutant p65 (C38S), whereas 11 α ,13-dihydrohelenalin acetate, which is devoid of the α -methylene- γ -lactone moiety, has a much weaker inhibitory effect.⁶⁹ Thus, as a major molecular target in the NF- κ B signaling pathway, helenalin can selectively alkylate the p65 subunit of NF- κ B at Cys-38, thereby interfering with its DNA-binding activity (Figure 3b).

Parthenolide (Figure 3a) is a sesquiterpene lactone that contains an α -methylene- γ -lactone moiety. It was identified as an NF- κ B inhibitor in the leaf extracts of Mexican Indian medicinal plants.⁷⁰ Parthenolide inhibits a common step in the activation of NF- κ B in response to many stimuli as well as in various cell types.^{69,71,72} It has been shown that parthenolide inhibits constitutively active IKK β (S177E/S181E) but not IKK β (C179A), which shows that parthenolide binds to IKK β and inhibits its kinase activity by the direct modification of Cys-179.⁷³ This is in agreement with the findings that parthenolide prevents IKK activation and subsequent I κ B α phosphorylation and degradation.^{71,72} However, it has also been reported that parthenolide does not effectively inhibit IKK activation, but rather inhibits the DNA binding of NF- κ B in different cell systems.^{69,74} Parthenolide has been found to inhibit the DNA-binding activity of wild-type p65, but not that of p65 (C38S).^{69,74} Collectively, it seems most likely that both Cys-38 of p65 and Cys-179 of IKK β are target residues of parthenolide, with Cys-38 of p65 being more preferentially alkylated under certain experimental settings (Figure 3b). Similarly, it has been shown that 15-deoxy- $\Delta^{12,14}$ -PGJ₂ targets both Cys-179 of IKK β and Cys-38 of p65.⁵⁶ As one of the sesquiterpene lactones that contain an α -methylene- γ -lactone moiety, artemisolid has been reported to inhibit IKK β activity by targeting its Cys-179.⁷⁵

Intercellular adhesion molecule-1 (ICAM-1; CD54) is a cell-surface glycoprotein that belongs to the immunoglobulin superfamily. It serves as a ligand for lymphocyte-function-associated antigen-1 (LFA-1; CD11a/CD18) and Mac-1 (CD11b/CD18). ICAM-1 is expressed at low levels on many types of cells and its expression is predominantly upregulated at the transcriptional level by NF- κ B in response to pro-inflammatory cytokines. A series of guaianolide and eudesmane types of sesquiterpenes have been synthesized or isolated from plant extracts, and investigated for their ability to inhibit surface

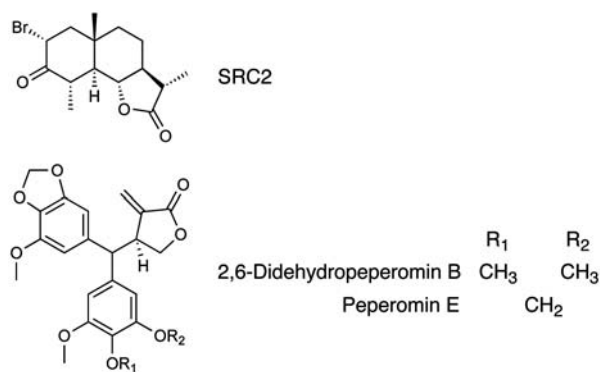


Figure 4 Structures of SRC2 ((11S)-2 α -bromo-3-oxoeudesmano-13,6 α -lactone) and peperomins.

ICAM-1 expression in human lung carcinoma A549 cells stimulated with IL-1 or TNF- α . Guaianolide derivatives possessing α -methylene- γ -lactone moieties, such as dehydrocostus lactone, exert inhibitory effects at IC₅₀ values lower than 10 μ M, whereas other α -methyl- γ -lactone derivatives show much weaker inhibitory effects.^{76–78} These findings clearly show that an α -methylene- γ -lactone moiety is crucial to inhibit the induction of ICAM-1 expression. This notion is consistent with the structure–activity relationship study of the effect of sesquiterpene lactones on NF- κ B-binding activity in TNF- α -stimulated cells, which shows that various guaianolides and eudesmanes containing α -methylene- γ -lactones manifest inhibitory effects.⁷⁹ We have also synthesized (11S)-2 α -bromo-3-oxoeudesmano-13,6 α -lactone (SRC2, as shown in Figure 4) from the starting material 1- α -santonin.⁸⁰ SRC2 is devoid of the α -methylene- γ -lactone moiety, but has a bromoketone structure at the A-ring. SRC2 inhibits the induction of cell-surface ICAM-1 expression in response to IL-1 stimulation by blocking the signaling pathway upstream of I κ B degradation.⁸⁰ Investigations of the molecular mechanism by which SRC2 inhibits NF- κ B activation are in progress.

Peperomins are secolignans isolated from the *Peperomia* family of plants. Recently, we have reported that several secolignans isolated from the extract of *Peperomia dindygulensis* inhibit cell-surface ICAM-1 expression induced by pro-inflammatory cytokines.⁸¹ However, except for their anti-inflammatory activity,⁸¹ multidrug resistance reversal activity⁸¹ and anticancer activity,^{81,82} the biological activities of peperomins are little understood. Peperomin E and 2,6-didehydropeperomin B (Figure 4) are structural analogs of peperomin A and peperomin B in which the α -methylene- γ -lactone groups are replaced with α -methyl- γ -lactone groups, respectively. We have recently shown that peperomin E and 2,6-didehydropeperomin B, but not peperomin A or peperomin B, inhibit I κ B α degradation induced by TNF- α or IL-1 in A549 cells.⁸³ In the NF- κ B signaling pathway, peperomin E and 2,6-didehydropeperomin B are able to block TNF- α -induced IKK activation.⁸³ However, in contrast to α -methylene- γ -lactone types of sesquiterpene lactones, such as parthenolide or artemisolid, peperomin E and 2,6-didehydropeperomin B do not inhibit IKK β activity directly.⁸³ Therefore, peperomin E and 2,6-didehydropeperomin B do not primarily block IKK β activity by the modification of Cys-179, but are likely to target other protein(s) required for IKK activation.

EPOXYQUINOIDS

Natural and synthetic epoxyquinoids, such as cycloepoxydon,^{84,85} dehydroxymethylepoxyquinomicin (DHMEQ),⁸⁶ epoxyquinol A,⁸⁷

epoxyquinol B,⁸⁸ epoxyquinone A monomer,⁸⁷ jesterone dimer,^{89,90} manumycin A⁶⁰ and panepoxydone,⁹¹ have been reported to inhibit NF- κ B activation. Epoxyquinoids contain the epoxide structure that is known to react with nucleophiles, such as cysteine thiol groups. Given that the reactivity of epoxyquinoids to proteins is similar to that of compounds containing α,β -unsaturated carbonyl moieties, it is speculated that epoxyquinoids selectively target critical cysteine residues of IKK β and p65 in the NF- κ B signaling pathway. With regard to some epoxyquinoids, novel molecular mechanisms involved in the suppression of NF- κ B activation have been revealed.

Epoxyquinols A and B (Figure 5a), which are naturally occurring pentaketide dimers, have been isolated from fungal metabolites and found to possess potent antiangiogenic activity.^{92,93} It has also been shown that both epoxyquinols A and B block TNF- α -induced NF- κ B activation.^{87,88} Compared with epoxyquinol A, its structural derivative, epoxyquinone A monomer (Figure 5a), is a potent inhibitor of TNF- α -induced NF- κ B activation.⁸⁷ Similar to sesquiterpene lactones, epoxyquinone A monomer inhibits IKK β and p65 by targeting Cys-179 and Cys-38, respectively (Figure 5b).⁹⁴ Jesterone dimer (Figure 5a), which was reported to exert 10- to 100-fold greater

antitumor activity than jesterone, has been shown to block TNF- α -induced IKK activation.^{89,90} Indeed, jesterone dimer converts constitutively active IKK β into stable higher molecular mass forms, irrespective of its Cys-179 mutation (Figure 5b).⁹⁰ It has also been shown that epoxyquinol B is able to bind covalently to cysteine residues of several proteins and to crosslink proteins through the cysteine residues by opening its epoxide ring.^{88,95} In the NF- κ B signaling pathway upstream of IKK activation, epoxyquinol B does not block TNF- α -induced RIP1 polyubiquitination; rather, it inhibits TAK1 phosphorylation.⁸⁸ As a molecular target, TAK1 has been identified to be crosslinked to high molecular weight complexes by itself or to other proteins by epoxyquinol B (Figure 5b).⁸⁸ Therefore, it seems likely that epoxyquinoid dimers, such as epoxyquinol B, preferentially crosslink TAK1 or IKK β , whereas epoxyquinoid monomers may target critical cysteine residues of IKK β or p65. As a direct TAK1 inhibitor with a different mode of action, 5Z-7-oxozeaenol has been identified to be a selective and ATP-competitive inhibitor with an IC₅₀ value of 8 nM, in a screening of 90 compounds (including 59 compounds that have been reported to inhibit protein kinases) with an *in vitro* kinase assay system using purified TAK1 and TAB1 proteins expressed in insect cells.⁹⁶

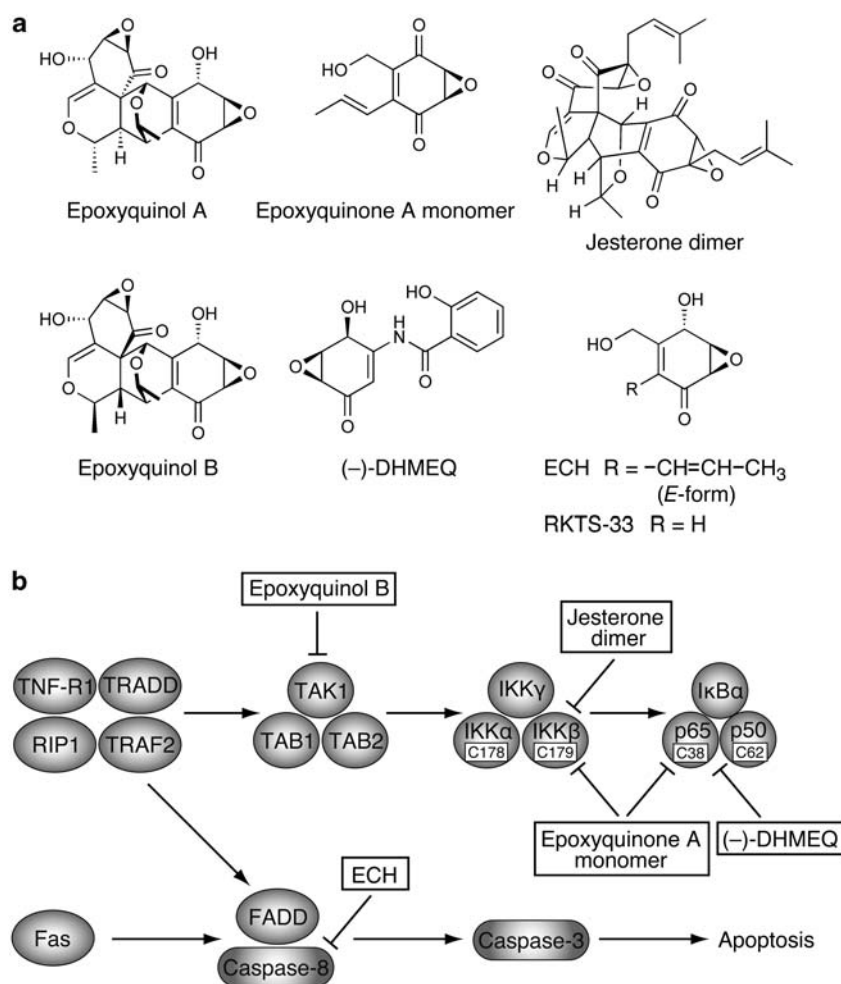


Figure 5 Structures of epoxyquinoids and their molecular targets. (a) Structures of epoxyquinoids. (b) Target proteins of epoxyquinoids in the tumor necrosis factor receptor 1 (TNF-R1) and Fas signaling pathways are shown. On TNF- α stimulation, TNF receptor 1 (TNF-R1) recruits adaptor proteins (TNF receptor-associated death domain (TRADD), receptor-interacting protein 1 (RIP1) and TNF receptor-associated factor 2 (TRAF2)), which subsequently activates the inhibitor of nuclear factor- κ B kinase (IKK) complex (IKK α , IKK β and IKK γ) through the TGF β -activated kinase (TAK1) complex (TAK1, TAB1 and TAB2). On Fas ligand stimulation, Fas recruits FADD (Fas-associated death domain) and caspase-8. Caspase-8 is activated by self-processing and thereby cleaves specific substrates such as caspase-3, leading to apoptosis execution.

(-)-DHMEQ (Figure 5a) has been designed as an NF- κ B inhibitor on the basis of the epoxyquinomicin C structure.⁸⁶ It has been shown that (-)-DHMEQ exerts anti-inflammatory activity in various *in vivo* models. At the cell level, (-)-DHMEQ inhibits TNF- α -induced nuclear translocation of NF- κ B and subsequent binding to DNA, whereas it does not inhibit TNF- α -induced I κ B phosphorylation and degradation.⁹⁷ Thus, unlike other epoxyquinoids, (-)-DHMEQ selectively inhibits the nuclear translocation of NF- κ B in response to various stimuli. It has been recently reported that (-)-DHMEQ covalently binds specific cysteine residues of Rel family proteins located close to the DNA-binding sites (Cys-38 of p65, Cys-144 of Rel B, Cys-27 of c-Rel and Cys-62 of p50) (Figure 5b).⁹⁸ (-)-DHMEQ thereby blocks the DNA-binding activity of wild-type, but not mutated (Cys to Ser), Rel family proteins in their purified forms.⁹⁸

As for the bioactive epoxyquinoids, we have shown that (2*R*, 3*R*, 4*S*)-2,3-epoxy-4-hydroxy-5-hydroxymethyl-6-(1*E*)-propenyl-cyclohex-5-en-1-one (ECH, as shown in Figure 5a) and its structural derivatives specifically inhibit Fas-mediated apoptosis.^{99,100} Fas is a cell-surface receptor belonging to the TNF receptor superfamily and has a cytoplasmic death domain essential for the induction of apoptosis in a FADD- and caspase-8-dependent manner.¹¹ ECH specifically inhibits the activation of caspase-8, but not its recruitment to the death-inducing signaling complex (DISC) in Fas ligand (FasL)-stimulated cells, thereby preventing caspase-8-dependent apoptosis.⁹⁹ Although ECH is the oxidized form of the epoxyquinone A monomer, it does not seem to inhibit IKK β activity, as TNF- α -induced I κ B α degradation still proceeds in the presence of ECH.⁹⁹ As a selective target in the Fas signaling pathway, ECH binds covalently to caspase-8, as revealed by an immunoprecipitation study using biotinylated ECH.⁹⁹ Thus, ECH is most likely to inactivate caspase-8 through the modification of a cysteine residue critical for its catalytic activity (Figure 5b). This notion is supported by our finding that the mycotoxin penicillic acid directly binds to a critical cysteine residue within the active center in the catalytic domain of caspase-8 (Figure 6).¹⁰¹ In much the same manner as ECH, penicillic acid prevents the activation of caspase-8, but not its recruitment to DISC in response to FasL.¹⁰¹ ECH prevents caspase-8-dependent apoptosis induced by death receptors (Fas and TNF-R1), but not apoptosis induced by staurosporine, MG-132, C2-ceramide or UV irradiation.⁹⁹ Therefore, unlike other epoxyquinoids, ECH does not seem to be an NF- κ B inhibitor, but a specific inhibitor of caspase-8. The molecular mechanism by which epoxyquinoids recognize specific cysteine residues in target proteins is currently unclear and should be clarified to develop highly selective inhibitors.

Cytotoxic T lymphocytes (CTLs) and natural killer cells eliminate target cells, such as tumor and virus-infected cells, by inducing apoptosis through two distinct killing pathways that are dependent on perforin/granzyme B and FasL. We have shown that ECH and its close structural analog, RKTS-33 (Figure 5a), specifically prevent Fas-ligand-dependent apoptosis in CTL-mediated cytotoxicity, whereas these agents barely affect perforin/granzyme B-dependent CTL-mediated cytotoxicity.^{102,103} We have previously shown that the perforin/granzyme B-dependent CTL-mediated killing pathway is selectively blocked by concanamycin A, an 18-membered macrolide that specifically inhibits vacuolar-type H⁺-ATPase.¹⁰⁴ Therefore, in combination with concanamycin A, ECH can be used as a specific inhibitor of FasL-dependent killing pathway to evaluate the contribution of two distinct killing pathways in various CTL-target settings.

CARDENOLIDE GLYCOSIDES

Cardiac glycosides, such as ouabain (Figure 7a), comprise a large number of naturally occurring compounds and consist of three

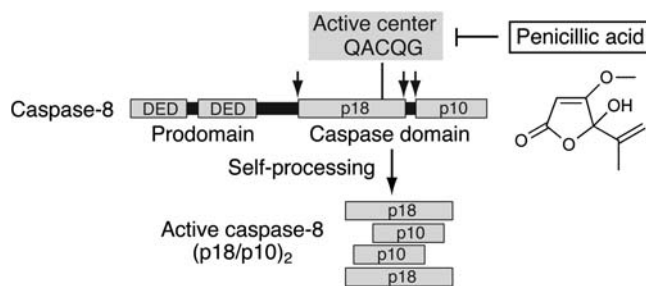


Figure 6 Structure of caspase-8 and its mechanism of activation. Caspase-8 is composed of two death effector domains (DED) as a prodomain and a caspase domain for its catalytic activity. The active center (QACQG) is located in the p18 subunit of the caspase domain. On dimerization, caspase-8 is cleaved into p18 and p10 subunits by self-processing, as indicated by arrows, and converted into the active tetramer (p18/p10)₂, which processes specific downstream substrates. Penicillic acid covalently binds to a cysteine residue in the active center and thereby prevents its enzymatic activity. The structure of penicillic acid is shown.

distinct structural motifs: a steroid core, a sugar moiety and a lactone moiety. Cardiac glycosides are further divided into cardenolides and bufadienolides having a five-membered butyrolactone ring and a six-membered unsaturated pyrone ring, respectively. Cardiac glycosides are defined as inhibitors of Na⁺/K⁺-ATPase, and used as drugs for treating heart failure and as anticancer drugs in clinical trials.¹⁰⁵ Na⁺/K⁺-ATPase is composed of a catalytic α -subunit and a regulatory β -subunit. It serves as a primary active transporter that is able to pump Na⁺ out and K⁺ in through hydrolysis of ATP, and maintains transmembrane Na⁺ and K⁺ gradients across the plasma membrane (Figure 7b).¹⁰⁶ Four isoforms of the α subunit (α 1, α 2, α 3 and α 4) exhibit unique tissue distributions. The α 1 isoform is present as the major housekeeping form in most tissues.¹⁰⁶ In addition to the binding sites for Na⁺, K⁺ and ATP, the α -subunit has highly conserved binding sites for cardiac glycosides.¹⁰⁶ All the four α isoforms are sensitive to ouabain in humans, whereas the α 1 isoform is ouabain-resistant in rodents. It is well established that the inhibition of Na⁺/K⁺-ATPase activity by cardiac glycosides leads to an increase in intracellular sodium ion levels in cardiac myocytes and subsequently an increase in calcium ion levels by Ca²⁺/Na⁺ exchange, thereby stimulating inotropic actions.¹⁰⁵

In addition to pumping ions, Na⁺/K⁺-ATPase has been shown to mediate various signal transductions in a manner independent of its function as an ion pump in response to cardiac glycosides (Figure 7b).¹⁰⁵ It has been shown that ouabain signals calcium oscillations through the inositol 1,4,5-triphosphate receptor that interacts with Na⁺/K⁺-ATPase and thereby induces NF- κ B activation at concentrations that do not inhibit Na⁺/K⁺-ATPase activity.^{107–109} In cardiac myocytes, ouabain has been reported to promote the rapid generation of reactive oxygen species, thereby inducing NF- κ B activation.¹¹⁰ As an early signaling pathway, Na⁺/K⁺-ATPase, on binding to cardiac glycosides, activates the cytoplasmic tyrosine kinase SRC, thereby activating the epidermal growth factor receptor and leading to the recruitment of adaptor proteins and the activation of the MAP kinase cascade that ultimately stimulates the mitochondrial production of reactive oxygen species.^{105,111}

Cardenolide glycosides, such as oleandrin and digitoxin (Figure 7a), have been reported to block the NF- κ B pathway activated either constitutively or in response to stimuli.^{112–118} Unlike ouabain, oleandrin inhibits NF- κ B activation upstream of I κ B degradation in response to many stimuli.^{112,113} In macrophage, oleandrin inhibits

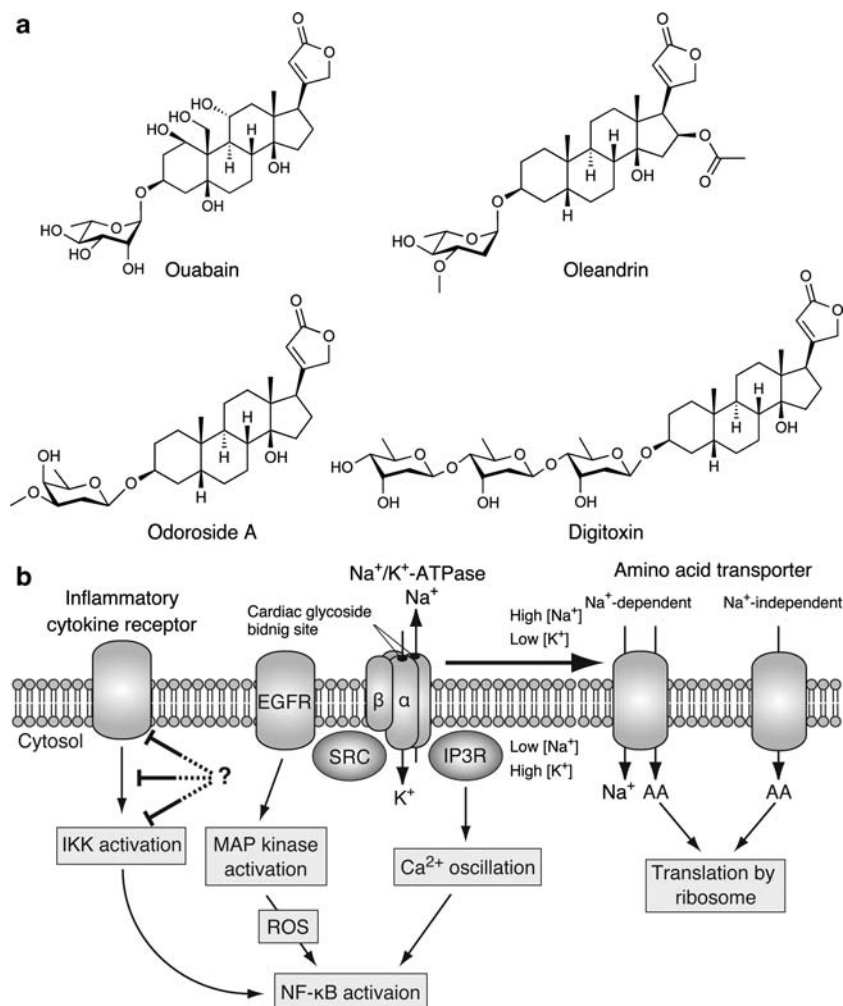


Figure 7 Structures of cardenolide glycosides and their mechanisms of actions. **(a)** Structures of cardenolide glycosides. **(b)** Na⁺/K⁺-ATPase is composed of α and β subunits and pumps Na⁺ out and K⁺ in to maintain transmembrane Na⁺ and K⁺ gradients across the plasma membrane. Amino acid transporters couple the uptake of amino acids with the electrical and chemical gradients through Na⁺/K⁺-ATPase. Na⁺/K⁺-ATPase interacts with inositol 1,4,5-triphosphate (IP3R), which is responsible for Ca²⁺ oscillation, leading to nuclear factor- κ B (NF- κ B) activation. Na⁺/K⁺-ATPase also interacts with the cytoplasmic tyrosine kinase SRC and thereby induces the activation of epidermal growth factor receptor (EGFR). EGFR recruits a set of adaptor proteins and activates the mitogen-activated protein (MAP) kinase cascade, which stimulates the mitochondrial production of reactive oxygen species (ROS), leading to NF- κ B activation. Cardenolide glycosides bind to the α -subunit of Na⁺/K⁺-ATPase at the extracellular region. Cardenolide glycosides exert different biological effects: the induction of NF- κ B activation, the inhibition of NF- κ B activation by inflammatory cytokine receptors at levels upstream of inhibitor of nuclear factor- κ B kinase (IKK) activation and the inhibition of NF- κ B-inducible protein expression by blocking Na⁺-dependent amino acid transport.

IL-8-induced activation by downregulating IL-8 receptor expression through membrane fluidity alteration, whereas it does not affect NF- κ B activation in response to many stimuli, including that of TNF- α and IL-1.¹¹⁵ It has been shown that digitoxin and oleandrin inhibit TNF- α -induced NF- κ B activation by blocking the recruitment of TRADD to TNF-R1.¹¹⁷ It has also been shown that digitoxin inhibits the IL-1-induced phosphorylation of IKK, but not the IL-1-induced phosphorylation of TAK1, indicating that digitoxin inhibits IL-1-induced NF- κ B activation at the IKK level.¹¹⁸ Therefore, cardenolide glycosides are likely to interfere with at least different steps in NF- κ B signaling, although it remains unclear whether the inhibition of NF- κ B activation by cardenolide glycosides is related to their inhibition of Na⁺/K⁺-ATPase activity (Figure 7b).

We have isolated cardenolide glycosides and their related compounds from *Nerium oleander* and *Phytolacca americana*, and conducted structure-activity relationship studies of their *in vitro*

anti-inflammatory activity. Among these compounds, odoroside A (Figure 7a) was found to inhibit ICAM-1 expression induced by TNF- α or IL-1 at IC₅₀ values < 1 μ M.^{119–123} Odoroside A has been shown to directly inhibit the ATP-hydrolyzing activity of Na⁺/K⁺-ATPase as potently as ouabain.¹²⁴ However, in contrast to previous studies, we have found that odoroside A and ouabain affect neither TNF- α -induced early NF- κ B signaling pathway nor mRNA expression, but rather prevent NF- κ B-inducible protein expression by blocking Na⁺-dependent amino acid transport.¹²⁴

Amino acid transport across the plasma membrane in mammalian cells is catalyzed by a broad range of discrete systems that consist of different gene products and distinct substrate specificities.¹²⁵ Amino acid transporters are known to couple amino acid transport with the electrical and chemical gradients initiated by Na⁺/K⁺-ATPase (Figure 7b).¹²⁵ This notion is in agreement with our finding that Na⁺-dependent amino acid transport is preferentially prevented by

odoroside A and ouabain compared with Na⁺-independent amino acid transport.¹²⁴ Inhibition of *de novo* protein synthesis by odoroside A has been observed at least in three cancer cell lines.¹²⁴ Therefore, it seems that cardenolide glycosides generally prevent NF- κ B-inducible gene expression at the translation level. However, it is currently unclear how either the early NF- κ B signaling pathway or the late NF- κ B-dependent protein expression is inhibited when cells are exposed to cardenolide glycosides. This may be influenced by the structures of cardenolide glycosides, their doses and durations, as well as cell-type specificity, including the expression levels of Na⁺/K⁺-ATPase isoforms, amino acid transporters and signaling proteins that regulate Na⁺/K⁺-ATPase signal transduction.

PROTEIN SYNTHESIS INHIBITORS

Protein synthesis inhibitors, such as cycloheximide (CHX, as shown in Figure 8a), are thought to block the translational stage of NF- κ B-inducible anti-apoptotic proteins, and thus have been often used to sensitize many types of cells to TNF- α -induced apoptosis.¹² Therefore, it is believed that protein synthesis inhibitors do not affect the early NF- κ B signaling pathway on TNF- α stimulation. In the course of screening for microbial secondary metabolites, we have initially identified acetoxycycloheximide (Ac-CHX, as shown in Figure 8a) as an active compound that inhibits TNF- α -induced ICAM-1 expression at 800-fold lower concentration than that used to inhibit IL-1-induced ICAM-1 expression.¹²⁶ In fact, Ac-CHX shows ~10-fold stronger protein synthesis blocking activity than CHX.^{126,127} However, Ac-CHX has been found to block TNF- α -induced I κ B α degradation, but not IL-1-induced I κ B α degradation, indicating that Ac-CHX specifically inhibits the TNF- α -induced early NF- κ B signaling pathway.¹²⁶ As a novel molecular mechanism, we have recently shown that Ac-CHX inhibits TNF- α -induced NF- κ B activation by inducing the ectodomain shedding of cell-surface TNF-R1 (Figure 8b).¹²⁸ CHX is also capable of inducing the ectodomain shedding of TNF-R1, although ~100-fold higher concentrations are required compared with Ac-CHX.¹²⁸

Tumor necrosis factor- α -converting enzyme (TACE), also referred to as a disintegrin and metalloprotease 17 (ADAM17), is a cell-surface type I transmembrane protein that was initially identified to process membrane-bound precursor TNF- α to its mature soluble form.^{129,130} Ectodomain shedding is a critical posttranslational mechanism for the regulation of the function of membrane-anchored ligands and receptors. In addition to TNF- α , TACE is able to process other ligands and receptors, such as TNF-R1 and TNF-R2.^{129,130} It has been shown that Ac-CHX induces the cleavage of cell-surface TNF-R1 into smaller soluble forms in a TACE-dependent manner and that the inhibition of TACE activity reverses TNF- α -induced NF- κ B activation in Ac-CHX-treated cells.¹²⁸

Ribotoxic stress response caused by some protein synthesis inhibitors triggers the activation of the MAP kinase superfamily, thereby eliciting cellular responses such as gene expression and apoptosis.^{126–128,131–135} Protein synthesis inhibitors that share the property of inducing alterations in the 28S rRNA, such as anisomycin (Figure 8a), are known to induce ribotoxic stress response.^{131–133} With regard to the structure–activity relationship, it seems that the acetoxyl groups of Ac-CHX and anisomycin are crucial to induce ribotoxic stress response, as their deacetoxyl and deacetyl analogs, respectively, are much less active to elicit ribotoxic stress response.^{126–128,133}

Extracellular signal-regulated kinase (ERK) and p38 MAP kinase have been reported to regulate ectodomain shedding mediated by TACE.^{136–140} In fact, Ac-CHX, and to a much lesser extent CHX, are able to promote the sustained activation of ERK and p38 MAP

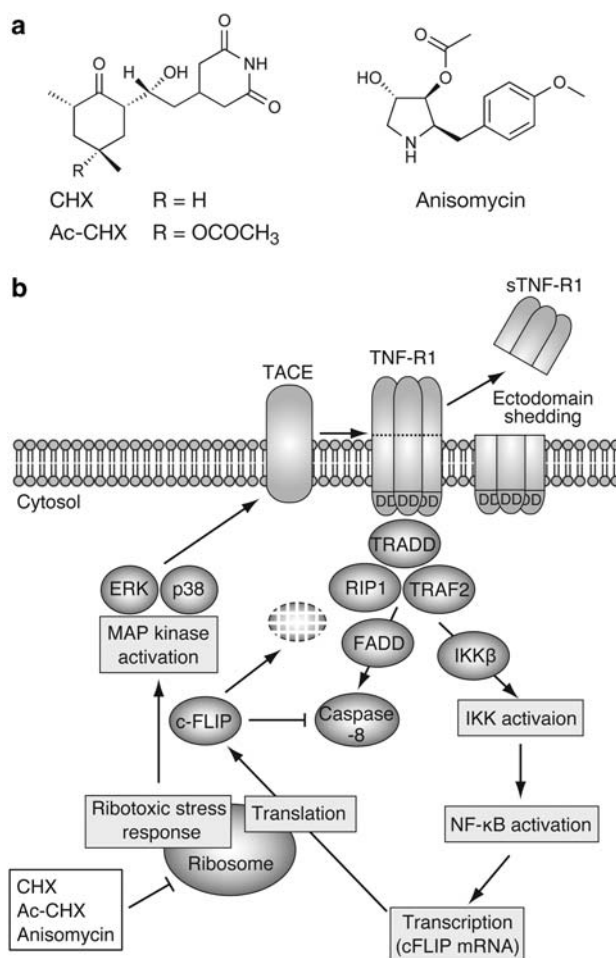


Figure 8 Structures of protein synthesis inhibitors and their mechanisms of actions on nuclear factor- κ B (NF- κ B) and apoptosis signaling pathways. (a) Structures of protein synthesis inhibitors. (b) Protein synthesis inhibitors such as acetoxycycloheximide (Ac-CHX) and anisomycin induce ribotoxic stress response, which triggers the activation of the mitogen-activated protein (MAP) kinase superfamily. Extracellular signal-regulated kinase (ERK) and p38 MAP kinase are responsible for the induction of the ectodomain shedding of TNF receptor 1 (TNF-R1) by TNF- α -converting enzyme (TACE), thereby preventing the TNF-R1-dependent NF- κ B signaling pathway. c-FLIP (cellular FADD-like IL-1 β -converting enzyme-inhibitory protein) is a short-lived protein regulated by the ubiquitin–proteasome pathway, but upregulated in an NF- κ B-dependent manner. Protein synthesis inhibitors such as cycloheximide (CHX) prevent the *de novo* synthesis of c-FLIP at the level of translation, thereby allowing the activation of caspase-8.

kinase.^{127,131,132,134} The MEK (MAP/ERK kinase) inhibitor, U0126, and the p38 MAP kinase inhibitor, SB203580, prevent ectodomain shedding of TNF-R1 induced by Ac-CHX.¹³⁴ The nonsteroidal anti-inflammatory drug, sodium salicylate, is known to block I κ B degradation in response to stimuli.¹⁴¹ In addition to the direct inhibition of IKK β activity by sodium salicylate,¹⁴² it has been shown that sodium salicylate blocks TNF- α -mediated I κ B α phosphorylation through p38 MAP kinase activation and that it causes rapid shedding of TNF-R1 in a p38 MAP kinase-dependent manner.^{143–145} Therefore, these findings are in line with our findings that ERK and p38 MAP kinase induce the downregulation of TNF-R1 by ribotoxic stress response.^{128,134}

Table 2 Profiles of natural and synthetic compounds that inhibit NF- κ B signaling pathway

| Compound | Origin | Molecular target ^a | Concentration (μ M) ^b | Reference |
|--|--|---|---------------------------------------|---|
| Acetoxycycloheximide | Unidentified actinomycete | Ribosome | 0.1–10 | Sugimoto <i>et al.</i> ¹²⁶ ; Ogura <i>et al.</i> ¹²⁸ |
| Arsenite | Environmental toxin | IKK β | 12.5–100 | Kapahi <i>et al.</i> ⁵³ |
| Artemisolid | Plant (<i>Artemisia asiatica</i>) | IKK β | 5–15 | Kim <i>et al.</i> ⁷⁵ |
| Auranofin | Gold compound | IKK β | 10–30 | Jeon <i>et al.</i> ⁵⁹ |
| Berberine | Plant | IKK β | 10–50 | Pandey <i>et al.</i> ⁶³ |
| Butein | Plant | IKK β | 10–50 | Pandey <i>et al.</i> ⁶² |
| CDDO-Im | Synthetic derivative of oleanolic acid | IKK β | 0.5–2 | Yore <i>et al.</i> ⁵⁸ |
| CDDO-Me | Synthetic derivative of oleanolic acid | IKK β | 0.25–1 | Ahmad <i>et al.</i> ⁵⁷ |
| Celastrol | Plant (<i>Celastrus orbiculatus</i>) | IKK β | 0.22–2.2 | Lee <i>et al.</i> ⁶¹ |
| Cycloepoxydon | Deuteromycete | ND | 4.2–8.4 ^c | Gehrt <i>et al.</i> ⁸⁴ |
| 15-Deoxy- $\Delta^{12,14}$ -PGJ ₂ | Natural prostaglandin derivative | IKK β /p65 | 1–6 | Rossi <i>et al.</i> ⁵⁴ ; Straus <i>et al.</i> ⁵⁶ |
| (–)-DHMEQ | Synthetic derivative of epoxyquinomycin C ^d | Rel family proteins | 2.7–27 | Matsumoto <i>et al.</i> ⁸⁶ ; Ariga <i>et al.</i> ⁹⁷ |
| Digitoxin | Plant | Na ⁺ /K ⁺ -ATPase | 0.003–0.1 | Tabary <i>et al.</i> ¹¹⁶ ; Yang <i>et al.</i> ¹¹⁷ ; Jagielska <i>et al.</i> ¹¹⁸ |
| Epoxyquinol A | Uncharacterized fungus | ND | 11 ^c | Li <i>et al.</i> ⁸⁷ |
| Epoxyquinone A monomer | Synthetic derivative of epoxyquinol A | IKK β /p65 | 2.3 ^c | Li <i>et al.</i> ⁸⁷ ; Liang <i>et al.</i> ⁹⁴ |
| Epoxyquinol B | Uncharacterized fungus | TAK1 | 3–30 | Kamiyama <i>et al.</i> ⁸⁸ |
| Gambogic acid | Plant (<i>Garcinia hanburyi</i>) | IKK β | 0.5–1.5 | Palempalli <i>et al.</i> ⁶⁵ |
| Helenalin | Plant | p65 | 10–40 | Lyss <i>et al.</i> ⁶⁸ ; García-Piñeres <i>et al.</i> ⁶⁹ |
| Jesterone dimer | Synthetic derivative of jesterone ^e | IKK β | 2.5–20 | Liang <i>et al.</i> ⁹⁰ |
| Manumycin A | <i>Streptomyces parvulus</i> | IKK β | 2–20 | Bernier <i>et al.</i> ⁶⁰ |
| Oleandrin | Plant | Na ⁺ /K ⁺ -ATPase | 0.017–17 | Manna <i>et al.</i> ¹¹² ; Sreenivasan <i>et al.</i> ¹¹³ ; Srivastava <i>et al.</i> ¹¹⁴ ; Manna <i>et al.</i> ¹¹⁵ |
| 5Z-7-oxozeaenol | Fungus | TAK1 | 0.083 ^c | Ninomiya-Tsuji <i>et al.</i> ⁹⁶ |
| Panepoxydone | <i>Lentinus crinitus</i> | ND | 7.15–9.52 ^c | Erkel <i>et al.</i> ⁹¹ |
| Parthenolide | Plant | IKK β /p65 | 5–40 | García-Piñeres <i>et al.</i> ⁶⁹ ; Hehner <i>et al.</i> ⁷¹ ; Hehner <i>et al.</i> ⁷² |
| Peperomin E | Plant (<i>Peperomia dindygulensis</i>) | ND | 10.5 ^c | Wu <i>et al.</i> ⁸¹ |
| SRC2 | Synthetic derivative of L- α -santonin | ND | 5.9 ^c | Kawai <i>et al.</i> ⁸⁰ |
| Xanthohumol | Plant | IKK β /p65 | 10–50 | Harikumar <i>et al.</i> ⁶⁴ |

Abbreviations: CDDO-Im, 1-(2-cyano-3,12-dioxooleana-1,9-dien-28-oyl)imidazole; CDDO-Me, 2-cyano-3,12-dioxooleana-1,9-dien-28-oic acid methyl ester; DHMEQ, dehydroxymethylepoxyquinomicin; IKK β , inhibitor of nuclear factor- κ B kinase- β ; ND, not determined; NF- κ B, nuclear factor- κ B; SRC2, (11S)-2 α -bromo-3-oxoeudesmano-13,6 α -lactone; TAK1, tumor growth factor- β -activated kinase.

^aMolecular targets in the NF- κ B signaling pathways or specific intracellular targets are shown.

^bThe concentration range used to inhibit NF- κ B activation in the cell-based assay is shown.

^cThe IC₅₀ values are shown.

^dProduced by *Amycolatopsis* sp.

^eProduced by *Pestalotiopsis jesteri*.

In the presence of TACE inhibitors, TNF- α -induced caspase-8 activation is greatly increased when A549 cells are treated with CHX or Ac-CHX.¹²⁸ As TACE is widely expressed in adult and fetal tissues, TNF- α /CHX-induced apoptosis may be more pronounced in various types of cells in the presence of TACE inhibitors. Given that TNF- α -induced NF- κ B activation induces the upregulation of c-FLIP, TACE-dependent ectodomain shedding induced by ERK and p38 MAP kinase is regarded as a posttranslational mechanism that immediately controls long-lived TNF-R1 on the cell surface (Figure 8b). Therefore, the ectodomain shedding of cell-surface TNF-R1 is likely to have a role in conferring resistance to TNF- α -induced apoptosis and in delaying the onset of TNF- α -induced apoptosis for a certain period.

CONCLUSION

In this review, the identification and biological properties of NF- κ B inhibitors (summarized in Table 2), which are classified into natural and synthetic IKK inhibitors, sesquiterpene lactones, epoxyquinoids, cardenolide glycosides and protein synthesis inhibitors have been described. Some of them are often used as specific NF- κ B inhibitors and as bioprobes to characterize intracellular biological responses and cell functions in various experimental models. Although not described

in this review, there are still many other interesting small molecules with unique structures and inhibitory profiles. Therefore, the elucidation of their molecular mechanisms would contribute to characterizing the NF- κ B signaling pathway at the molecular level as well as to developing novel lead compounds that target the NF- κ B signaling pathway in response to pro-inflammatory cytokines.

ACKNOWLEDGEMENTS

I thank Professor Masaya Imoto for giving me an opportunity to prepare this review.

- Karin, M. & Greten, F. R. NF- κ B: linking inflammation and immunity to cancer development and progression. *Nat. Rev. Immunol.* **5**, 749–759 (2005).
- Baud, V. & Karin, M. Is NF- κ B a good target for cancer therapy? Hopes and pitfalls. *Nat. Rev. Drug Discov.* **8**, 33–40 (2009).
- Ghosh, S. & Hayden, M. S. New regulators of NF- κ B in inflammation. *Nat. Rev. Immunol.* **8**, 837–848 (2008).
- Hayden, M. S. & Ghosh, S. Shared principles in NF- κ B signaling. *Cell* **132**, 344–362 (2008).
- Scheidereit, C. I κ B kinase complexes: gateways to NF- κ B activation and transcription. *Oncogene* **25**, 6685–6705 (2006).
- Solt, L. A. & May, M. J. The I κ B kinase complex: master regulator of NF- κ B signaling. *Immunol. Res.* **42**, 3–18 (2008).

- 7 Lee, F. S., Peters, R. T., Dang, L. C. & Maniatis, T. MEKK1 activates both I κ B kinase α and I κ B kinase β . *Proc. Natl Acad. Sci. USA* **95**, 9319–9324 (1998).
- 8 Zandi, E., Chen, Y. & Karin, M. Direct phosphorylation of I κ B by IKK α and IKK β : discrimination between free and NF- κ B-bound substrate. *Science* **281**, 1360–1363 (1998).
- 9 Chen, Z. J. Ubiquitin signalling in the NF- κ B pathway. *Nat. Cell Biol.* **7**, 758–765 (2005).
- 10 Bhoj, V. G. & Chen, Z. J. Ubiquitylation in innate and adaptive immunity. *Nature* **458**, 430–437 (2009).
- 11 Locksley, R. M., Killeen, N. & Lenardo, M. J. The TNF and TNF receptor superfamilies: integrating mammalian biology. *Cell* **104**, 487–501 (2001).
- 12 Aggarwal, B. B. Signalling pathways of the TNF superfamily: a double-edged sword. *Nat. Rev. Immunol.* **3**, 745–756 (2003).
- 13 Micheau, O. & Tschopp, J. Induction of TNF receptor I-mediated apoptosis via two sequential signaling complexes. *Cell* **114**, 181–190 (2003).
- 14 Ea, C. K., Deng, L., Xia, Z. P., Pineda, G. & Chen, Z. J. Activation of IKK by TNF α requires site-specific ubiquitination of RIP1 and polyubiquitin binding by NEMO. *Mol. Cell* **22**, 245–257 (2006).
- 15 Li, H., Kobayashi, M., Blonska, M., You, Y. & Lin, X. Ubiquitination of RIP is required for tumor necrosis factor α -induced NF- κ B activation. *J. Biol. Chem.* **281**, 13636–13643 (2006).
- 16 Wu, C. J., Conze, D. B., Li, T., Srinivasula, S. M. & Ashwell, J. D. Sensing of Lys 63-linked polyubiquitination by NEMO is a key event in NF- κ B activation. *Nat. Cell Biol.* **8**, 398–406 (2006).
- 17 Kataoka, T. The caspase-8 modulator c-FLIP. *Crit. Rev. Immunol.* **25**, 31–58 (2005).
- 18 Budd, R. C., Yeh, W. C. & Tschopp, J. cFLIP regulation of lymphocyte activation and development. *Nat. Rev. Immunol.* **6**, 196–204 (2006).
- 19 Chang, L. *et al.* The E3 ubiquitin ligase Itch couples JNK activation to TNF α -induced cell death by inducing c-FLIP₁ turnover. *Cell* **124**, 601–613 (2006).
- 20 Janssens, S. & Beyaert, R. Functional diversity and regulation of different interleukin-1 receptor associated kinase (IRAK) family members. *Mol. Cell* **11**, 293–302 (2003).
- 21 Shimada, T. *et al.* IKK- i , a novel lipopolysaccharide-inducible kinase that is related to I κ B kinase. *Int. Immunol.* **11**, 1357–1362 (1999).
- 22 Peters, R. T., Liao, S. M. & Maniatis, T. IKK ϵ is part of a novel PMA-inducible I κ B kinase complex. *Mol. Cell* **5**, 513–522 (2000).
- 23 Kishore, N. *et al.* IKK- i and TBK-1 are enzymatically distinct from the homologous enzyme IKK-2: comparative analysis of recombinant human IKK- i , TBK-1, and IKK-2. *J. Biol. Chem.* **277**, 13840–13847 (2002).
- 24 Hideshima, T. *et al.* NF- κ B as a therapeutic target in multiple myeloma. *J. Biol. Chem.* **277**, 16639–16647 (2002).
- 25 Castro, A. C. *et al.* Novel IKK inhibitors: β -carboline. *Bioorg. Med. Chem. Lett.* **13**, 2419–2422 (2003).
- 26 Nagashima, K. *et al.* Rapid TNFR1-dependent lymphocyte depletion *in vivo* with a selective chemical inhibitor of IKK β . *Blood* **107**, 4266–4273 (2006).
- 27 Wen, D. *et al.* A selective small molecule I κ B kinase β inhibitor blocks nuclear factor κ B-mediated inflammatory responses in human fibroblast-like synoviocytes, chondrocytes, and mast cells. *J. Pharmacol. Exp. Ther.* **317**, 989–1001 (2006).
- 28 Kishore, N. *et al.* A selective IKK-2 inhibitor blocks NF- κ B-dependent gene expression in interleukin-1 β -stimulated synovial fibroblasts. *J. Biol. Chem.* **278**, 32861–32871 (2003).
- 29 Baxter, A. *et al.* Hit-to-lead studies: the discovery of potent, orally active, thiophene-carboxamide IKK-2 inhibitors. *Bioorg. Med. Chem. Lett.* **14**, 2817–2822 (2004).
- 30 Bonafoux, D. *et al.* Inhibition of IKK-2 by 2-[(aminocarbonyl)amino]-5-acetylenyl-3-thiophenecarboxamides. *Bioorg. Med. Chem. Lett.* **15**, 2870–2875 (2005).
- 31 Podolin, P. L. *et al.* Attenuation of murine collagen-induced arthritis by a novel, potent, selective small molecule inhibitor of I κ B kinase 2, TPCA-1 (2-[(aminocarbonyl)amino]-5-(4-fluorophenyl)-3-thiophenecarboxamide), occurs via reduction of proinflammatory cytokines and antigen-induced T cell proliferation. *J. Pharmacol. Exp. Ther.* **312**, 373–381 (2005).
- 32 Sugiyama, H. *et al.* Synthesis and structure activity relationship studies of benzothieno[3,2-*b*]furan derivatives as a novel class of IKK β inhibitors. *Chem. Pharm. Bull.* **55**, 613–624 (2007).
- 33 Murata, T. *et al.* Discovery of novel and selective IKK- β serine-threonine protein kinase inhibitors. Part 1. *Bioorg. Med. Chem. Lett.* **13**, 913–918 (2003).
- 34 Murata, T. *et al.* Synthesis and structure-activity relationships of novel IKK- β inhibitors. Part 3: orally active anti-inflammatory agents. *Bioorg. Med. Chem. Lett.* **14**, 4019–4022 (2004).
- 35 Sanda, T. *et al.* Growth inhibition of multiple myeloma cells by a novel I κ B kinase inhibitor. *Clin. Cancer Res.* **11**, 1974–1982 (2005).
- 36 Frelin, C. *et al.* AS602868, a pharmacological inhibitor of IKK2, reveals the apoptotic potential of TNF- α in Jurkat leukemic cells. *Oncogene* **22**, 8187–8194 (2003).
- 37 Heckmann, A. *et al.* IKK2 inhibitor alleviates kidney and wasting diseases in a murine model of human AIDS. *Am. J. Pathol.* **164**, 1253–1262 (2004).
- 38 Burke, J. R. *et al.* BMS-345541 is a highly selective inhibitor of I κ B kinase that binds at an allosteric site of the enzyme and blocks NF- κ B-dependent transcription in mice. *J. Biol. Chem.* **278**, 1450–1456 (2003).
- 39 Beaulieu, F. *et al.* Synthesis and biological evaluation of 4-amino derivatives of benzimidazoquinoline, benzimidazoquinoline, and benzopyrazoloquinazoline as potent IKK inhibitors. *Bioorg. Med. Chem. Lett.* **17**, 1233–1237 (2007).
- 40 Belega, M. *et al.* Synthesis and structure-activity relationship of imidazo[1,2-*a*]thieno[3,2-*e*]pyrazines as IKK- β inhibitors. *Bioorg. Med. Chem. Lett.* **17**, 4284–4289 (2007).
- 41 Onai, Y. *et al.* Inhibition of I κ B phosphorylation in cardiomyocytes attenuates myocardial ischemia/reperfusion injury. *Cardiovasc. Res.* **63**, 51–59 (2004).
- 42 Tanaka, A. *et al.* A novel NF- κ B inhibitor, IMD-0354, suppresses neoplastic proliferation of human mast cells with constitutively activated *c-kit* receptors. *Blood* **105**, 2324–2331 (2005).
- 43 Tegeder, I. *et al.* Specific inhibition of I κ B kinase reduces hyperalgesia in inflammatory and neuropathic pain models in rats. *J. Neurosci.* **24**, 1637–1645 (2004).
- 44 Waelchli, R. *et al.* Design and preparation of 2-benzamido-pyrimidines as inhibitors of IKK. *Bioorg. Med. Chem. Lett.* **16**, 108–112 (2006).
- 45 Bamborough, P. *et al.* 5-(1-*H*-Benzimidazol-1-yl)-3-alkoxy-2-thiophenecarbonitriles as potent, selective, inhibitors of IKK- ϵ kinase. *Bioorg. Med. Chem. Lett.* **16**, 6236–6240 (2006).
- 46 Christopher, J. A. *et al.* The discovery of 2-amino-3,5-diarylbenzamide inhibitors of IKK- α and IKK- β kinases. *Bioorg. Med. Chem. Lett.* **17**, 3972–3977 (2007).
- 47 Christopher, J. A. *et al.* Discovery of 6-aryl-7-alkoxyisoquinoline inhibitors of I κ B kinase- β (IKK- β). *J. Med. Chem.* **52**, 3098–3102 (2009).
- 48 Liddle, J. *et al.* 4-Phenyl-7-azaindoles as potent and selective IKK2 inhibitors. *Bioorg. Med. Chem. Lett.* **19**, 2504–2508 (2009).
- 49 Mbalaviele, G. *et al.* A novel, highly selective, tight binding I κ B kinase-2 (IKK-2) inhibitor: a tool to correlate IKK-2 activity to the fate and functions of the components of the nuclear factor- κ B pathway in arthritis-relevant cells and animal models. *J. Pharmacol. Exp. Ther.* **329**, 14–25 (2009).
- 50 Sommers, C. D. *et al.* Novel tight-binding inhibitory factor- κ B kinase (IKK-2) inhibitors demonstrate target-specific anti-inflammatory activities in cellular assays and following oral and local delivery in an *in vivo* model of airway inflammation. *J. Pharmacol. Exp. Ther.* **330**, 377–388 (2009).
- 51 Ling, L., Cao, Z. & Goeddel, D. V. NF- κ B-inducing kinase activates IKK- α by phosphorylation of Ser-176. *Proc. Natl Acad. Sci. USA* **95**, 3792–3797 (1998).
- 52 Delhase, M., Hayakawa, M., Chen, Y. & Karin, M. Positive and negative regulation of I κ B kinase activity through IKK β subunit phosphorylation. *Science* **284**, 309–313 (1999).
- 53 Kapahi, P. *et al.* Induction of NF- κ B activation by arsenite through reaction with a critical cysteine in the activation loop of I κ B kinase. *J. Biol. Chem.* **275**, 36062–36066 (2000).
- 54 Rossi, A. *et al.* Anti-inflammatory cyclopentenone prostaglandins are direct inhibitors of I κ B kinase. *Nature* **403**, 103–108 (2000).
- 55 Byun, M. S., Choi, J. & Jue, D. M. Cysteine-179 of I κ B kinase β plays a critical role in enzyme activation by promoting phosphorylation of activation loop serines. *Exp. Mol. Med.* **38**, 546–552 (2006).
- 56 Straus, D. S. *et al.* 15-Deoxy- $\Delta^{12,14}$ -prostaglandin J₂ inhibits multiple steps in the NF- κ B signaling pathway. *Proc. Natl Acad. Sci. USA* **97**, 4844–4849 (2000).
- 57 Ahmad, R., Raina, D., Meyer, C., Kharbada, S. & Kufe, D. Triterpenoid CDDO-Me blocks the NF- κ B pathway by direct inhibition of IKK β on Cys-179. *J. Biol. Chem.* **281**, 35764–35769 (2006).
- 58 Yore, M. M., Liby, K. T., Honda, T., Gribble, G. W. & Sporn, M. B. The synthetic triterpenoid 1-[2-cyano-3,12-dioxoleana-1,9(11)-dien-28-oyl]imidazole blocks nuclear factor- κ B activation through direct inhibition of I κ B kinase β . *Mol. Cancer Ther.* **5**, 3232–3239 (2006).
- 59 Jeon, K. I., Byun, M. S. & Jue, D. M. Gold compound auranofin inhibits I κ B kinase (IKK) by modifying Cys-179 of IKK β subunit. *Exp. Mol. Med.* **35**, 61–66 (2003).
- 60 Bernier, M. *et al.* Binding of manumycin A inhibits I κ B kinase β activity. *J. Biol. Chem.* **281**, 2551–2561 (2006).
- 61 Lee, J. H. *et al.* Inhibition of NF- κ B activation through targeting I κ B kinase by celastrol, a quinone methide triterpenoid. *Biochem. Pharmacol.* **72**, 1311–1321 (2006).
- 62 Pandey, M. K. *et al.* Butein, a tetrahydrochalcone, inhibits nuclear factor (NF)- κ B and NF- κ B-regulated gene expression through direct inhibition of I κ B α kinase β on cysteine 179 residue. *J. Biol. Chem.* **282**, 17340–17350 (2007).
- 63 Pandey, M. K. *et al.* Berberine modifies cysteine 179 of I κ B α kinase, suppresses nuclear factor- κ B-regulated antiapoptotic gene products, and potentiates apoptosis. *Cancer Res.* **68**, 5370–5379 (2008).
- 64 Harikumar, K. B. *et al.* Modification of the cysteine residues in I κ B α kinase and NF- κ B (p65) by xanthohumol leads to suppression of NF- κ B-regulated gene products and potentiation of apoptosis in leukemia cells. *Blood* **113**, 2003–2013 (2009).
- 65 Palempalli, U. D. *et al.* Gambogic acid covalently modifies I κ B kinase- β subunit to mediate suppression of lipopolysaccharide-induced activation of NF- κ B in macrophage. *Biochem. J.* **419**, 401–409 (2009).
- 66 Schmidt, T. J. Helenanolide-type sesquiterpene lactones—III. Rates and stereochemistry in the reaction of helenalin and related helenanolides with sulfhydryl containing biomolecules. *Bioorg. Med. Chem.* **5**, 645–653 (1997).
- 67 Lyss, G., Schmidt, T. J., Merfort, I. & Pahl, H. L. Helenalin, an anti-inflammatory sesquiterpene lactone from Arnica, selectively inhibits transcription factor NF- κ B. *Biol. Chem.* **378**, 951–961 (1997).
- 68 Lyss, G., Knorre, A., Schmidt, T. J., Pahl, H. L. & Mefort, I. The anti-inflammatory sesquiterpene lactone helenalin inhibits the transcription factor NF- κ B by directly targeting p65. *J. Biol. Chem.* **273**, 33508–33516 (1998).
- 69 García-Piñeres, A. J. *et al.* Cysteine 38 in p65/NF- κ B plays a crucial role in DNA binding inhibition by sesquiterpene lactones. *J. Biol. Chem.* **276**, 39713–39720 (2001).
- 70 Bork, P. M., Schmitz, M. L., Kuhnt, M., Escher, C. & Heinrich, M. Sesquiterpene lactone containing Mexican Indian medicinal plants and pure sesquiterpene lactones as potent inhibitors of transcription factor NF- κ B. *FEBS Lett.* **402**, 85–90 (1997).
- 71 Hehner, S. P. *et al.* Sesquiterpene lactones specifically inhibit activation of NF- κ B by preventing the degradation of I κ B- α and I κ B- β . *J. Biol. Chem.* **273**, 1288–1297 (1998).

- 72 Hehner, S. P., Hofmann, T. G., Dröge, W. & Schmitz, M. L. The antiinflammatory sesquiterpene lactone parthenolide inhibits NF- κ B by targeting the I κ B kinase complex. *J. Immunol.* **163**, 5617–5623 (1999).
- 73 Kwok, B. H. B., Koh, B., Nduhuisi, M. I., Elofsson, M. & Crews, C. M. The anti-inflammatory natural product parthenolide from the medicinal herb Feverfew directly binds to and inhibits I κ B kinase. *Chem. Biol.* **8**, 759–766 (2001).
- 74 García-Piñeres, A. J., Lindenmeyer, M. T. & Mefort, I. Role of cysteine residues of p65/NF- κ B on the inhibition by the sesquiterpene lactone parthenolide and N-ethyl maleimide, and on its transactivating potential. *Life Sci.* **75**, 841–856 (2004).
- 75 Kim, B. H. *et al.* Artemisolid is a typical inhibitor of I κ B kinase β targeting cysteine-179 residue and down-regulates NF- κ B-dependent TNF- α expression in LPS-activated macrophages. *Biochem. Biophys. Res. Commun.* **361**, 593–598 (2007).
- 76 Yuuya, S. *et al.* Guaianolides as immunomodulators. Synthesis and biological activities of dehydrocostus lactone, mokko lactone, eremanthin, and their derivatives. *J. Nat. Prod.* **62**, 22–30 (1999).
- 77 Higuchi, Y. *et al.* Synthetic approach to exo-endo cross-conjugated cyclohexadienones and its application to the syntheses of dehydrobrachylaenolide, isodehydrochamaecynone, and trans-isodehydrochamaecynone. *J. Nat. Prod.* **66**, 588–594 (2003).
- 78 Zhang, S. *et al.* Bioactive guaianolides from *Siyekucai* (*Ixeris chinensis*). *J. Nat. Prod.* **69**, 1425–1428 (2006).
- 79 Siedle, B. *et al.* Quantitative structure-activity relationship of sesquiterpene lactones as inhibitors of the transcription factor NF- κ B. *J. Med. Chem.* **47**, 6042–6054 (2004).
- 80 Kawai, S. *et al.* Santonin-related compound 2 inhibits the expression of ICAM-1 in response to IL-1 stimulation by blocking the signaling pathway upstream of I κ B degradation. *Immunopharmacology* **48**, 129–135 (2000).
- 81 Wu, J. *et al.* Bioactive secolignans from *Peperomia dindygulensis*. *J. Nat. Prod.* **69**, 790–794 (2006).
- 82 Xu, S. *et al.* Bioactive compounds from *Peperomia pellucida*. *J. Nat. Prod.* **69**, 247–250 (2006).
- 83 Tsutsui, C. *et al.* Peperomins as anti-inflammatory agents that inhibit the NF- κ B signaling pathway. *Bioorg. Med. Chem. Lett.* **19**, 4084–4087 (2009).
- 84 Gehrt, A., Erkel, G., Anke, T. & Sterner, O. Cycloepoxydon, 1-hydroxy-2-hydroxymethyl-3-pent-1-enylbenzene and 1-hydroxy-2-hydroxymethyl-3-pent-1,3-dienylbenzene, new inhibitors of eukaryotic signal transduction. *J. Antibiot.* **51**, 455–463 (1998).
- 85 Li, C. *et al.* Total synthesis of the NF- κ B inhibitor (–)-cycloepoxydon: utilization of tartrate-mediated nucleophilic epoxydation. *J. Am. Chem. Soc.* **123**, 11308–11309 (2001).
- 86 Matsumoto, N. *et al.* Synthesis of NF- κ B activation inhibitors derived from epoxyquinomycin C. *Bioorg. Med. Chem. Lett.* **10**, 865–869 (2000).
- 87 Li, C. *et al.* Angiogenesis inhibitor epoxyquinol A: total synthesis and inhibition of transcription factor NF- κ B. *Org. Lett.* **4**, 3267–3270 (2002).
- 88 Kamiyama, H. *et al.* Epoxyquinol B, a naturally occurring pentaketide dimer, inhibits NF- κ B signaling by crosslinking TAK1. *Biosci. Biotechnol. Biochem.* **72**, 1894–1900 (2008).
- 89 Hu, Y. *et al.* Exploring chemical diversity of epoxyquinoid natural products: synthesis and biological activity of (–)-jesterone and related molecules. *Org. Lett.* **3**, 1649–1652 (2001).
- 90 Liang, M. C. *et al.* Jesterone dimer, a synthetic derivative of the fungal metabolite jesterone, blocks activation of transcription factor nuclear factor κ B by inhibiting the inhibitor of κ B kinase. *Mol. Pharmacol.* **64**, 123–131 (2003).
- 91 Erkel, G., Anke, T. & Sterner, O. Inhibition of NF- κ B activation by panepoxydone. *Biochem. Biophys. Res. Commun.* **226**, 214–221 (1996).
- 92 Kakeya, H. *et al.* Epoxyquinol A, a highly functionalized pentaketide dimer with antiangiogenic activity isolated from fungal metabolites. *J. Am. Chem. Soc.* **124**, 3496–3497 (2002).
- 93 Kakeya, H. *et al.* Epoxyquinol B, a fungal metabolite with a potent antiangiogenic activity. *J. Antibiot.* **55**, 829–831 (2002).
- 94 Liang, M. C. *et al.* Inhibition of transcription factor NF- κ B signaling proteins IKK β and p65 through specific cysteine residues by epoxyquinone A monomer: correlation with its anti-cancer cell growth activity. *Biochem. Pharmacol.* **71**, 634–645 (2006).
- 95 Kamiyama, H. *et al.* Fungal metabolite, epoxyquinol B, crosslinks proteins by epoxythiol conjugation. *J. Antibiot.* **61**, 94–97 (2008).
- 96 Ninomiya-Tsuji, J. *et al.* A resorcylic acid lactone, 5Z-7-oxozeaenol, prevents inflammation by inhibiting the catalytic activity of TAK1 MAPK kinase. *J. Biol. Chem.* **278**, 18485–18490 (2003).
- 97 Ariga, A., Namekawa, J., Matsumoto, N., Inoue, J. & Umezawa, K. Inhibition of tumor necrosis factor- α -induced nuclear translocation and activation of NF- κ B by dehydroxymethylepoxyquinomycin. *J. Biol. Chem.* **277**, 24625–24630 (2002).
- 98 Yamamoto, M., Horie, R., Takeiri, M., Kozawa, I. & Umezawa, K. Inactivation of NF- κ B components by covalent binding of (–)-dehydroxymethylepoxyquinomycin to specific cysteine residues. *J. Med. Chem.* **51**, 5780–5788 (2008).
- 99 Miyake, Y., Kakeya, H., Kataoka, T. & Osada, H. Epoxycyclohexenone inhibits Fas-mediated apoptosis by blocking activation of pro-caspase-8 in the death-inducing signaling complex. *J. Biol. Chem.* **278**, 11213–11220 (2003).
- 100 Kakeya, H. *et al.* Novel non-peptide inhibitors targeting death receptor-mediated apoptosis. *Bioorg. Med. Chem. Lett.* **13**, 3743–3746 (2003).
- 101 Bando, M. *et al.* The mycotoxin penicillic acid inhibits Fas ligand-induced apoptosis by blocking self-processing of caspase-8 in death-inducing signaling complex. *J. Biol. Chem.* **278**, 5786–5793 (2003).
- 102 Mitsui, T., Miyake, Y., Kakeya, H., Osada, H. & Kataoka, T. ECH, an epoxycyclohexenone derivative that specifically inhibits Fas ligand-dependent apoptosis in CTL-mediated cytotoxicity. *J. Immunol.* **172**, 3428–3436 (2004).
- 103 Mitsui, T. *et al.* RKTs-33, an epoxycyclohexenone derivative that specifically inhibits Fas ligand-dependent apoptosis in CTL-mediated cytotoxicity. *Biosci. Biotechnol. Biochem.* **69**, 1923–1928 (2005).
- 104 Kataoka, T. *et al.* Concanamycin A, a powerful tool for characterization and estimation of contribution of perforin- and Fas-based lytic pathways in cell-mediated cytotoxicity. *J. Immunol.* **156**, 3678–3686 (1996).
- 105 Prassas, I. & Diamandis, E. P. Novel therapeutic applications of cardiac glycosides. *Nat. Rev. Drug. Discov.* **7**, 926–935 (2008).
- 106 Kaplan, J. H. Biochemistry of Na,K-ATPase. *Ann. Rev. Biochem.* **71**, 511–535 (2002).
- 107 Aizman, O., Uhlén, P., Lal, M., Brismar, H. & Aperia, A. Ouabain, a steroid hormone that signals with slow calcium oscillations. *Proc. Natl Acad. Sci. USA* **98**, 13420–13424 (2001).
- 108 Miyakawa-Naito, A. *et al.* Cell signaling microdomain with Na,K-ATPase and inositol 1,4,5-triphosphate receptor generates calcium oscillations. *J. Biol. Chem.* **278**, 50355–50361 (2003).
- 109 Li, J., Zelenin, S., Aperia, A. & Aizman, O. Low doses of ouabain protect from serum deprivation-triggered apoptosis and stimulate kidney cell proliferation via activation of NF- κ B. *J. Am. Soc. Nephrol.* **17**, 1848–1857 (2006).
- 110 Xie, Z. *et al.* Intracellular reactive oxygen species mediate the linkage of Na⁺/K⁺-ATPase to hypertrophy and its marker genes in cardiac myocytes. *J. Biol. Chem.* **274**, 19323–19328 (1999).
- 111 Xie, Z. & Cai, T. Na⁺/K⁺-ATPase-mediated signal transduction: from protein interaction to cellular function. *Mol. Interv.* **3**, 157–168 (2003).
- 112 Manna, S. K., Sah, N. K., Newman, R. A., Cisneros, A. & Aggarwal, B. B. Oleandrin suppresses activation of nuclear transcription factor- κ B, activator protein-1, and c-Jun NH₂-terminal kinase. *Cancer Res.* **60**, 3838–3847 (2000).
- 113 Sreenivasan, Y., Sarkar, A. & Manna, S. K. Oleandrin suppresses activation of nuclear transcription factor- κ B and activator protein-1 and potentiates apoptosis induced by ceramide. *Biochem. Pharmacol.* **66**, 2223–2239 (2003).
- 114 Srivastava, M. *et al.* Digitoxin mimics gene therapy with CFTR and suppresses hypersecretion of IL-8 from cystic fibrosis lung epithelial cells. *Proc. Natl Acad. Sci. USA* **101**, 7693–7698 (2004).
- 115 Manna, S. K., Sreenivasan, Y. & Sarkar, A. Cardiac glycoside inhibits IL-8-induced biological responses by downregulating IL-8 receptors through altering membrane fluidity. *J. Cell. Physiol.* **207**, 195–207 (2006).
- 116 Tabary, O. *et al.* Calcium-dependent regulation of NF- κ B activation in cystic fibrosis airway epithelial cells. *Cell Signal.* **18**, 652–660 (2006).
- 117 Yang, Q. *et al.* Cardiac glycosides inhibit TNF- α /NF- κ B signaling by blocking recruitment of TNF receptor-associated death domain to the TNF receptor. *Proc. Natl Acad. Sci. USA* **102**, 9631–9636 (2005).
- 118 Jagielska, J., Salguero, G., Schieffer, B. & Bavendiek, U. Digitoxin elicits anti-inflammatory and vasoprotective properties in endothelial cells: therapeutic implications for the treatment of atherosclerosis? *Atherosclerosis* **206**, 390–396 (2009).
- 119 Fu, L. *et al.* Three new triterpenes from *Nerium oleander* and biological activity of the isolated compounds. *J. Nat. Prod.* **68**, 198–206 (2005).
- 120 Zhao, M. *et al.* Taraxasterane- and ursane-type triterpenes from *Nerium oleander* and their biological activities. *J. Nat. Prod.* **69**, 1164–1167 (2006).
- 121 Bai, L. *et al.* Bioactive pregnanes from *Nerium oleander*. *J. Nat. Prod.* **70**, 14–18 (2007).
- 122 Zhao, M. *et al.* Bioactive cardenolides from the stems and twigs of *Nerium oleander*. *J. Nat. Prod.* **70**, 1098–1103 (2007).
- 123 Wang, L. *et al.* Bioactive triterpene saponins from the roots of *Phytolacca americana*. *J. Nat. Prod.* **71**, 35–40 (2008).
- 124 Takada, Y. *et al.* Odoricide A and ouabain inhibit Na⁺/K⁺-ATPase and prevent NF- κ B-inducible protein expression by blocking Na⁺-dependent amino acid transport. *Biochem. Pharmacol.* **78**, 1157–1166 (2009).
- 125 Hyde, R., Taylor, P. M. & Hundal, H. S. Amino acid transporters: roles in amino acid sensing and signalling in animal cells. *Biochem. J.* **373**, 1–18 (2003).
- 126 Sugimoto, H. *et al.* E-73, an acetoxyl analogue of cycloheximide, blocks the tumor necrosis factor-induced NF- κ B signaling pathway. *Biochem. Biophys. Res. Commun.* **277**, 330–333 (2000).
- 127 Kadohara, K. *et al.* Acetoxycycloheximide (E-73) rapidly induces apoptosis mediated by the release of cytochrome c via activation of c-Jun N-terminal kinase. *Biochem. Pharmacol.* **69**, 551–560 (2005).
- 128 Ogura, H. *et al.* Ectodomain shedding of TNF receptor 1 induced by protein synthesis inhibitors regulates TNF- α -mediated activation of NF- κ B and caspase-8. *Exp. Cell Res.* **314**, 1406–1414 (2008).
- 129 Schlöndorff, J. & Blobel, C. P. Metalloprotease-disintegrins: modular proteins capable of promoting cell-cell interactions and triggering signals by protein-ectodomain shedding. *J. Cell Sci.* **112**, 3603–3617 (1999).
- 130 Moss, M. L., White, J. M., Lambert, M. H. & Andrews, R. C. TACE and other ADAM proteases as targets for drug discovery. *Drug Discov. Today* **6**, 417–426 (2001).
- 131 Iordanov, M. S. *et al.* Ribotoxic stress response: activation of the stress-activated protein kinase JNK1 by inhibitors of the peptidyl transferase reaction and by sequence-specific RNA damage to the α -sarcin/ricin loop in the 28S rRNA. *Mol. Cell. Biol.* **17**, 3373–3381 (1997).
- 132 Sidhu, J. S. & Omiecinski, C. J. Protein synthesis inhibitors exhibit a nonspecific effect on phenobarbital-inducible cytochrome P450 gene expression in primary rat hepatocytes. *J. Biol. Chem.* **273**, 4769–4775 (1998).

- 133 Shifrin, V. I. & Anderson, P. Trichothecene mycotoxins trigger a ribotoxic stress response that activates c-Jun N-terminal kinase and p38 mitogen-activated protein kinase and induces apoptosis. *J. Biol. Chem.* **274**, 13985–13992 (1999).
- 134 Ogura, H. *et al.* ERK and p38 MAP kinase are involved in downregulation of cell surface TNF receptor 1 induced by acetoxycycloheximide. *Int. Immunopharmacol.* **8**, 922–926 (2008).
- 135 Kadohara, K. *et al.* Caspase-8 mediates mitochondrial release of pro-apoptotic proteins in a manner independent of its proteolytic activity in apoptosis induced by the protein synthesis inhibitor acetoxycycloheximide in human leukemia Jurkat cells. *J. Biol. Chem.* **284**, 5478–5487 (2009).
- 136 Fan, H. & Derynck, R. Ectodomain shedding of TGF- α and other transmembrane proteins is induced by receptor tyrosine kinase activation and MAP kinase signaling cascades. *EMBO J.* **18**, 6962–6972 (1999).
- 137 Díaz-Rodríguez, E., Montero, J. C., Esparís-Ogando, A., Yuste, L. & Pandiella, A. Extracellular signal-regulated kinase phosphorylates tumor necrosis factor α -converting enzyme at threonine 735: a potential role in regulated shedding. *Mol. Biol. Cell* **13**, 2031–2044 (2002).
- 138 Weskamp, G. *et al.* Evidence for a critical role of the tumor necrosis factor α convertase (TACE) in ectodomain shedding of the p75 neurotrophin receptor (p75^{NTR}). *J. Biol. Chem.* **279**, 4241–4249 (2004).
- 139 Soond, S. M., Everson, B., Riches, D. W. H. & Murphy, G. ERK-mediated phosphorylation of Thr735 in TNF α -converting enzyme and its potential role in TACE protein trafficking. *J. Cell Sci.* **118**, 2371–2380 (2005).
- 140 Deng, X. *et al.* p38 Mitogen-activated protein kinase-dependent tumor necrosis factor- α -converting enzyme is important for liver injury in hepatotoxic interaction between lipopolysaccharide and ranitidine. *J. Pharmacol. Exp. Ther.* **326**, 144–152 (2008).
- 141 Kopp, E. & Ghosh, S. Inhibition of NF- κ B by sodium salicylate and aspirin. *Science* **265**, 956–959 (1994).
- 142 Yin, M. J., Yamamoto, Y. & Gaynor, R. B. The anti-inflammatory agents aspirin and salicylate inhibit the activity of I κ B kinase- β . *Nature* **396**, 77–80 (1998).
- 143 Schwenger, P., Alpert, D., Skolnik, E. Y. & Vilcek, J. Activation of p38 mitogen-activated protein kinase by sodium salicylate leads to inhibition of tumor necrosis factor-induced I κ B α phosphorylation and degradation. *Mol. Cell. Biol.* **18**, 78–84 (1998).
- 144 Alpert, D., Schwenger, P., Han, J. & Vilcek, J. Cell stress and MKK6b-mediated p38 MAP kinase activation inhibit tumor necrosis factor-induced I κ B phosphorylation and NF- κ B activation. *J. Biol. Chem.* **274**, 22176–22183 (1999).
- 145 Madge, L. A., Sierra-Honigsmann, M. R. & Poher, J. S. Apoptosis-inducing agents cause rapid shedding of tumor necrosis factor receptor 1 (TNFR1). *J. Biol. Chem.* **274**, 13643–13649 (1999).

ORIGINAL ARTICLE

Activation of secondary metabolite–biosynthetic gene clusters by generating *rsmG* mutations in *Streptomyces griseus*

Yukinori Tanaka^{1,2}, Shinji Tokuyama² and Kozo Ochi¹

Unlike other *Streptomyces* spp., the streptomycin producer *Streptomyces griseus* IFO13189 shows emergence of a small fraction of *rsmG* and *rpsL* mutants among spontaneous low- or high-level streptomycin-resistant mutants. *rsmG*, but not *rpsL*, mutants showed greater ability (two- to threefold) to produce streptomycin, accompanied by enhanced transcription of *metK* and *strR*, together with streptomycin biosynthetic genes, such as *strB1*, *strD* and *strF*, thus underlying the observed increase in streptomycin production in the *rsmG* mutants. Moreover, *rsmG* mutation was effective for activating the ‘silent’ or poorly expressed secondary metabolite–biosynthetic genes present in *S. griseus*.

The Journal of Antibiotics (2009) 62, 669–673; doi:10.1038/ja.2009.97; published online 9 October 2009

Keywords: *rsmG*; silent genes; *Streptomyces griseus*; streptomycin resistance

INTRODUCTION

Actinomycetes produce a variety of natural products that are of major importance in the pharmaceutical industry. More than 50% of all anti-infective and anticancer compounds developed over the past 25 years have been natural products or derivatives thereof.¹ In the past several years, the complete genome sequences of many organisms have been reported. The information from these genome projects indicated that *Streptomyces coelicolor*, *S. avermitilis* and *S. griseus* have 20, 25 and 34 clusters of genes involved in secondary metabolism, respectively, but only a few secondary metabolites are known in each case.^{2–4} Recently, we described a practical method for increasing antibiotic production in bacteria by modulating ribosomal components (ribosomal proteins or rRNA), specifically by generating mutations conferring drug resistance, such as streptomycin resistance.^{5–7} This approach, called ‘ribosome engineering’,⁸ has several advantages including the ability to screen for drug resistance mutations by simple selection on drug-containing plates, even if the mutation frequency is extremely low (for example, $<10^{-10}$), and has been shown to be effective for improving the industrial strains, which had been bred to produce large amount of antibiotics.^{9,10} *S. griseus* is a filamentous, soil-living, Gram-positive bacteria, which produces an aminoglycoside antibiotic, streptomycin, and is characterized by the presence of a streptomycin self-resistance gene, *aphD*, which encodes streptomycin-6-phosphotransferase. Here, we showed that *rsmG* and *rpsL* (conferring low and high levels of resistance to streptomycin, respectively) mutations can be generated in *S. griseus*, although this organism already possesses a relatively high level of self-resistance to this antibiotic produced by the organism itself. The effects of *rsmG* and *rpsL* mutations on streptomycin production were examined, along with those

of many other ‘silent’ secondary metabolite–biosynthetic genes present in this organism.

MATERIALS AND METHODS

Bacterial strains and culture conditions

Streptomyces griseus IFO13189, a prototrophic streptomycin-producing wild-type strain, was used as the parental strain. Spontaneous streptomycin-resistant mutants were obtained as colonies that grew within 5–7 days after spores were spread on glucose–yeast extract–malt extract (GYM) agar¹¹ containing various concentrations of streptomycin. Mutations in *rpsL* or *rsmG* genes were determined by DNA sequencing using the primers listed in Table 1. Cultivation was performed at 30 °C (for preculture) or 25 °C (for main culture) using SPY medium¹¹ with rotary shaking at 220 r.p.m.

Assay for streptomycin and determination of minimum inhibitory concentrations

Streptomycin was determined by bioassay using *Bacillus subtilis* ATCC6633 as the test organism. Minimum inhibitory concentrations (MICs) were determined by spotting spore solutions ($\sim 10^6$) onto streptomycin-containing GYM plates, followed by incubation for 5 days at 30 °C.

Total RNA preparation

Total cellular RNA was prepared using Isogen reagent (Nippon Gene, Toyama, Japan). Each pellet was resuspended in 1 ml of Isogen reagent and incubated at 50 °C for 10 min. After cooling, 0.2 ml of chloroform was added. Each sample was mixed well by vortexing and centrifuged at 16 000 × g for 10 min, and 0.6 ml of the aqueous phase (top layer) was transferred to a clean tube. To each test tube, 0.4 ml of chloroform was added and each sample was mixed by repeated inversions and centrifuged at 16 000 × g for 10 min. A portion (0.6 ml) of the aqueous phase (top layer) was transferred to a clean tube. The RNA in each

¹National Food Research Institute, Tsukuba, Ibaraki, Japan and ²Faculty of Agriculture, Department of Applied Biological Chemistry, Shizuoka University, Shizuoka, Japan

Correspondence: Dr K Ochi, National Food Research Institute, 2–1–12 Kannondai, Tsukuba, Ibaraki 305-8642, Japan.

E-mail: kochi@affrc.go.jp

Received 14 July 2009; revised 10 September 2009; accepted 18 September 2009; published online 9 October 2009

Table 1 The primers used in this study

| Purpose | Primer | Oligonucleotide sequence (5' → 3') | Reference |
|------------------------------------|----------------------------------|--|------------------------------------|
| PCR and sequencing for <i>rpsL</i> | rpsL-F1 rpsL-R1 | CGACACACCCGACCGCTGGG CGGGTCGATGATACCGGGCGCTTC | Tanaka <i>et al.</i> ⁶ |
| PCR and sequencing for <i>rsmG</i> | rsmG-F2 rsmG-R2 | CGGAAGGACGGTCCCGTG GAGCGACGTTTCACGTGAAACACGATGC | Tanaka <i>et al.</i> ⁶ |
| Real-time qPCR for <i>hrdB</i> | SGR1701 hrdB F SGR1701 hrdB R | GAAGGTCATCGAGGTCCAGAAG GTGGCGGAGCTTCGACATC | Ohnishi <i>et al.</i> ⁴ |
| Real-time qPCR for <i>adpA</i> | adpA-77F adpA-130R | TTGCCGTGCTGCTGTTCA AAACGAGAGCGGGATGGA | This study |
| Real-time qPCR for <i>metK</i> | metK-F2 metK-R2 | CAACCTCGTGCGCAACAA CACAGGAAGCACCGTCGAA | This study |
| Real-time qPCR for <i>strR</i> | SGR5931 strR F SGR5931 strR R | AATTATCCCGCTGACAATGG GGATGGGTCTCCAGGACAC | Ohnishi <i>et al.</i> ⁴ |
| Real-time qPCR for <i>strB1</i> | strB1-F2 strB1-R2 | ACTACGAGAGCCAGGAGCAGAT TGACTCCGAGCTTGGTCAACT | This study |
| Real-time qPCR for <i>strD</i> | strD-F2 strD-R2 | ACCCACACGTCTGCGAAAC TGGCCTCCAGCCATAGA | This study |
| Real-time qPCR for <i>strF</i> | StrF-F2 StrF-R2 | GACTACGACAAGGTGCACGACTA AAGCGGATGTTCTCGATGGT | This study |
| Real-time qPCR for SGR 281 | 281-802F 281-874R | CGCACGATCTGGAAGAACCT GGTAGTAGAGGCGATCGACGTAGA | This study |
| Real-time qPCR for SGR 443 | 443-643F 443-727R | GTGCAGTCCCGGAGATG GGTAGCGCCGTTCTGTTGTC | This study |
| Real-time qPCR for SGR 593 | 593-44F 593-101R | GTTCTTGCTGACCTGAATG CGCGAGAGAAGCGGATCA | This study |
| Real-time qPCR for SGR 604 | 604-15F 604-78R | GCCCTACTACGAACTGCGTCAT GTAGACGTTGCCGACCAGGTT | This study |
| Real-time qPCR for SGR 811 | 811-F825 811-R899 | CCTGCCCTACCTGATGTTTCC CAGTTCTGTTCCGGTGAACCATTC | This study |
| Real-time qPCR for SGR 896 | 896-F702 896-R770 | GGAGTGCCGCGAGATCTTC TCGAGGACGGCGATGCTT | This study |
| Real-time qPCR for SGR 962 | 962-551F 962-627R | TCCCCCTAACATCTACGACTT GCGTTTCGCGGAGACGAT | This study |
| Real-time qPCR for SGR 2079 | 2079-190F 2079-245R | GCCACACAGGCCCATCTC ACCAGGAAGGCCAGAAAA | This study |
| Real-time qPCR for SGR 2488 | 2488-501F 2488-582R | GTCCGCTCGATCGTCAAC GTGCTTGGCCGCGACGTA | This study |
| Real-time qPCR for SGR 2594 | 2594-825F 2594-889R | CGTCTTCGGCATGGTCATG ATCTGCTCGACGGTTCCA | This study |
| Real-time qPCR for SGR 3267 | 3267-F945 3267-R1007 | CGTCGTCACGCTCTGGAA TCCTCAGGACGGTCAACAC | This study |
| Real-time qPCR for SGR 4413 | 4413-140F 4413-199R | TCGCCGGTACTTCTTCATC TGAGGCGCAGCCGTACGT | This study |
| Real-time qPCR for SGR 5295 | 5295-F189 5295-R253 | CAACGACTACCTGGGCATGA GCAGGGTGGAGGCGATCT | This study |
| Real-time qPCR for SGR 6072 | 6072-F27 6072-R99 | CACCGTCCTGGAGTACTTCCA GTCCGTGGCGAACAGCTT | This study |
| Real-time qPCR for SGR 6178 | 6178-F372 6178-R424 | CCGGGCTCCGGTGATC CGTCATCGCCCCTCAGATG | This study |
| Real-time qPCR for SGR 6367 | 6367-F142 6367-R198 | GCGTTACGTCCTTTCC GCTCGGGCGACACA | This study |
| Real-time qPCR for SGR 6717 | 6717-864F 6717-922R | CGCGCAGTTCATCATGGAA TCATCACGTACTTGGGCATCTC | This study |
| Real-time qPCR for SGR 6780 | 6780-F381 6780-R457 | CGCGCTCCGAGCAGAT CGTTGTGGTTGGCGATGAC | This study |

Abbreviation: qPCR, quantitative PCR.

tube was precipitated with an equal volume of isopropanol, and rinsed with 70% ethanol. The Isogen reagent treatment was repeated once more to prepare pure RNA and finally suspended with an appropriate volume of diethylpyrocarbonate-treated water.

Transcriptional analysis by real-time quantitative PCR

The total RNAs were prepared as described above. Contaminating DNA was removed by incubating each total RNA sample (1 µg) with 1 U of DNase I (Invitrogen, Carlsbad, CA, USA) for 15 min at 25 °C. Reverse transcription

Table 2 Characterization of streptomycin resistance mutations of *Streptomyces griseus*

| Streptomycin concentration ($\mu\text{g ml}^{-1}$) used for selection | Mutation in ^a | | Amino acid substitution | Frequency of mutants with the same mutation | Minimum inhibitory concentration to streptomycin ($\mu\text{g ml}^{-1}$) ^b | Streptomycin productivity ($\mu\text{g ml}^{-1}$) ^c | Designation of mutant |
|---|--------------------------|-------------------------------|----------------------------------|---|---|--|-----------------------|
| | <i>rsmG</i> | <i>rpsL</i> | | | | | |
| — ^d | | | | | 70 | 65 ± 6 | |
| 70 | Δ73G–76T | | Frameshift | 1/86 | 300 | 118 ± 27 | KO-1057 |
| | Insertion of AGCTC at 88 | | Frameshift | 1/86 | 300 | 117 ± 27 | KO-1058 |
| | 173T→C | | Leu58→Pro | 1/86 | 300 | 154 ± 30 | KO-1059 |
| | 268G→C | | Gly90→Arg | 1/86 | 300 | 192 ± 21 | KO-1060 |
| | Insertion of CCA at 277 | | Insertion of Pro at 93 | 1/86 | 300 | 124 ± 17 | KO-1061 |
| | 280G→C | | Ala94→Pro | 1/86 | 300 | 144 ± 18 | KO-1062 |
| | 331C→T | | Arg111→Trp | 1/86 | 300 | 124 ± 17 | KO-1063 |
| | 332G→A | | Arg111→Gln | 1/86 | 300 | 130 ± 5 | KO-1064 |
| | Δ389T–398G | | Frameshift | 1/86 | 300 | 139 ± 33 | KO-1065 |
| | Insertion of G at 465 | | Frameshift | 1/86 | 300 | 121 ± 18 | KO-1066 |
| | 500A501G→C | | Frameshift | 1/86 | 300 | 151 ± 8 | KO-1067 |
| | Insertion of G at 585 | | Frameshift | 1/86 | 300 | 164 ± 36 | KO-1069 |
| | Δ623T | | Frameshift | 1/86 | 300 | 125 ± 4 | KO-1070 |
| | ND ^e | | ND | 72/86 | — ^f | — ^f | |
| 100 | Δ260G–291G | | Frameshift | 1/30 | 300 | 140 ± 8 | KO-1050 |
| | Δ389T–398G | | Frameshift | 1/30 | 300 | 162 ± 17 | KO-1051 |
| | ND | | ND | 28/30 | — ^f | — ^f | |
| 500 | | 262A→G | Lys88→Glu | 4/59 | 2000 | 57 ± 13 | KO-1052~1055 |
| | | ND | ND | 55/59 | — ^f | — ^f | |
| 1000 | | Insertion of GGCGTGCGT at 250 | Insertion of Gly, Val, Arg at 84 | 1/20 | 3000 | 29 ± 7 | KO-1056 |
| | | ND | ND | 19/20 | — ^f | — ^f | |
| 2000 | | ND | ND | 9/9 | — ^f | — ^f | |

Abbreviation: GYM, glucose–yeast extract–malt extract.

^aNumbered from the start codon of the open reading frame of *S. griseus*.^bDetermined after 5 days of incubation on GYM medium.^cStrains were grown in SPY medium at 25 °C for 3 days.^dWild-type strain.^eMutations were not detected in either *rsmG* or *rpsL* gene.^fNot determined.

reaction was carried out using a high-capacity RNA-to-cDNA Kit (Applied Biosystems, Foster City, CA, USA) according to the manufacturer's instructions. The samples were diluted with an appropriate volume of water and analyzed using the 7300 real-time quantitative PCR (qPCR) system and Power SYBR Green PCR master mix (Applied Biosystems). Each transcriptional assay was normalized to the corresponding transcriptional level of the *hrdB* gene encoding the principal sigma factor. Primers used for real-time qPCR are listed in Table 1. All reactions were performed under the following conditions: 2 min at 50 °C, 10 min at 95 °C, followed by 40 cycles of 15 s at 95 °C for denaturing, 30 s at 60 °C for annealing and 30 s at 72 °C for extension.

RESULTS AND DISCUSSION

Isolation and characterization of streptomycin-resistant mutants

In various actinomycetes, high-level resistance to streptomycin is often due to mutations in *rpsL*, which encodes the ribosomal protein S12, whereas low-level resistance is due to mutations in *rsmG*, which encodes a 16S rRNA methyltransferase.^{5,6} Unlike other *Streptomyces* spp. (MIC to streptomycin, 0.2–2 $\mu\text{g ml}^{-1}$), the streptomycin producer *S. griseus* IFO13189 showed a relatively high level of resistance (MIC=70 $\mu\text{g ml}^{-1}$). We isolated a total of 204 resistant mutant strains

that had developed spontaneously on GYM agar plates containing various concentrations (70–2000 $\mu\text{g ml}^{-1}$) of streptomycin. Of these mutants, 15 had mutations in the *rsmG* gene and were characterized by the frequent appearance of deletion or insertion mutations that resulted in frameshift, and five carried mutations in *rpsL*, including the K88E mutation and novel insertion mutation (Table 2). These results were in contrast with those of previous studies in other *Streptomyces* spp. in which >50% of resistant strains were due to mutations in *rpsL* or *rsmG*.⁶ This observation suggested that *S. griseus* harbors a wide range of resistance systems, in addition to inactivation of streptomycin by streptomycin-6-phosphotransferase, to survive in the presence of its own antibiotic, streptomycin. The *rsmG* mutants showed impaired ability to form aerial mycelia, and were somewhat deficient in sporulation.

We reported previously that, in the *rsmG* mutant background, *rpsL* mutants with high-level streptomycin resistance emerge at a frequency 200-fold greater than that in the wild-type strain of *S. coelicolor*, and this elevated frequency in the emergence of high-level streptomycin resistance was facilitated by a mutation pattern in *rpsL* more varied than that obtained by selection of the wild-type strain.^{5,6} Similarly,

Table 3 Genes of *Streptomyces griseus* IFO13189 analyzed in this study

| Gene ^a | Product | Secondary metabolite biosynthetic gene cluster |
|-------------------|--|--|
| <i>metK</i> | S-adenosylmethionine synthetase | — ^b |
| <i>adpA</i> | Transcriptional regulator | — ^b |
| <i>strR</i> | Streptomycin biosynthesis operon regulator | Streptomycin |
| <i>strB1</i> | Scyllo-inosamine-4-phosphate amidinotransferase | Streptomycin |
| <i>strD</i> | Putative glucose-1-phosphate thymidyltransferase | Streptomycin |
| <i>strF</i> | StrF protein | Streptomycin |
| SGR281 | Hypothetical protein | PKS–NRPS hybrid (SGR278–SGR283) |
| SGR443 | Putative ABC transporter ATPase and permease component | NRPS for siderophore (SGR443–SGR455) |
| SGR593 | Hypothetical protein | NRPS (SGR574–SGR593) |
| SGR604 | Putative enediyne biosynthesis protein | Enediyne PKS (SGR604–SGR611) |
| SGR811 | Putative oxidoreductase | PKS–NRPS hybrid (SGR810–SGR815) |
| SGR896 | Putative O-methyltransferase | NRPS (SGR895–SGR901) |
| SGR962 | Putative squalene–hopene cyclase | Hopanoid (SGR962–SGR966) |
| SGR2079 | Putative terpene cyclase | Terpene (SGR2079) |
| SGR2488 | Putative dehydrogenase | Type I PKS, NRPS (SGR2482–SGR2489) |
| SGR2594 | Putative integral membrane ion antiporter | NRPS (SGR2586–SGR2598) |
| SGR3267 | Putative cytochrome P450 | Type II PKS, NRPS (SGR3239–SGR3288) |
| SGR4413 | Putative lantibiotic biosynthesis protein | Lantibiotic (SGR4408–SGR4421) |
| SGR5295 | 5-Aminolevulinic synthase | Unknown (SGR5285–SGR5295) |
| SGR6072 | Putative ketosteroid isomerase | Type I PKS (SGR6071–SGR6083) |
| SGR6178 | Putative thioesterase | Type I PKS (SGR6177–SGR6183) |
| SGR6367 | Putative oxidoreductase | Type I PKS (SGR6360–SGR6387) |
| SGR6717 | Putative ABC transporter ATPase and permease component | NRPS for siderophore (SGR6709–SGR6717) |
| SGR6780 | Putative malonyl-CoA: ACP transacylase | Type I PKS, PKS–NRPS hybrid (SGR6776–SGR6786) |

^aGene names are obtained from the reference Ohnishi *et al.*⁴

^bThese are not the secondary metabolite biosynthetic gene cluster.

S. griseus rsmG mutant, KO-1050, generated the mutants resistant to high-level streptomycin (1000 µg ml⁻¹) at high frequency. However, no *rpsL* mutants were detected among the 30 resistant mutants tested, again characterizing the specific feature of *S. griseus*.

Effects of *rsmG* and *rpsL* mutations on streptomycin production

Mutations in *rsmG* were effective in enhancing streptomycin production, leading to a two- to threefold increase in streptomycin production, whereas *rpsL* K88E mutation and *rpsL* insertion mutation were not effective (Table 2). In addition, the mutants with no mutations in either *rsmG* or *rpsL* (that is, ND mutants) showed the impaired ability to produce streptomycin, as examined with 12 ND mutants (data not shown). In *S. coelicolor*, enhanced expression of the *metK* gene encoding S-adenosylmethionine synthetase corresponds to the enhanced production of streptomycin and actinorhodin caused by *rsmG* mutations.^{5,12} Moreover, addition of S-adenosylmethionine causes overproduction of streptomycin in *S. griseus*, accompanied by enhanced transcription of *adpA* and *strR*.^{13,14} We analyzed transcription of *metK*, *adpA* and *strR*, together with several genes involved in biosynthesis of streptomycin (*strB1*, *strF* and *strD*) (Table 3).

As expected, the *rsmG* mutant, but not the *rpsL* K88E mutant, exhibited elevated levels of *metK*, *strR*, *strB1*, *strF* and *strD* expression compared with the wild-type strain at late growth phase (36 h) (Figure 1), thus underlying the enhanced production of streptomycin in the *rsmG* mutant. StrR is a regulator of the streptomycin biosynthesis operon¹⁵ and AdpA acts as a central transcriptional regulator in the A-factor regulatory cascade of *S. griseus*.¹⁶ Although the elevated levels of *metK* and *strR* expression account well for the marked enhancement of biosynthetic gene expression (*strB1*, *strD* and *strF*), it is not yet clear why *adpA* gene expression was not activated in the *rsmG* mutant.

Effects of *rsmG* mutation on transcription of secondary metabolite–biosynthetic gene clusters

A recent study in our laboratory indicated that certain mutations in *rpoB* (encoding RNA polymerase β-subunit) or *rpsL* genes can activate ‘silent’ genes of actinomycetes, leading to the discovery of novel antibacterial agents.¹⁷ The activation of silent genes by generating *rpoB* H437D or *rpoB* H437L mutations in *Streptomyces* sp. 631689 was attributed, at least partly, to the increased affinity of the mutant RNA polymerase for promoters.¹⁷ Thus, we analyzed the expression of secondary metabolite–biosynthetic gene clusters in the *S. griseus rsmG* mutant, KO-1050. A total of 18 genes belonging to 18 secondary metabolite–biosynthetic gene clusters (Table 3) were subjected to transcriptional analysis by real-time qPCR, and the results indicated that the levels of expression of these genes are quite low (1/10–1/1000 compared with that of *strB1*), thus representing silent or poorly expressed genes. Strikingly, analysis of cells harvested at late growth phase (36 h) indicated that the *rsmG* mutation affected not only streptomycin biosynthesis but also the expression of other secondary metabolite–biosynthetic genes, although the effects were not dramatic (Figure 2). Enhancement of expression was pronounced in SGR3267 (putative cytochrome P450 involved in Type II polyketide synthases or non-ribosomal peptide synthetases) and SGR962 (putative squalene–hopene cyclase involved in hopanoid synthesis). By contrast, the *rpsL* K88E mutant, KO-1052, did not show any enhanced expression of those genes (data not shown).

CONCLUDING REMARKS

We showed that *rsmG* mutation is effective not only for enhancement of streptomycin production but also for activation of silent or poorly expressed genes in *S. griseus*. Although a biochemical approach (for example, measurement of *in vitro* protein synthesis activity) was not

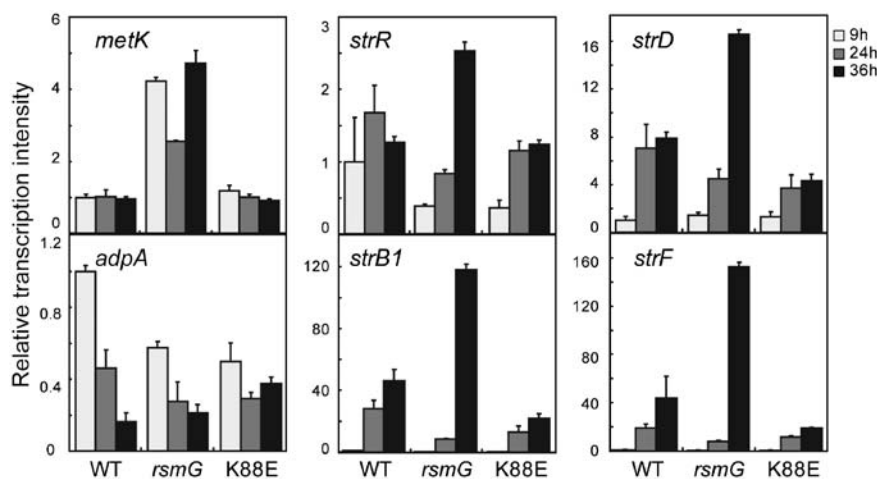


Figure 1 Transcriptional analysis of *adpA*, *metK*, *strR*, *strB1*, *strD* and *strF* by real-time quantitative PCR (qPCR). The RNAs were extracted from cells of wild-type (13189), *rsmG* (KO-1050) and *rpsL* K88E (KO-1052) mutant strains grown to early growth phase (9 h), mid growth phase (24 h) or late growth phase (36 h) in SPY medium. Total RNA preparation and real-time qPCR were performed as described in Materials and Methods. The error bars indicate the standard deviations of the means of three or more samples.

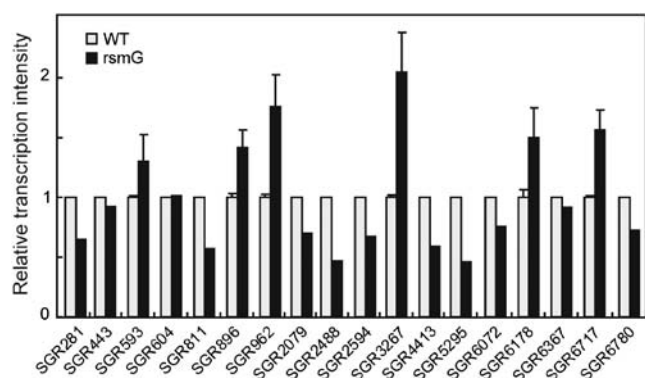


Figure 2 Transcriptional analysis of the genes involved in the secondary metabolite–biosynthetic gene clusters. The RNAs were extracted from cells of wild-type (13189) and *rsmG* (KO-1050) mutant strains grown to late growth phase (36 h). Total RNA preparation and real-time quantitative PCR was performed as described in Materials and Methods. Error bars indicate the standard deviations of the means of three or more samples.

employed in the present study, it is possible that the expression of pathway-specific regulatory genes is governed by higher-order regulatory proteins and expression of such higher-order regulatory proteins may be significantly affected under conditions associated with enhanced *metK* expression in mutants. The present method, together with other methods reported recently,^{6,7,17–20} may be useful for activating silent genes, eventually leading to the discovery of novel antibacterial agents.

ACKNOWLEDGEMENTS

This work was supported by grants to KO (Effective Promotion of Joint Research of Special Coordination Funds) from the Ministry of Education, Culture, Sports and Technology of the Japanese Government.

CONFLICT OF INTEREST

The authors declare no conflict of interest.

- Bentley, S. D. *et al.* Complete genome sequence of the model actinomycete *Streptomyces coelicolor* A3(2). *Nature* **417**, 141–147 (2002).
- Ikeda, H. *et al.* Complete genome sequence and comparative analysis of the industrial microorganism *Streptomyces avermitilis*. *Nat. Biotechnol.* **21**, 526–531 (2003).
- Ohnishi, Y. *et al.* Genome sequence of the streptomycin-producing microorganism *Streptomyces griseus* IFO 13350. *J. Bacteriol.* **190**, 4050–4060 (2008).
- Nishimura, K., Hosaka, T., Tokuyama, S., Okamoto, S. & Ochi, K. Mutations in *rsmG*, encoding a 16S rRNA methyltransferase, result in low-level streptomycin resistance and antibiotic overproduction in *Streptomyces coelicolor* A3(2). *J. Bacteriol.* **189**, 3876–3883 (2007).
- Tanaka, Y. *et al.* Antibiotic overproduction by *rpsL* and *rsmG* mutants of various actinomycetes. *Appl. Environ. Microbiol.* **75**, 4919–4922 (2009).
- Wang, G., Hosaka, T. & Ochi, K. Dramatic activation of antibiotic production in *Streptomyces coelicolor* by cumulative drug resistance mutations. *Appl. Environ. Microbiol.* **74**, 2834–2840 (2008).
- Ochi, K. From microbial differentiation to ribosome engineering. *Biosci. Biotechnol. Biochem.* **71**, 1373–1386 (2007).
- Tamehiro, N. *et al.* Innovative approach for improvement of an antibiotic-overproducing industrial strain of *Streptomyces albus*. *Appl. Environ. Microbiol.* **69**, 6412–6417 (2003).
- Beltrametti, F., Rossi, R., Selva, E. & Marinelli, F. Antibiotic production improvement in the rare actinomycete *Planobispora rosea* by selection of mutants resistant to the aminoglycosides streptomycin and gentamycin and to rifamycin. *J. Ind. Microbiol. Biotechnol.* **33**, 283–288 (2006).
- Ochi, K. Metabolic initiation of differentiation and secondary metabolism by *Streptomyces griseus*: significance of the stringent response (ppGpp) and GTP content in relation to A factor. *J. Bacteriol.* **169**, 3608–3616 (1987).
- Okamoto, S., Lezhava, A., Hosaka, T., Okamoto Hosoya, Y. & Ochi, K. Enhanced expression of S-adenosylmethionine synthetase causes overproduction of actinorhodin in *Streptomyces coelicolor* A3(2). *J. Bacteriol.* **185**, 601–609 (2003).
- Saito, N., Kurosawa, K., Xu, J., Okamoto, S. & Ochi, K. Effect of S-adenosylmethionine on antibiotic production in *Streptomyces griseus* and *Streptomyces griseoflavus*. *Actinomycetologica* **17**, 47–49 (2003).
- Shin, S. K., Xu, D., Kwon, H. J. & Suh, J. W. S-adenosylmethionine activates *adpA* transcription and promotes streptomycin biosynthesis in *Streptomyces griseus*. *FEMS Microbiol. Lett.* **259**, 53–59 (2006).
- Retzlaff, L. & Distler, J. The regulator of streptomycin gene expression, StrR, of *Streptomyces griseus* is a DNA binding activator protein with multiple recognition sites. *Mol. Microbiol.* **18**, 151–162 (1995).
- Ohnishi, Y., Yamazaki, H., Kato, J. Y., Tomono, A. & Horinouchi, S. AdpA, a central transcriptional regulator in the A-factor regulatory cascade that leads to morphological development and secondary metabolism in *Streptomyces griseus*. *Biosci. Biotechnol. Biochem.* **69**, 431–439 (2005).
- Hosaka, T. *et al.* Antibacterial discovery in actinomycetes strains with mutations in RNA polymerase or ribosomal protein S12. *Nat. Biotechnol.* **27**, 462–464 (2009).
- Rigali, S. *et al.* Feast or famine: the global regulator DasR links nutrient stress to antibiotic production by *Streptomyces*. *EMBO Rep.* **9**, 670–675 (2008).
- Carata, E. *et al.* Phenotypes and gene expression profiles of *Saccharopolyspora erythraea* rifampicin-resistant (*rif*) mutants affected in erythromycin production. *Microb. Cell. Fact.* **8**, 18 (2009).
- Tala, A. *et al.* Activation of dormant bacterial genes by *Nonomuraea* sp. strain ATCC 39727 mutant-type RNA polymerase. *J. Bacteriol.* **191**, 805–814 (2009).

1 Newman, D. J. & Cragg, G. M. Natural products as sources of new drugs over the last 25 years. *J. Nat. Prod.* **70**, 461–477 (2007).

ORIGINAL ARTICLE

In vitro activity of various combinations of antimicrobials against carbapenem-resistant *Acinetobacter* species in Singapore

Tze-Peng Lim^{1,4}, Thean-Yen Tan², Winnie Lee¹, Surantran Sasikala², Thuan-Tong Tan³, Li-Yang Hsu⁴ and Andrea L Kwa¹

Outbreaks of carbapenem-resistant *Acinetobacter* species have emerged, especially in Singapore. Combination therapy may be the only viable option until new antibiotics are available. The objective of this study was to identify potential antimicrobial combinations against carbapenem-resistant *Acinetobacter baumannii* and *Acinetobacter* species in Singapore. From an ongoing surveillance program, two isolates of *A. baumannii* and an isolate of *Acinetobacter* species that were multidrug resistant were selected on the basis of their unique resistance mechanisms. The two *A. baumannii* isolates carried the carbapenemase *bla*_{OXA-23}-like gene and the *Acinetobacter* species carried a metallo- β -lactamase IMP-4 gene. Time-kill studies were conducted with approximately 10^5 CFU ml⁻¹ at baseline with 0.5 times minimum inhibitory concentrations (MICs) of polymyxin B and tigecycline, and at a maximally achievable clinical concentration of meropenem (64 μ g ml⁻¹) and rifampicin (2 μ g ml⁻¹), alone and in combinations. The MICs (μ g ml⁻¹) of *Acinetobacter* species A105, *A. baumannii* AB112 and *A. baumannii* AB8879 to polymyxin B/tigecycline/rifampicin/meropenem were found to be 1/0.5/4/64, 1/4/4/32 and 2/2/2/64, respectively. In time-kill studies, enhanced combined killing effects were observed in the tigecycline–rifampicin combination; the tigecycline–rifampicin and rifampicin–polymyxin B combination; and the rifampicin–polymyxin B combination for *Acinetobacter* species A105, *A. baumannii* AB112 and *A. baumannii* AB8879, respectively, with > 5 log kill at 24 h suggesting synergism, with no regrowth observed at 72 h. These findings demonstrate that *in vitro* synergy of antibiotic combinations in carbapenem-resistant *Acinetobacter* species may be strain dependent. It may guide us in choosing a preemptive therapy for carbapenem-resistant *Acinetobacter* species infections and warrants further investigations.

The Journal of Antibiotics (2009) 62, 675–679; doi:10.1038/ja.2009.99; published online 30 October 2009

Keywords: *Acinetobacter* species; carbapenem resistance; combination therapy

INTRODUCTION

Microbial resistance to antimicrobial agents is a serious problem that renders development of new treatment options an urgent priority. The alarming spread of antimicrobial resistance is threatening our therapeutic armamentarium.^{1,2} It is likely that effective treatment may not be available for many common infections in the near future, and we are at risk of returning to the preantibiotic era in the event of an outbreak.³ Broad-spectrum antimicrobial resistance in Gram-negative bacteria (for example, *Acinetobacter baumannii* and *Pseudomonas aeruginosa*) is especially worrisome and has worldwide implications.

Acinetobacter baumannii is an emerging Gram-negative bacillus associated with serious nosocomial infections; it is also associated with multiple mechanisms of resistance to various antimicrobial agents.⁴ Carbapenem resistance is now observed worldwide in *A. baumannii*, leading to limited therapeutic options.⁵ Several

mechanisms are responsible for resistance to carbapenem in *A. baumannii*. These are reduced outer membrane permeability, penicillin-binding protein changes and carbapenemases.⁶ Treatment of multidrug-resistant *Acinetobacter* infections often represents a challenge to clinicians,^{7–9} and there are very few agents in the advanced stage of development designed to target multidrug-resistant Gram-negative bacteria. As a result, a task force from the Infectious Diseases Society of America (IDSA) has recently identified *A. baumannii* as a 'particularly problematic pathogen,' for which there is an urgent need for new and effective treatment strategies.¹⁰

Most of our carbapenem-resistant isolates were sensitive only to polymyxin/colistin. However, colistin treatment failures as a result of colistin resistance were reported. Furthermore, heterogeneous colistin resistance among multidrug-resistant isolates is now recognized in this region.^{11,12} Hence, the need for an effective combination antimicrobial

¹Department of Pharmacy, Singapore General Hospital, Singapore; ²Department of Microbiology, Changi General Hospital, Singapore; ³Singapore General Hospital, National University of Singapore, Singapore and ⁴Department of Medicine, Yong Loo Lin School of Medicine, National University of Singapore, Singapore
Correspondence: Dr AL Kwa, Department of Pharmacy, Singapore General Hospital, Outram Road, Singapore 169609, Singapore.
E-mail: andrea.kwa.l.h@sgh.com.sg

Received 15 July 2009; revised 9 September 2009; accepted 18 September 2009; published online 30 October 2009

therapy is urgent. The objective of this study was to identify potential antimicrobial combinations against carbapenem-resistant *Acinetobacter* species in Singapore. It is hoped that we can provide a robust assessment of the activity of different antimicrobial agents when used in combination and assist clinicians to efficiently identify potential antimicrobial combinations for such difficult-to-treat infections.

MATERIALS AND METHODS

Species identification and OXA screening for test isolates

Two clinical multidrug-resistant strains of *A. baumannii* (*A. baumannii* AB112 and *A. baumannii* AB8879) and an *Acinetobacter* species (*Acinetobacter* sp. A105) from isolates collected for surveillance were used in the time-kill studies.¹³ The three isolates were screened for blaOXA-23-like, blaOXA-24-like, blaOXA-58-like and blaOXA-51-like genes using a multiplex PCR assay. Putative metallo- β -lactamase genes were amplified from the collection by using published degenerate primers.^{3,14–16} Selected PCR products were further sequenced to confirm their gene products. The ISAbal–OXA complex was detected with forward and reverse primers of the named genes, using the PCR protocol described by Turton *et al.*¹⁷ Another PCR-based multiplex assay was used to differentiate *A. baumannii* from other *Acinetobacter* species.¹⁸

Minimum inhibitory concentration testing

Minimum inhibitory concentrations (MICs) to a panel of antibiotics were obtained by commercial dehydrated microbroth dilution panels (Trek Diagnostics, East Grinstead, UK), performed according to the manufacturer's recommendations. MICs to rifampicin were obtained by a modified broth macrodilution method as described by the Clinical and Laboratory Standards Institute (CLSI).¹⁹ The studies were conducted in duplicate and were repeated at least once on a separate day.

Antimicrobial agents

Meropenem was obtained from Astra Zeneca (Dainippon Sumitomo Pharma Company Ltd, Oita, Japan). Polymyxin B and rifampicin were obtained from Sigma-Aldrich (St Louis, MO, USA). Tigecycline was obtained from Wyeth Pharmaceuticals (Pearl River, NY, USA). For polymyxin B and meropenem, a stock solution of each antimicrobial agent in sterile water was prepared, aliquoted and stored at -70°C . Tigecycline in solution was freshly prepared before each experiment. Before each susceptibility test, an aliquot of the drug was thawed and diluted to the desired concentrations with Cation-adjusted Mueller-Hinton broth (CAMHB). Conversely, rifampicin was dissolved in dimethyl sulfoxide and was then serially diluted to the desired final drug concentration. The final dimethyl sulfoxide concentration had no effect on *Acinetobacter* species and *A. baumannii* growth.

Time-kill studies

Time-kill studies were conducted with each antibiotic tested individually and in combination. For the purposes of our study, the maximum clinically achievable meropenem concentration of $64\ \mu\text{g ml}^{-1}$, which represented a free peak concentration arising from a 2 g, 3 h infusion, was simulated.²⁰ Rifampicin was tested at $2\ \mu\text{g ml}^{-1}$, which represented a free peak concentration arising from a 600 mg, daily oral dose to maximize the use of the drug.²¹ The concentrations of polymyxin B and tigecycline were tested at $0.5\times$ MIC to yield attainable experimental end points.

An overnight culture of the isolate was diluted into prewarmed CAMHB and incubated further at 35°C until log-phase growth was reached. The bacterial suspension was diluted with CAMHB according to absorbance at 630 nm; 15 ml of the suspension was transferred to 50-ml sterile conical flasks, each containing 1 ml of a drug dilution at 16 times the target concentration. The final concentration of the bacterial suspension in each flask was approximately 10^5 CFU ml⁻¹ (ranging from 1×10^5 to 5×10^5 CFU ml⁻¹).

Flasks were incubated in a shaker water bath at 35°C . Serial samples of broth were obtained from each flask at 0 h (baseline), and then at 2, 4, 8, 12 and 24 h after incubation. Samples were obtained in duplicate at each time period, except for the 24 h sample, which was tested in triplicate. Harvested broth samples (0.5 ml) were first centrifuged at $10\,000\times g$ for 15 min and then reconstituted with sterile normal saline to their original volumes in order to

minimize drug carryover. The total bacterial count for each sample was quantified by depositing serial 10-fold dilutions of broth samples onto Mueller Hinton agar plates using a spiral-plater (Interscience, St Nom La Breteche, France). Inoculated plates were incubated in a humidified incubator (35°C) for 18–24 h, bacterial colonies were visually counted and the original bacterial density from the original sample was calculated on the basis of the dilution factor. Synergy was defined as $\geq 2\ \log_{10}$ decrease in CFU ml⁻¹ for the antibiotic combination compared with its more active constituent, whereas additive effect was defined as $1\ \log_{10}$ decrease in CFU ml⁻¹ for the combination compared with its more active constituent at 24 h. Bactericidal effect was defined as $\geq 3\ \log_{10}$ decrease in CFU ml⁻¹, whereas antagonism was defined as the combination that yields colony counts higher than those detected with the more active single drug alone, at 24 h.

RESULTS

Susceptibility

All isolates were resistant to meropenem, imipenem, ampicillin/sulbactam, ciprofloxacin, gentamicin, piperacillin/tazobactam, cefepime and amikacin, but were susceptible to polymyxin B. There are no current CLSI susceptibility break points for rifampicin and tigecycline against *Acinetobacter* species. The MIC values are shown in Table 1.

Resistance mechanisms

Acinetobacter sp. A105 was positive for OXA-58 and IMP-type carbapenamases. *A. baumannii* AB112 and *A. baumannii* AB8879 were positive for OXA-23 and OXA-51 β -lactamases.²²

Time-kill studies

Figures 1a, 2a and 3a show the microbiological responses observed in single-drug time-kill studies. The number of CFU ml⁻¹ over time in response to the tested antibiotic(s) depicts the microbiological response. Polymyxin B was the only single antibiotic to demonstrate consistent bactericidal activity against all three test isolates. The second most active single antibiotic was meropenem, in two out of the three test strains. However, isolate regrowth was observed for all single antibiotics by 24 h.

For test strain *Acinetobacter* sp. A105, all antibiotic combinations showed rapid bactericidal activity within 2 h of initial inoculation. Bacterial counts fell below the lower threshold of detection within 2 h for tigecycline–rifampicin, meropenem–rifampicin and polymyxin B–meropenem antibiotic combinations, and tigecycline–rifampicin combination remained so throughout the 24-h testing period. These three combinations fulfilled the microbiological definition of

Table 1 Minimum inhibitory concentration ($\mu\text{g ml}^{-1}$) results against the two *A. baumannii* isolates and one *Acinetobacter* species

| Antimicrobial | <i>Acinetobacter</i> species A105 | <i>A. baumannii</i> AB112 | <i>A. baumannii</i> AB8879 |
|-------------------------|--------------------------------------|------------------------------|-------------------------------|
| Meropenem | 64 | 32 | 64 |
| Polymyxin B | 1 | 1 | 2 |
| Rifampicin | 4 | 4 | 2 |
| Tigecycline | 0.5 | 4 | 2 |
| Ampicillin-sulbactam | ≥ 128 | 16 | ≥ 128 |
| Ciprofloxacin | ≥ 16 | ≥ 16 | ≥ 16 |
| Gentamicin | ≥ 64 | ≥ 64 | ≥ 64 |
| Minocycline | ≤ 0.25 | 1 | 4 |
| Piperacillin-tazobactam | ≥ 256 | ≥ 256 | ≥ 256 |
| Cefepime | ≥ 64 | ≥ 64 | ≥ 64 |
| Amikacin | ≥ 128 | ≥ 128 | ≥ 128 |
| Ceftazidime | ≥ 128 | ≥ 128 | ≥ 128 |

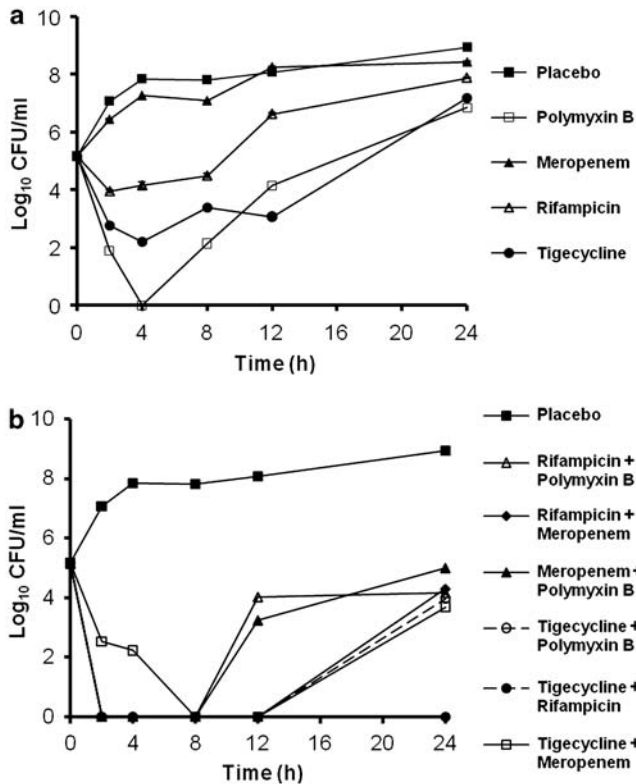


Figure 1 Microbiological responses observed in *Acinetobacter* sp. A105: single-drug system (a), two antimicrobial combinations (b). The number of CFU ml⁻¹ over time in response to the tested antibiotic(s) depicts microbiological responses. A considerable reduction (>99%) in bacterial burden was observed at 24 h for the tigecycline–rifampicin combination.

antibiotic synergy for all the tested time periods. Synergistic activity was intermittently present for the other antibiotic combinations during the 24-h testing time period, but bacterial regrowth was observed at the 24-h end point.

For test strain *A. baumannii* AB112, all antibiotic combinations other than meropenem–tigecycline rapidly achieved a >3 log₁₀ reduction in bacterial counts within the first 4 h of testing. Only the two most effective bactericidal combinations of tigecycline–rifampicin and rifampicin–polymyxin B showed synergistic activity at the end of the 24-h testing period. The least-effective combination for this isolate was meropenem–rifampicin, with only marginally increased activity compared with meropenem alone.

For test strain *A. baumannii* AB8879, all antibiotic combinations with polymyxin B achieved bactericidal and synergistic activity in the first 4 h of testing, but only the rifampicin–polymyxin B combination maintained synergistic activity at 24 h. The least-effective combination for this isolate was meropenem–rifampicin, with only marginal improvement for the combination when compared with the activity of meropenem alone.

DISCUSSION

Few treatment options remain for serious infections caused by multi-drug-resistant and carbapenem-resistant *A. baumannii*. Combination therapy (in view of potential synergistic activity) for multidrug-resistant Gram-negative bacteria may be more effective than monotherapy,²³ and may allow the use of antibiotics with marginal activity against the target organism.

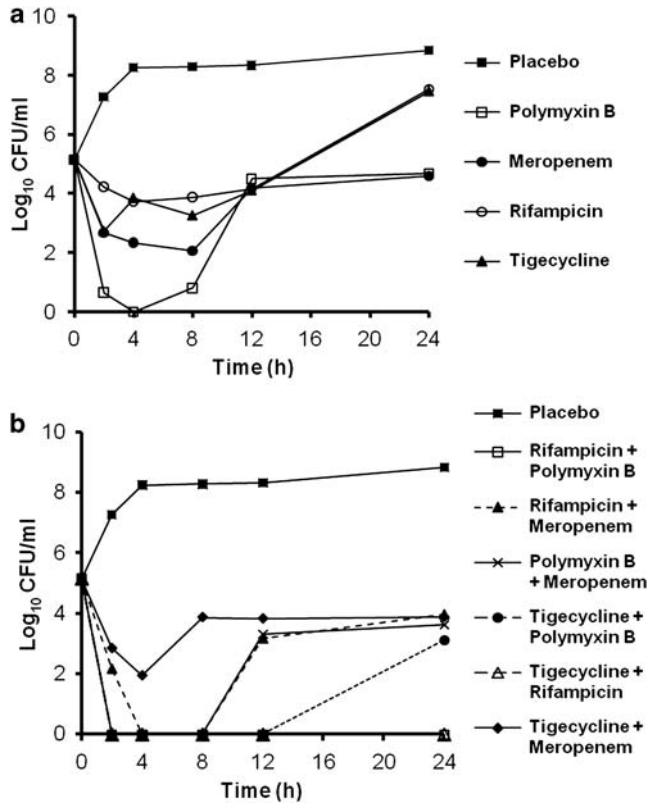


Figure 2 Microbiological responses observed in *A. baumannii* AB112: single-drug system (a), two antimicrobial combinations (b). The number of CFU ml⁻¹ over time in response to the tested antibiotic(s) depicts microbiological responses. A considerable reduction (>99%) in bacterial burden was observed at 24 h for tigecycline–rifampicin and rifampicin–polymyxin B combinations.

Carbapenem-hydrolyzing OXA enzymes are the most important cause of carbapenem resistance in *A. baumannii* worldwide. Although these oxacillinases are weaker hydrolyzers of carbapenems *in vitro* than are metallo-β-lactamase, the presence of the promoter sequence, ISAbal, can result in clinically significant resistance to carbapenems. *A. baumannii* carrying OXA-23 is now found in most parts of the world and are often responsible for many outbreaks.⁶ Previous investigations revealed that the most common carbapenemase gene responsible in carbapenem-resistant isolates in our institutions was bla_{OXA-23} and not bla_{OXA-51}.^{22,24} The two tested *A. baumannii* strains in this study carried both the bla_{OXA-23}-like and bla_{OXA-51}-like carbapenemase gene, and both isolates possessed ISAbal upstream of the bla_{OXA-23} gene (results not shown). *A. sp.* A 105 (with bla_{OXA-58}-like and bla_{IMP-4}-like genes) was selected for the presence of IMP-4 metallo-β-lactamase, as metallo-β-lactamase genes are increasingly being reported.^{25,26} It is likely that as multidrug-resistant isolates become more common, we will need to define and target in our selection of antibiotics a combination based on a library of data such as those presented here on various combinations that are useful in strains with different resistance determinants.

In this study, clinically achievable concentrations of the tested antibiotics were used. For example, previous studies have shown that extending the infusion duration of meropenem from 30 min to 3 h increases the probability of bactericidal target attainment.^{20,27} Despite this, synergistic activity between meropenem and other antibiotic combinations was only observed in one out of three strains.

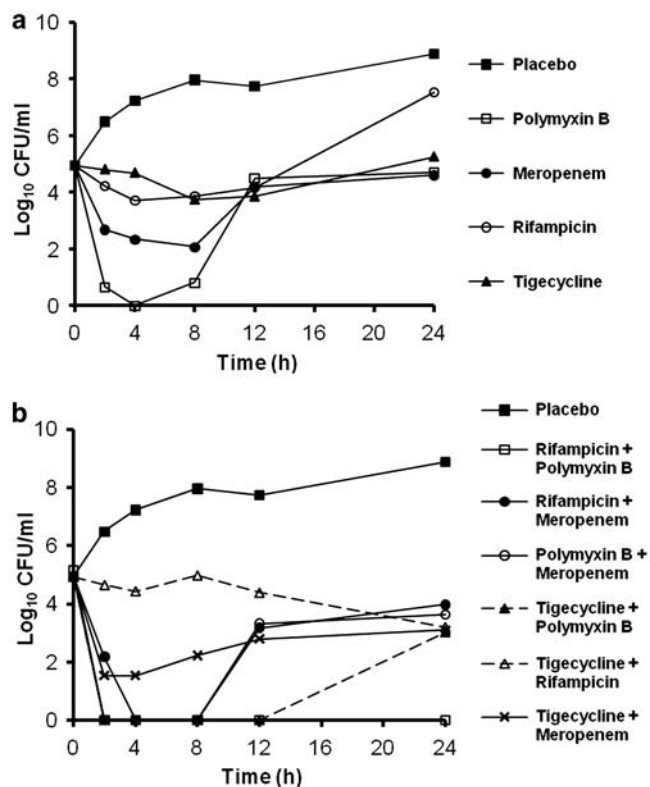


Figure 3 Microbiological responses observed in *A. baumannii* AB8879: single-drug system (a), two antimicrobial combinations (b). The number of CFU ml⁻¹ over time in response to the tested antibiotic(s) depicts microbiological responses. A considerable reduction (>99%) in bacterial burden was observed at 24 h for the rifampicin–polymyxin B combination.

There was no antibiotic combination that reliably demonstrated synergistic activity against all isolates, although rifampicin–polymyxin and tigecycline–rifampicin combinations were bactericidal and synergistic for two of the three isolates, respectively.

Time-kill studies are labor intensive for routine use and will not provide results in a clinically relevant time frame. However, screening for useful antibiotic combinations in a local population of antibiotic-resistant *Acinetobacter* species with well-defined resistance mechanisms may allow the empirical selection of combination antibiotic therapy, where clinically indicated. Clearly, more quantitative information regarding such synergistic and antagonistic relationships is both valuable and necessary for evaluating the effectiveness of various antimicrobial agent combinations. Other potential models that have been used to determine synergistic activity include an *in vitro* pharmacodynamic infection model in which human-like (fluctuating) drug concentration profiles are simulated, and checker-board titrations, Etest and *in vivo* animal testing are carried out. However, it is worth noting that the correlation between each model and actual clinical outcomes remains to be clearly elucidated. For example, studies have found conflicting results for the same antimicrobial combinations comparing animal *in vivo* studies with a follow-up clinical pilot study.^{28,29}

In this study, we performed time-kill analysis only for three different *Acinetobacter* species with similar MICs against various antimicrobial agents. The differences in the mechanisms of resistance seemed to result in different effective antibiotic combinations. Hence, one effective antimicrobial combination for one isolate cannot be assumed to be effective for another isolate of the same species. Either

combination testings are carried out for every carbapenem-resistant isolates or lengthy experiments are conducted to determine phenotypic response to different combinations of resistance genes. Neither of the two methods mentioned are technically easy nor practically feasible, but may prove necessary under pressure of the spread of such bacteria.

In *A. baumannii*, the AdeABC efflux pump, a member of the resistance-nodulation-cell-division family, has been well characterized. Aminoglycosides, tetracyclines, erythromycin, chloramphenicol, trimethoprim, fluoroquinolones, some β -lactams and also recently tigecycline were found to be substrates for this pump. Drugs, as substrates for the AdeABC pump, can increase the expression of AdeABC genes, leading to multidrug resistance.³⁰ Although AdeABC multidrug efflux pumps are intrinsic to *A. baumannii*, and the AdeDE and AdeXY pumps are found predominantly in *Acinetobacter* genospecies 3,³¹ we did not have any additional data to confirm the overexpression of these efflux genes, which can contribute to multidrug resistance in our isolates. Hence, with the knowledge of different carbapenemase genes (which confer expression of different types of carbapenemases) in our isolates, we can only postulate why carbapenem as a part of combination antibiotics does not work in synergism, whereas combinations using non- β -lactams work better against our isolates.

CONCLUSION

Various antibiotic combinations against carbapenem-resistant *Acinetobacter* species were tested and reported with varied efficacies. Thus, it is clear that antibacterial effects can differ according to resistance mechanisms.³²

We selected strains that had mechanisms common in our settings, according to our surveillance program. For example, *A. baumannii* AB8879 was an outbreak strain in our burns unit. We propose that combination testings be made a part of molecular mechanisms surveillance programs to be effective. This study demonstrated the utility of synergy testing in a selection of multidrug-resistant *Acinetobacter* species to determine the activity of specific antibiotic combinations. This may facilitate the optimal use of antimicrobial agents by guiding a rational selection of future antibiotic combinations for therapy.

CONFLICT OF INTEREST

The authors declare no conflict of interest.

ACKNOWLEDGEMENTS

This study was supported in part by National Medical Research Council and SingHealth Foundation.

- Gold, H. S. & Moellering, R. C. Jr. Antimicrobial-drug resistance. *N. Engl. J. Med.* **335**, 1445–1453 (1996).
- Neu, H. C. The crisis in antibiotic resistance. *Science* **257**, 1064–1073 (1992).
- Landman, D. *et al.* Citywide clonal outbreak of multiresistant *Acinetobacter baumannii* and *Pseudomonas aeruginosa* in Brooklyn, NY: the preantibiotic era has returned. *Arch. Intern. Med.* **162**, 1515–1520 (2002).
- Bonomo, R. A. & Szabo, D. Mechanisms of multidrug resistance in *Acinetobacter* species and *Pseudomonas aeruginosa*. *Clin. Infect. Dis.* **43**(Suppl 2), S49–S56 (2006).
- Peleg, A. Y., Seifert, H. & Paterson, D. L. *Acinetobacter baumannii*: emergence of a successful pathogen. *Clin. Microbiol. Rev.* **21**, 538–582 (2008).
- Poirel, L. & Nordmann, P. Carbapenem resistance in *Acinetobacter baumannii*: mechanisms and epidemiology. *Clin. Microbiol. Infect.* **12**, 826–836 (2006).
- Maragakis, L. L. & Perl, T. M. *Acinetobacter baumannii*: epidemiology, antimicrobial resistance, and treatment options. *Clin. Infect. Dis.* **46**, 1254–1263 (2008).

- 8 Levin, A. S. *et al.* Intravenous colistin as therapy for nosocomial infections caused by multidrug-resistant *Pseudomonas aeruginosa* and *Acinetobacter baumannii*. *Clin. Infect. Dis.* **28**, 1008–1011 (1999).
- 9 Centers for Disease Control and Prevention (CDC). *Acinetobacter baumannii* infections among patients at military medical facilities treating injured U.S. service members, 2002–2004. *MMWR Morb. Mortal. Wkly. Rep.* **53**, 1063–1066 (2004).
- 10 Talbot, G. H. *et al.* Bad bugs need drugs: an update on the development pipeline from the Antimicrobial Availability Task Force of the Infectious Diseases Society of America. *Clin. Infect. Dis.* **42**, 657–668 (2006).
- 11 Li, J. *et al.* Heteroresistance to colistin in multidrug-resistant *Acinetobacter baumannii*. *Antimicrob. Agents. Chemother.* **50**, 2946–2950 (2006).
- 12 Yau, W. *et al.* Colistin hetero-resistance in multidrug-resistant *Acinetobacter baumannii* clinical isolates from the Western Pacific region in the SENTRY antimicrobial surveillance programme. *J. Infect.* **58**, 138–144 (2009).
- 13 Hsu, L. Y. *et al.* Antimicrobial drug resistance in Singapore hospitals. *Emerg. Infect. Dis.* **13**, 1944–1947 (2007).
- 14 Woodford, N. *et al.* Multiplex PCR for genes encoding prevalent OXA carbapenemases in *Acinetobacter* spp. *Int. J. Antimicrob. Agents* **27**, 351–353 (2006).
- 15 Brown, S., Young, H. K. & Amyes, S. G. Characterisation of OXA-51, a novel class D carbapenemase found in genetically unrelated clinical strains of *Acinetobacter baumannii* from Argentina. *Clin. Microbiol. Infect.* **11**, 15–23 (2005).
- 16 Nordmann, P. & Poirel, L. Emerging carbapenemases in Gram-negative aerobes. *Clin. Microbiol. Infect.* **8**, 321–331 (2002).
- 17 Turton, J. F. *et al.* The role of ISAba1 in expression of OXA carbapenemase genes in *Acinetobacter baumannii*. *FEMS Microbiol. Lett.* **258**, 72–77 (2006).
- 18 Chen, T. L. *et al.* Comparison of one-tube multiplex PCR, automated ribotyping and intergenic spacer (ITS) sequencing for rapid identification of *Acinetobacter baumannii*. *Clin. Microbiol. Infect.* **13**, 801–806 (2007).
- 19 Clinical and Laboratory Standards Institute. *Performance Standards for Antimicrobial Testing: Seventeenth Informational Supplement M100-S17* (CLSI: Wayne, Pennsylvania, USA, 2007).
- 20 Jaruratanasirikul, S., Sriwiriyan, S. & Punyo, J. Comparison of the pharmacodynamics of meropenem in patients with ventilator-associated pneumonia following administration by 3-h infusion or bolus injection. *Antimicrob. Agents. Chemother.* **49**, 1337–1339 (2005).
- 21 Gumbo, T. *et al.* Concentration-dependent mycobacterium tuberculosis killing and prevention of resistance by rifampin. *Antimicrob. Agents. Chemother.* **51**, 3781–3788 (2007).
- 22 Tan, T. T., Widjaya, L., Hsu, L. Y. & Koh, T. H. Characterization of resistance genes among *Acinetobacter* spp. isolates in Singaporean Hospitals. 18th European Congress of Clinical Microbiology and Infectious Diseases. Barcelona Spain, 2008.
- 23 Urban, C., Segal-Maurer, S. & Rahal, J. J. Considerations in control and treatment of nosocomial infections due to multidrug-resistant *Acinetobacter baumannii*. *Clin. Infect. Dis.* **36**, 1268–1274 (2003).
- 24 Koh, T. H., Sng, L. H., Wang, G. C., Hsu, L. Y. & Zhao, Y. IMP-4 and OXA beta-lactamases in *Acinetobacter baumannii* from Singapore. *J. Antimicrob. Chemother.* **59**, 627–632 (2007).
- 25 Tognim, M. C., Gales, A. C., Penteado, A. P., Silbert, S. & Sader, H. S. Dissemination of IMP-1 metallo-beta-lactamase-producing *Acinetobacter* species in a Brazilian teaching hospital. *Infect. Control. Hosp. Epidemiol.* **27**, 742–747 (2006).
- 26 Wang, H. *et al.* Molecular epidemiology of clinical isolates of carbapenem-resistant *Acinetobacter* spp. from Chinese hospitals. *Antimicrob. Agents. Chemother.* **51**, 4022–4028 (2007).
- 27 Li, C., Kuti, J. L., Nightingale, C. H. & Nicolau, D. P. Population pharmacokinetic analysis and dosing regimen optimization of meropenem in adult patients. *J. Clin. Pharmacol.* **46**, 1171–1178 (2006).
- 28 Montero, A. *et al.* Antibiotic combinations for serious infections caused by carbapenem-resistant *Acinetobacter baumannii* in a mouse pneumonia model. *J. Antimicrob. Chemother.* **54**, 1085–1091 (2004).
- 29 Saballs, M. *et al.* Rifampicin/imipenem combination in the treatment of carbapenem-resistant *Acinetobacter baumannii* infections. *J. Antimicrob. Chemother.* **58**, 697–700 (2006).
- 30 Wieczorek, P. *et al.* Multidrug resistant *Acinetobacter baumannii*—the role of AdeABC (RND family) efflux pump in resistance to antibiotics. *Folia. Histochem. Cytobiol.* **46**, 257–267 (2008).
- 31 Koh, T. H., Sng, L. H., Wang, G. C., Hsu, L. Y. & Zhao, Y. Carbapenemase and efflux pump genes in *Acinetobacter calcoaceticus*–*Acinetobacter baumannii* complex strains from Singapore. *J. Antimicrob. Chemother.* **60**, 1173–1174 (2007).
- 32 Song, J. Y. *et al.* *In vitro* activities of carbapenem/sulbactam combination, colistin, colistin/rifampicin combination and tigecycline against carbapenem-resistant *Acinetobacter baumannii*. *J. Antimicrob. Chemother.* **60**, 317–322 (2007).

ORIGINAL ARTICLE

Solid-phase synthesis and biological activity of malformin C and its derivatives

Yasuhiro Kojima¹, Toshiaki Sunazuka¹, Kenichiro Nagai¹, Tomoyasu Hirose¹, Miyuki Namatame², Aki Ishiyama², Kazuhiko Otoguro² and Satoshi Ōmura¹

We accomplished the solid-phase total synthesis of malformin C, which is adaptable for the easy preparation of various derivatives. A solid-phase total synthesis of malformin C was achieved by on-resin macrolactamization and disulfide bond formation, with concurrent cleavage from the resin. Antimalarial and antitrypanosomal activities were examined, which helped elucidate partial structure–activity relationships. Results indicate that the disulfide bond is essential and branched amino acids are also crucial components if the compound is to exhibit potent antimalarial and antitrypanosomal properties.

The Journal of Antibiotics (2009) 62, 681–686; doi:10.1038/ja.2009.100; published online 30 October 2009

Keywords: antimalarial activity; antitrypanosomal activity; cyclic pentapeptide; disulfide bond; malformins; solid-phase synthesis

INTRODUCTION

Malformins, produced from *Aspergillus niger*, are a group of cyclic pentapeptides with a disulfide bond formed from two cysteine thiols. The compounds express various biological activities, such as inducing root curvatures and malformations in plants,^{1–4} antibacterial activity against Gram-positive and Gram-negative bacteria,^{5–7} enhanced fibrinolytic activity⁸ and inhibitory activity of the G₂ checkpoint.⁹ Owing to their unique structures and diverse biological profiles, several processes for the synthesis of malformins have been examined.^{10–13} More recently, our research group has found that malformin C^{14,15} exhibits bioactivity against malarial parasites and trypanosomes, with IC₅₀ values of 70 and 1.6 ng ml⁻¹, respectively.

Malaria, caused by *Plasmodium* species, occurs in more than 90 countries worldwide, and it was estimated that there were over 247 million clinical cases of malaria and 881 000 malaria-caused deaths in 2006.¹⁶ Many antimalarial agents have been developed, but widespread drug resistance has rendered many of them ineffective, with the current exception of artemisinin and its derivatives. More recently, resistance to members of the antimalarial artemisinin class of drugs is being reported from Southeast Asia, especially from the Cambodia region, which is causing significant alarm and concern for the future of this class of drugs (<http://sciencenow.sciencemag.org/cgi/content/full/2009/729/3>). Therefore, development of new, safe and potent antimalarial drugs, with new modes of action and structural features, is urgently required.

Human African trypanosomiasis (HAT), also known as sleeping sickness, is recognized as one of Africa's most neglected diseases and is a significant cause of mortality and morbidity in sub-Saharan Africa. The World Health Organization (WHO) estimated that, in 2000,

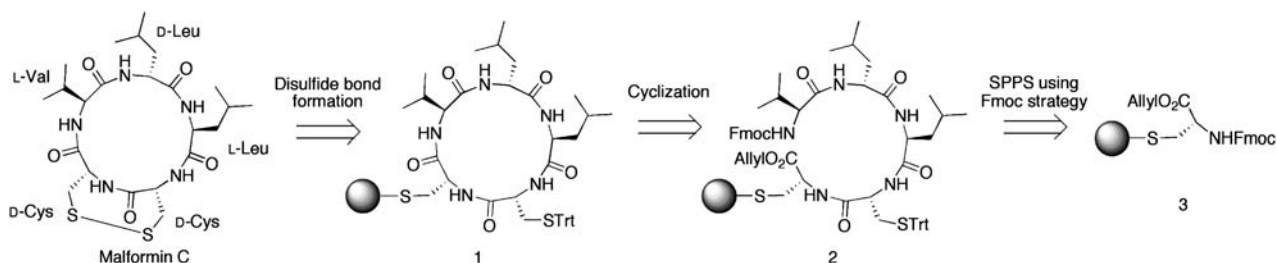
approximately 300 000 Africans were affected by the disease, a figure much larger than the 27 000 cases diagnosed and treated that year. Owing to increased surveillance activities in the past 7 years, recent estimates indicate that there are now approximately 50 000–70 000 cases of HAT annually. In 2007, the number of new cases reported had actually decreased to 10 769 (http://www.who.int/trypanosomiasis_african/disease/en/index.html). Currently, only four drugs, including pentamidine, are registered for the treatment of HAT. All four are unsatisfactory, as they cannot be administered orally and are hampered by severe toxicity and increasing resistance of the parasites.

Consequently, there is a pressing need for new antitrypanosomal drugs that have new structures and mechanisms of action and are both safe and effective. The global need for such antimalarial and antitrypanosomal drugs led us to develop a new methodology for the preparation of malformin analogs to elucidate structure–activity relationships. We had already completed a total synthesis of malformin C in liquid-phase sequences,¹³ but sought to discover a solid-phase synthesis that would provide the advantages of speeding up reactions, allow the use of a large amount of reagent and allow all remaining reagents and side products to be removed easily by washing with solvent, as well as create the possibility of rapidly synthesizing analogs with different amino acids. In this study, we report the total synthesis of malformin C using a solid-phase route, easily adaptable for analog preparation and for evaluation of the antimalarial and antitrypanosomal activities of malformin C and various analogs.

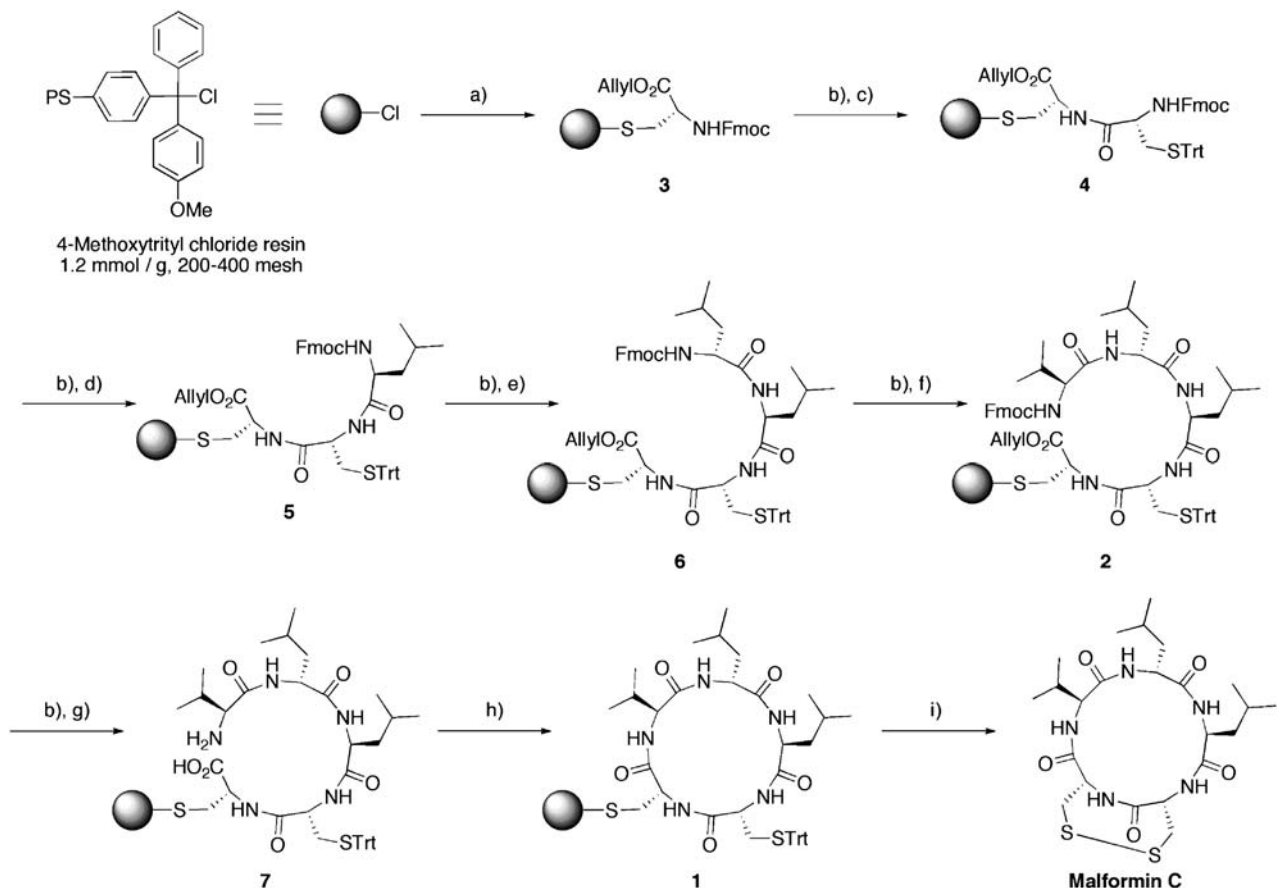
RESULT AND DISCUSSION

Our retrosynthetic analysis of malformin C is shown in Scheme 1. We focused on the development of a solid-phase strategy that would

¹Kitasato Institute, Kitasato Institute for Life Science and Graduate School of Infection Control Sciences, Kitasato University, Tokyo, Japan and ²Research Center for Tropical Diseases, Kitasato Institute for Life Science, Kitasato University, Tokyo, Japan
Correspondence: Professor T Sunazuka or Professor S Ōmura, Kitasato Institute for Life Science and Graduate School of Infection Control Sciences, Kitasato University, 5-9-1 Shirokane, Minato-ku, Tokyo, 108-8641, Japan. E-mails: sunazuka@lisci.kitasato-u.ac.jp or omuras@insti.kitasato-u.ac.jp
Received 13 July 2009; revised 23 September 2009; accepted 28 September 2009; published online 30 October 2009



Scheme 1 Retrosynthetic analysis of malformin C with resin.



Scheme 2 Solid-phase synthesis of malformin C; (a) Fmoc-D-Cys-OAllyl, *i*-Pr₂NEt, CH₂Cl₂; (b) 20% piperidine/DMF; (c) Fmoc-D-Cys(S-Trt)-OH, PyBOP, *i*-Pr₂NEt, DMF; (d) Fmoc-L-Leu-OH, PyBOP, *i*-Pr₂NEt, DMF; (e) Fmoc-D-Leu-OH, PyBOP, *i*-Pr₂NEt, DMF; (f) Fmoc-L-Val-OH, PyBOP, *i*-Pr₂NEt, DMF; (g) Pd(PPh₃)₄, 5,5-dimethyl-1,3-hexanedione, THF; (h) HBTU, HOBT, *i*-Pr₂NEt, 20% DMF/CH₂Cl₂; (i) I₂, DMF, 15% overall yield of malformin C from **3**.

enable the preparation of various malformin analogs. Malformin C could be synthesized through oxidative disulfide formation of the cyclic peptide (**1**) in which one of two Cys residues is protected with a trityl (Trt) group and the other is bound on a Trt linker. Compound **1** could be prepared by selective deprotection and subsequent on-resin cyclization of the pentapeptide (**2**). We chose the allyl ester for C-terminal protection of the peptide chain because it can be tolerant under 9-fluorenylmethyloxycarbonyl (Fmoc) and *tert*-butoxycarbonyl deprotection conditions and removed by Pd-catalyzed chemistry without interference with S-Trt functionalities. The amide linkage between D-cysteine and L-valine residues was chosen for on-resin macrolactamization. The peptide chain could be elongated by the Fmoc solid-phase peptide synthesis method.

We used 4-methoxytrityl chloride linker, which is useful for immobilization of thiol groups.^{17,18} As shown in Scheme 2, Fmoc-D-Cys-OAllyl was loaded through the thiol group onto the 4-methoxytrityl chloride resin to yield the cysteine derivative (**3**). The loading yield was estimated to be quantitative by acid cleavage from the resin with 50% trifluoroacetic acid (TFA)/CH₂Cl₂. The four amino acid derivatives, Fmoc-D-Cys(S-Trt)-OH, Fmoc-L-Leu-OH, Fmoc-D-Leu-OH and Fmoc-L-Val-OH, were sequentially introduced, using 20% piperidine/*N,N'*-dimethylformamide (DMF) for deprotection and benzotriazole-*yl*-oxy-tris-pyrrolidino-phosphonium hexafluorophosphate (PyBOP) as a coupling reagent, to yield **2**. After deprotection of the Fmoc group and Allyl group of **2**, cyclization of the linear peptide (**7**) was performed, with

O-benzotriazole-1-yl-*N,N,N'*-tetramethyluroniumhexafluorophosphate (HBTU) and 1-hydroxybenzotriazole (HOBT) as coupling reagents, to yield **1**. Other coupling reagents such as diphenylphosphoryl azide and *N,N'*-diisopropylcarbodiimide did not result in the cyclic compound. Finally, oxidative disulfide formation with iodine in DMF,¹⁹ and then release from the resin by treatment with 50% TFA/CH₂Cl₂ and triisopropylsilane,²⁰ resulted in malformin C in 15% overall yield for 13 steps after silica gel chromatography. The melting point, [α]_D, IR, ¹H and ¹³C NMR and high-resolution mass spectra were found to be identical to those of the natural product. It is assumed that the relatively low yield is because of the poor solubility of malformin C in organic solvents. Although **1** was obtained in almost quantitative yield, the crude yield of malformin C was moderate. Thus, in the final step, oxidative conditions might cause undesired intermolecular interactions with the solid support, resulting in a relatively low yield. Oxidation by the liquid phase of the dithiol compound obtained from resin treatment with 50% TFA/CH₂Cl₂ and triisopropylsilane was not productive; thus, malformin C was synthesized using the above-mentioned method in spite of the low yield.

To demonstrate the flexibility of this methodology, malformins A1,^{21–23} we also synthesized A2²⁴ and B2^{25–27} (in 6, 13 and 7% yield, respectively). Spectroscopic data of synthetic malformins were identical to references. Synthesis of unnatural malformin (**8**), which introduced less hindered L-Ala instead of the L-Leu of malformin C, was performed to examine the effect of the L-Leu residue on antimalarial and antitrypanosomal activities. Because the bioactivity of malformins A1 and C is significantly different, because of the impact of the L-Leu residue on the inhibitory activity on G₂ checkpoint,⁹ sulfide (**9**) and thiol (**10**) were synthesized to investigate the importance of the disulfide bond in antiparasitic activity (Table 1). The synthetic compounds were purified by silica gel column chromatography, characterized by HPLC and ESI-MS, and subjected to assay for antimalarial and antitrypanosomal activities.

Assay results are summarized in Table 1. Artemether,²⁸ an effective antimalarial reagent, showed activity with an IC₅₀ value of 2.3 ng ml⁻¹, and pentamidine,²⁹ an effective antitrypanosomal reagent, showed activity with an IC₅₀ value of 1.58 ng ml⁻¹. Malformin C has antitrypanosomal activity with an IC₅₀ value of 1.6 ng ml⁻¹ equal to that of pentamidine, and antimalarial activity with an IC₅₀ value of 70 ng ml⁻¹, a little lower than that of artemether. However, **9** and **10** exhibited reduced activity against both parasites. Thus, the disulfide bond of malformin C seems to be necessary for antiparasitic activity. To compare antitrypanosomal and antimalarial activities, we calculated the selectivity index (SI: antitrypanosomal activity (IC₅₀ for the GUTat 3.1 strain)/antimalarial activity (IC₅₀ for the K1 strain)) (Table 1). What is interesting is that the SIs of malformin A1, A2 and **8** were reversed with malformin C. Therefore, both activities of malformins A1, A2 and **8**, incorporating amino acid residues instead of the L-Leu of malformin C, were different by substituent, suggesting that L-Leu residues were important for the activity. A comparison of **8** with others indicates that a degree of the bulk at the position of L-Leu of malformin C is necessary for antimalarial activity, whereas malformin B2 showed the strongest activity against *Plasmodium falciparum*. These correlations suggest that the replacement of the D-Leu moiety of malformin C to a smaller amino acid residue may express better potency for antimalarial activity. Considering the bioactivity results of malformin C and B2, it would seem that L-Leu is necessary for antitrypanosomal activity.

In conclusion, we demonstrated a solid-phase synthesis of malformin C and used this to produce a variety of derivative compounds. As the result of the synthesis of these compounds, we obtained substantial information with respect to the structure–activity

relationships of antimalarial and antitrypanosomal activities. We also discovered that malformin B2 exhibits more potent antimalarial activity than does malformin C.

EXPERIMENTAL SECTION

General

Reagents of the highest commercial quality were purchased and were used without further purification, unless otherwise specified. Reactions were monitored by TLC using Merck F60₂₅₄ silica gel plates (Merck, Tokyo, Japan). Spots were visualized with UV light (254 nm) and stained with phosphomolybdic acid. Silica gel chromatography was performed on a Merck Kieselgel 60 (Art. 1.09385).

FT-IR spectra were recorded in KBr pellets on a Horiba FT-210 spectrometer (Horiba, Kyoto, Japan). Mass spectra were recorded on a JEOL JMS-700V (Jeol, Tokyo, Japan) or JMS-T100LP Mass Spectrometer (Jeol). ¹H NMR spectra were recorded at 270, 300 or 400 MHz and ¹³C NMR spectra were recorded at 67.5, 75 or 100 MHz on JEOL JNM-EX270 (270 MHz), MERCURY-300 (300 MHz), Varian XL-400 (400 MHz) or Varian UNITY-400 (400 MHz) spectrometers (Varian, Tokyo, Japan) in CDCl₃ or DMSO-*d*₆. ¹H NMR spectral data are reported as follows: chemical shifts relative to CHCl₃ (7.26 p.p.m.) or dimethyl sulfoxide (DMSO) (2.49 p.p.m.), integration, multiplicity (s=singlet, d=doublet, t=triplet, q=quartet, m=multiplet, br=broad) and coupling constant. Optical rotation was obtained with a JASCO DIP-370 polarimeter (Jasco, Tokyo, Japan). ¹³C NMR spectral data are reported in p.p.m. relative to CHCl₃ (77.0 p.p.m.) or DMSO (39.7 p.p.m.). Melting points were measured with a Yanaco micro melting point apparatus (Yanaco, Kyoto, Japan). HPLC analysis was conducted on a Hitachi ELITE LaChrom (Hitachi, Tokyo, Japan) (Column; Senshu Pak PEGASIL ODS 4.6φ×250 mm with a flow rate of 1.0 ml min⁻¹. Mobile phase was 0.05% TFA in 45% MeCN/H₂O).

Allyl *N*-9-fluorenylmethoxycarbonyl-D-cysteinate

To a solution of Fmoc-D-Cys(S-Trt)-OAllyl (5.35 g, 8.56 mmol) in CH₂Cl₂ (85.6 ml) was added triethylsilane (4.1 ml, 25.7 mmol) and dropwise TFA (1.98 ml, 25.7 mmol) at room temperature (RT) under N₂ atmosphere. After stirring at RT for 2 h, the reaction mixture was concentrated. The residue was purified by flash chromatography on silica gel (hexane/EtOAc=10/1 to hexane/EtOAc=5/1) to yield the thiol (3.01 g, 92%) as a white solid. The spectra data corresponded to the known substance.³⁰

Allyl *N*-9-fluorenylmethoxycarbonyl-D-S-4-methoxytrityl resin cysteinate (**3**)

4-Methoxytrityl chloride resin (30.0 mg, 1.2 mmol g⁻¹) was swollen with CH₂Cl₂ for 30 min at RT. Subsequently, Fmoc-D-Cys-OAllyl (27.6 mg, 72 μmol) was dissolved in CH₂Cl₂ (0.72 ml), and the resin and *N,N*-diisopropylethylamine (DIPEA) (37.6 μl, 216 μmol) were added. The mixture was then agitated for 3 h at RT. MeOH was added to cap any unreacted site, and the reaction mixture was agitated for an additional 10 min. The resin was then washed with DMF (3×2 min), CH₂Cl₂/MeOH=10/1 (2 min) and CH₂Cl₂ (3×2 min).

General procedure for deprotection of the Fmoc group

The resin was swollen with DMF (1.5 ml) for 30 min, filtered and treated with 20% piperidine in DMF (1.5 ml) for 1 h at RT. The mixture was filtered and washed with DMF (3×2 min), CH₂Cl₂/MeOH=10/1 (2 min) and CH₂Cl₂ (3×2 min).

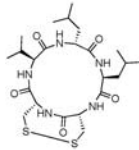
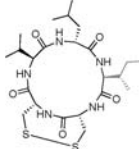
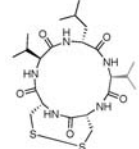
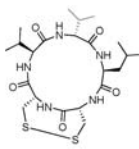
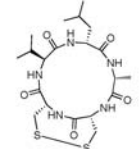
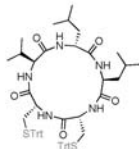
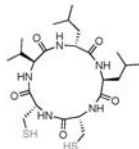
General procedure for elongation of the peptide chain

The resin was swollen with DMF for 30 min at RT. Fmoc-amino acid (2.0 equivalents) was then dissolved in DMF (0.72 ml); thereafter, PyBOP (3.0 equivalents, 56.2 mg, 108 μmol), DIPEA (6.0 equivalents, 37.6 μl, 216 μmol) and the resin were added. The mixture was subsequently agitated for 3 h at RT. The resin was filtered and washed with DMF (3×2 min), CH₂Cl₂/MeOH=10/1 (2 min) and CH₂Cl₂ (3×2 min).

General procedure for deprotection of the Allyl group

The resin was swollen with tetrahydrofuran (THF) (1.5 ml) for 1 h at RT under N₂ atmosphere, and excess THF was drained using a syringe. A solution of

Table 1 Structure of synthetic compounds, result of assay and synthetic yields

| Compounds | IC ₅₀ (µg/ml) | | Selectivity Index (SI) *2 / *1 | Synthetic yields |
|---|---|---|-----------------------------------|---------------------|
| | Anti-malarial activity* ¹ | Anti-trypanoso- mal activity* ² | | |
| Malformin C  | 0.07 | 0.0016 | 0.023 | 15% |
| Malformin A1  | 0.056 | 0.19 | 3.4 | 6% |
| Malformin A2  | 0.095 | 0.56 | 5.9 | 13% |
| Malformin B2  | 0.019 | 0.0052 | 0.27 | 7% |
| Unnatural malformin (8)  | 0.24 | 0.70 | 2.9 | 3% |
| (9)  | >12.5 | 1.52 | <0.12 | 35%* ³ |
| (10)  | 3.8 | 0.17 | 0.045 | 66% |
| Existing medication | | | | |
| Artemether | 0.0023 | — | — | — |
| Chloroquine | 0.184 | — | — | — |
| Pentamidine | — | 0.00158 | — | — |

*1 *Plasmodium falciparum* K1, *2 *Trypanosoma brucei brucei* GUTat 3.1*3 prepared by liquid-phase synthesis¹³

Pd(PPh₃)₄ (62.4 mg, 54 μmol) and 5,5-dimethyl-1,3-hexanedione (50.5 mg, 360 μmol) in THF (1.5 ml) was added to the resin, and the mixture was agitated for 1 h at RT under N₂ atmosphere. The resin was filtered and washed with THF (4×2 min), DMF (4×2 min), CH₂Cl₂ (4×2 min), 0.02 M sodium N,N-diethylthio carbamate trihydrate in DMF (3×15 min), DMF (5×2 min) and CH₂Cl₂ (3×2 min).

General procedure for cyclization of linear peptide

The resin was swollen with DMF/CH₂Cl₂=1/4 for 30 min at RT. Next, HBTU (3.0 equivalents, 41 mg, 108 μmol) was dissolved in DMF/CH₂Cl₂=1/4 (0.72 ml), after which HOBT (3.0 equivalents, 16.5 mg, 108 μmol), DIPEA (6.0 equivalents, 37.6 μl, 216 μmol) and the resin were added. The mixture was then agitated for 3 h at RT, after which it was filtered and washed with DMF (3×2 min), CH₂Cl₂/MeOH=10/1 (2 min) and CH₂Cl₂ (3×2 min).

General procedure for synthesis of malformins

The resin was swollen with DMF for 30 min at RT under N₂ atmosphere. A solution of I₂ (5.0 equivalents, 45.7 mg, 180 μmol) and triisopropylsilane (4.0 equivalents, 29.5 μl, 144 μmol) in DMF (1.5 ml) was added to the resin, and the mixture was agitated for 1 h at RT under N₂ atmosphere. The resin was filtered and cleaved from solid phase by treatment with 50% TFA/CH₂Cl₂ for 1 h. The product was filtered, washed with CH₂Cl₂ and the combined filtrates were concentrated. The residue was purified by flash column chromatography on silica gel (CHCl₃ to CHCl₃/MeOH=30/1) to yield malformins as white solids (2.9 mg, 15% of malformin C, 1.2 mg, 6% of malformin A1, 2.3 mg, 13% of malformin A2, 1.5 mg, 7% of malformin B2, 0.6 mg, 3% of 9).

Malformin C. The ¹H-NMR data and HPLC analysis of solid-phase synthetic malformin C corresponded to the previously synthetic one.

Malformin A1. m.p. > 300 °C; [α]_D²⁵ -42.2 (c 0.10, 2-methoxyethanol); IR (NaCl) cm⁻¹: 3266, 2958, 1633, 1535; ¹H NMR (400 MHz, DMSO-*d*₆) δ 8.84 (1H, d, *J*=4.2 Hz), 8.59 (1H, d, *J*=6.9 Hz), 7.95 (1H, d, *J*=8.9 Hz), 7.39 (1H, d, *J*=9.4 Hz), 7.10 (1H, d, *J*=10.8 Hz), 4.70 (1H, dt, *J*=4.4, 11.0 Hz), 4.46 (1H, dt, *J*=6.1, 9.3 Hz), 3.95 (1H, dd, *J*=3.2, 7.1 Hz), 3.92 (1H, dd, *J*=9.0, 10.3 Hz), 3.86 (1H, dd, *J*=6.8, 10.5 Hz), 3.50 (1H, dd, *J*=3.7, 14.6 Hz), 3.11–3.24 (3H, m), 2.03 (1H, dq, *J*=6.7, 13.3 Hz), 1.65–1.72 (1H, m), 1.35–1.59 (4H, m), 1.09–1.18 (1H, m), 0.88 (3H, d, *J*=6.6 Hz), 0.85 (3H, d, *J*=6.6 Hz), 0.80–0.82 (9H, m), 0.77 (3H, d, *J*=6.9 Hz); ¹³C NMR (100 MHz, DMSO-*d*₆) δ 173.9, 173.0, 172.7, 170.5, 169.7, 58.8, 58.0, 52.9, 52.3, 50.3, 46.2, 45.2, 33.9, 30.4, 26.8, 24.7, 24.4, 22.7, 21.7, 19.7, 18.7, 14.9, 9.9; MS (ESI+) *m/z* 530.2450 [M+H]⁺ (530.2470 calcd for C₂₃H₄₀O₅N₅S₂ [M+H]).

Natural malformin A1^{23,25}. [α]_D²⁵ -39.0 (2-methoxyethanol); ¹H NMR (DMSO-*d*₆) δ 8.87 (1H, d, *J*=4.03 Hz), 8.61 (1H, d, *J*=6.60 Hz), 7.96 (1H, d, *J*=8.79 Hz), 7.41 (1H, d, *J*=9.16 Hz), 7.13 (1H, d, *J*=10.99 Hz), 4.74 (1H, dt, *J*=4.40, 10.99 Hz), 4.49 (1H, dt, *J*=6.23, 9.16 Hz), 4.01 (1H, dt, *J*=3.67, 6.60 Hz), 3.95 (1H, d, *J*=9.16 Hz), 3.90 (1H, dd, *J*=6.60, 10.26 Hz), 3.53 (1H, dd, *J*=3.30, 14.65 Hz), 3.28 (2H, m), 3.17 (1H, dd, *J*=3.3, 14.29 Hz), 2.06 (1H, m), 1.72 (1H, m), 1.58 (1H, m), 1.54 (1H, m), 1.40 (2H, m), 1.17 (1H, m), 0.79–0.92 (18H, m); ¹³C NMR (DMSO-*d*₆) δ 173.7, 172.7, 172.4, 170.4, 169.6, 58.6, 57.8, 52.8, 52.3, 50.3, 46.1, 45.0, 40.6, 34.0, 26.8, 24.6, 24.3, 22.5, 21.6, 19.4, 18.4, 14.7, 9.8; HRMS *m/z* 529.2411 [M⁺] (529.2392 calcd for C₂₃H₃₉O₅N₅S₂ [M]).

Malformin A2. m.p. > 300 °C; [α]_D²⁸ -29.6 (c 0.10, 2-methoxyethanol); IR (NaCl) cm⁻¹: 3286, 2962, 1660, 1536, 1174; ¹H NMR (400 MHz, 1 drop *d*-TFA in CDCl₃) δ 7.98 (1H, d, *J*=5.9 Hz), 7.15–7.30 (3H, m), 7.03 (1H, d, *J*=8.3 Hz), 5.00 (1H, dt, *J*=3.6, 11.3 Hz), 4.42 (1H, m), 4.02 (1H, dd, *J*=7.5, 10.7 Hz), 3.86 (1H, dd, *J*=3.0, 15.3 Hz), 3.72 (1H, dt, *J*=3.3, 6.7 Hz), 3.36 (1H, dd, *J*=11.6, 15.6 Hz), 3.15–3.25 (2H, m), 2.09 (1H, dq, *J*=6.6, 13.1 Hz), 1.99 (1H, dq, *J*=6.7, 13.4 Hz), 1.51–1.65 (3H, m), 1.05 (3H, d, *J*=6.6 Hz), 0.99 (3H, d, *J*=6.1 Hz), 0.91–0.96 (12H, m), ¹H NMR (400 MHz, DMSO-*d*₆) δ 8.82 (1H, d, *J*=3.9 Hz), 8.54 (1H, d, *J*=6.8 Hz), 7.88 (1H, d, *J*=8.5 Hz), 7.41 (1H, d, *J*=9.2 Hz), 7.13 (1H, d, *J*=9.3 Hz), 4.70 (1H, dt, *J*=4.5, 10.9 Hz), 4.45 (1H, dt, *J*=6.3, 9.0 Hz), 3.97 (1H, dd, *J*=3.1, 6.9 Hz), 3.91 (1H, dt, *J*=6.0, 10.1 Hz), 3.77 (1H, dd, *J*=6.8, 9.9 Hz), 3.50 (1H, dd, *J*=3.3, 15.1 Hz), 3.11–3.24 (3H, m), 2.02 (1H, dq, *J*=6.9, 13.8 Hz), 1.83 (1H, dq, *J*=6.7, 13.3 Hz), 1.55 (1H, dt, *J*=7.1, 13.6 Hz), 1.37 (2H, m), 0.89 (3H, d, *J*=6.3 Hz), 0.88 (3H, d, *J*=6.2 Hz),

0.85 (3H, d, *J*=6.7 Hz), 0.80–0.82 (9H, m); ¹³C NMR (100 MHz, 1 drop *d*-TFA in CDCl₃) δ 175.7, 175.6, 174.2, 172.4, 171.1, 62.1, 60.5, 54.6, 52.8, 52.6, 47.1, 45.8, 29.7, 29.0, 27.2, 24.9, 22.1, 21.7, 19.2, 19.1, 19.0, 18.3; ¹³C NMR (100 MHz, DMSO-*d*₆) δ 174.4, 173.9, 173.1, 171.1, 170.2, 60.5, 59.3, 53.3, 52.8, 50.8, 46.6, 45.6, 29.4, 29.0, 27.4, 24.9, 23.1, 22.2, 20.1, 19.9, 19.4, 19.1; MS (FAB) *m/z* 516.2316 [M+H]⁺ (516.2314 calcd for C₂₂H₃₈O₅N₅S₂ [M+H]).

Natural malformin A2²³. ¹H NMR (DMSO-*d*₆) δ 8.75 (1H, d, *J*=4.28 Hz), 8.46 (1H, d, *J*=6.71 Hz), 7.73 (1H, d, *J*=8.54 Hz), 7.43 (1H, d, *J*=9.15 Hz), 7.15 (1H, d, *J*=10.99 Hz), 4.73 (1H, dt, *J*=4.89, 10.99 Hz), 4.47 (1H, dt, *J*=6.72, 9.15 Hz), 3.99 (1H, dt, *J*=3.66, 7.32 Hz), 3.94 (1H, dd, *J*=9.15, 9.77 Hz), 3.82 (1H, dd, *J*=7.32, 9.77 Hz), 3.52 (1H, m), 3.25 (2H, m), 3.20 (1H, m), 2.04 (1H, m), 1.86 (1H, m), 1.60 (1H, m), 1.41 (2H, m), 0.92 (3H, d, *J*=4.88 Hz), 0.90 (3H, d, *J*=6.71 Hz), 0.89 (3H, d, *J*=6.11 Hz), 0.85 (3H, d, *J*=6.72 Hz), 0.84 (3H, d, *J*=6.71 Hz); HRMS *m/z* 515.2227 [M⁺] (515.2235 calcd for C₂₂H₃₇O₅N₅S₂ [M]).

Malformin B2. m.p. > 300 °C; [α]_D²⁹ -47.7 (c 0.050, 2-methoxyethanol); IR (NaCl) cm⁻¹: 3266, 2925, 1671, 1546; ¹H NMR (400 MHz, DMSO-*d*₆) δ 8.92 (1H, d, *J*=4.3 Hz), 8.54 (1H, d, *J*=6.5 Hz), 8.27 (1H, d, *J*=9.1 Hz), 7.18 (1H, d, *J*=9.6 Hz), 6.94 (1H, d, *J*=11.2 Hz), 4.66 (1H, dt, *J*=3.8, 11.1 Hz), 4.18 (1H, dt, *J*=6.1, 9.4 Hz), 4.11 (1H, dd, *J*=7.5, 9.2 Hz), 3.89–3.94 (2H, m), 3.43–3.45 (1H, m), 3.23–3.26 (1H, m), 3.05–3.12 (2H, m), 1.94–2.04 (1H, m), 1.66–1.75 (1H, m), 1.44–1.58 (3H, m), 0.84 (3H, d, *J*=6.3 Hz), 0.76–0.80 (15H, m); ¹³C NMR (100 MHz, DMSO-*d*₆) δ 173.8, 173.1, 172.0, 170.7, 169.7, 58.6, 57.3, 52.8, 52.4, 51.6, 46.0, 45.2, 30.3, 29.0, 26.3, 24.0, 22.9, 21.5, 19.8, 19.0, 18.7, 18.5; MS (ESI+) *m/z* 516.2326 [M+H]⁺ (516.2314 calcd for C₂₂H₃₈O₅N₅S₂ [M+H]).

Natural malformin B2^{25,27}. [α]_D²⁵ -49.5 (c 0.73, 2-methoxyethanol); ¹H NMR (DMSO-*d*₆) δ 9.01 (1H, d, *J*=4.15 Hz), 8.61 (1H, d, *J*=6.35 Hz), 8.34 (1H, d, *J*=8.54 Hz), 7.26 (1H, d, *J*=9.52 Hz), 7.00 (1H, d, *J*=10.98 Hz), 4.73 (1H, dt, *J*=3.66, 10.99 Hz), 4.23 (1H, dt, *J*=6.1, 9.28 Hz), 4.17 (1H, dd, *J*=8.06, 8.79 Hz), 3.98 (1H, m), 3.97 (1H, dd, *J*=8.54, 10.5 Hz), 3.53 (1H, m), 3.30 (1H, dd, *J*=11.48, 14.89 Hz), 3.16 (1H, m), 3.13 (1H, m), 2.05 (1H, m), 1.77 (1H, m), 1.58 (1H, m), 1.54 (1H, m), 1.25 (1H, m), 0.80–0.95 (18H, m); ¹³C NMR (DMSO-*d*₆) δ 173.8, 173.2, 172.0, 170.8, 169.7, 58.7, 57.3, 52.8, 52.4, 51.6, 46.0, 45.2, 38.7, 30.3, 26.3, 24.0, 23.0, 21.5, 19.8, 19.0, 18.8, 18.5; HRMS *m/z* 515.2231 [M⁺] (515.2235 calcd for C₂₂H₃₇O₅N₅S₂ [M]).

Cyclo-(D-cysteinyl-D-valinyl-D-leucyl-L-alanyl)-, cyclic (1→2)-disulfide (8). m.p. > 300 °C; [α]_D²⁷ -28.8 (c 0.10, 2-methoxyethanol); IR (NaCl) cm⁻¹: 3286, 2958, 1652, 1538; ¹H NMR (400 MHz, DMSO-*d*₆) δ 8.75 (1H, d, *J*=2.9 Hz), 8.55 (1H, d, *J*=5.9 Hz), 7.69 (1H, d, *J*=8.5 Hz), 7.47 (1H, d, *J*=9.0 Hz), 7.28 (1H, d, *J*=10.9 Hz), 4.68 (1H, dt, *J*=3.0, 7.7 Hz), 4.39 (1H, dt, *J*=4.8, 9.7 Hz), 4.14–4.21 (1H, m), 3.94 (1H, dd, *J*=3.3, 6.8 Hz), 3.91 (1H, dd, *J*=2.4, 10.2 Hz), 3.49 (1H, dd, *J*=3.3, 15.0 Hz), 3.19 (2H, d, *J*=8.4 Hz), 3.14 (1H, dt, *J*=3.0, 15.2 Hz), 1.99 (1H, dq, *J*=5.8, 12.9 Hz), 1.63–1.56 (1H, m), 1.39–1.46 (2H, m), 1.14 (3H, d, *J*=7.1 Hz), 0.87 (3H, d, *J*=6.6 Hz), 0.84 (3H, d, *J*=6.6 Hz), 0.81–0.82 (6H, m); ¹³C NMR (100 MHz, DMSO-*d*₆) δ 174.0, 173.4, 172.8, 171.0, 169.8, 58.9, 52.9, 52.5, 50.3, 48.9, 46.2, 45.3, 29.0, 27.3, 24.4, 23.0, 21.3, 19.6, 18.7, 16.2; MS (ESI+) *m/z* 510.1814 [M+Na]⁺ (510.1820 calcd for C₂₀H₃₃O₅N₅S₂Na [M+Na]).

Cyclo-(D-cysteinyl-D-cysteinyl-L-valinyl-D-leucyl-L-leucyl)- (10). The resin was swollen with CH₂Cl₂ for 30 min at RT. A solution of 50% TFA/CH₂Cl₂ (1.5 ml) and triisopropylsilane (4.0 equivalents, 29.5 μl, 144 μmol) was added to the resin and the mixture was agitated for 1 h at RT. The product was filtered and washed with CH₂Cl₂, and the filtrate was combined and concentrated. The residue was purified by flash column chromatography on silica gel (CHCl₃ to CHCl₃/MeOH=10/1) to yield dithiol compound **10** as a white solid (13.6 mg, 66%); m.p. > 300 °C; [α]_D²³ -5.0 (c 0.05, 2-methoxyethanol); IR (KBr) cm⁻¹: 3280, 2962, 1637, 1546; ¹H NMR (400 MHz, DMSO-*d*₆) δ 8.66 (1H, d, *J*=8.6 Hz), 8.62 (1H, d, *J*=8.1 Hz), 8.54 (1H, d, *J*=6.6 Hz), 7.56 (1H, d, *J*=6.5 Hz), 7.48 (1H, d, *J*=9.2 Hz), 4.40 (1H, dt, *J*=5.0 Hz), 4.10–4.21 (3H, m), 3.94 (1H, t, *J*=9.7 Hz), 2.79–2.88 (1H, m), 2.59–2.73 (3H, m), 2.44 (1H, t, *J*=8.7 Hz), 2.11 (1H, t, *J*=8.6 Hz), 1.92–2.01 (1H, m), 1.37–1.59 (6H, m), 0.89 (3H, d, *J*=6.7 Hz), 0.87 (3H, d, *J*=6.9 Hz), 0.79–0.85 (12H, m); ¹³C NMR (100 MHz, DMSO-*d*₆) δ 173.1, 172.3, 171.0, 170.1, 168.7, 58.8, 56.5, 56.3, 52.3, 50.4, 40.7, 39.1, 26.9, 25.9, 24.5, 24.2, 23.0, 22.5, 22.4, 21.5, 19.5, 18.8; MS (ESI+) *m/z* 554.2442 [M+Na]⁺ (554.2447 calcd for C₂₃H₄₁O₅N₅S₂Na [M+Na]).

ACKNOWLEDGEMENTS

This work was supported in part by funds from the Drugs for Neglected Diseases initiative (DNDi); a grant for the All Kitasato Project Study (AKPS); and by the 21st Century COE Program, Ministry of Education, Culture, Sports, Science and Technology. We also thank Ms A Nakagawa, Dr K Nagai and Ms N Sato (School of Pharmaceutical Sciences, Kitasato University) for the various instrumental analyses.

- 1 Curtis, R. W. Curvatures and malformations in bean plants caused by culture filtrate of *Aspergillus niger*. *Plant Physiol.* **33**, 17–22 (1958).
- 2 Curtis, R. W. Root curvatures induced by culture filtrates of *Aspergillus niger*. *Science* **128**, 661–662 (1958).
- 3 Takahashi, N. & Curtis, R. W. Isolation and characterization of malformin. *Plant Physiol.* **36**, 30–36 (1961).
- 4 Curtis, R. W. Studies on response of bean seedlings & corn roots to malformin. *Plant Physiol.* **36**, 37–43 (1961).
- 5 Suda, S. & Curtis, R. W. Antibiotic properties of malformin. *Appl. Microbiol.* **14**, 475–476 (1966).
- 6 Kobbe, B., Cushman, M., Wagon, G. N. & Demain, A. L. Production and antibacterial activity of malformin C, a toxic metabolite of *Aspergillus niger*. *Appl. Environ. Microbiol.* **33**, 996–997 (1977).
- 7 Franck, B. Mycotoxins from mold fungi—weapons of uninvited fellow-boarders of man and animal: structures, biological activity, biosynthesis, and precautions. *Angew. Chem. Int. Ed.* **23**, 493–505 (1984).
- 8 Koizumi, Y. & Hasumi, K. Enhancement of fibrinolytic activity of U937 cells malformin A₁. *J. Antibiot.* **55**, 78–82 (2002).
- 9 Hagimori, K., Fukuda, T., Hasegawa, Y., Ōmura, S. & Tomoda, H. Fungal malformins bleomycin-induced G2 checkpoint in Jurkat cells. *Biol. Pharm. Bull.* **30**, 1379–1383 (2007).
- 10 Bodanszky, M. & Stahl, G. L. The structure and synthesis of malformin A. *Proc. Natl Acad. Sci. USA* **71**, 2791–2794 (1974).
- 11 Bodanszky, M., Stahl, G. L. & Curtis, R. W. Synthesis and biological activity of *enantio*-[5-Valine]malformin, a palindrome peptide. *J. Am. Chem. Soc.* **97**, 2857–2859 (1975).
- 12 Kurath, P. Preparation and antimicrobial activity of *enantio*-[1-Valine]malformin. *Helvetica Chimica Acta* **59**, 1127–1132 (1976).
- 13 Kojima, Y. *et al.* Total synthesis of malformin C, an inhibitor of bleomycin-induced G2 arrest. *J. Antibiot.* **61**, 297–302 (2008).
- 14 Anderegg, R. J., Biemann, K., Büchi, G. & Cushman, M. Malformin C, a new metabolite of *Aspergillus niger*. *J. Am. Chem. Soc.* **98**, 3365–3370 (1976).
- 15 Mustafa, V. & Phillip, C. Biosynthetically diverse compounds from a saltwater culture of sponge-derived *Aspergillus niger*. *J. Nat. Prod.* **63**, 41–43 (2000).
- 16 World Health Organization. World Malaria Report 2008. Available at <http://apps.who.int/malaria/wmr2008/malaria2008.pdf>
- 17 Mourtas, S., Gatos, D., Karavoltos, M., Katakalous, C. & Barlos, K. Resin-bound mercapto acids: synthesis and application. *Tetrahedron Lett.* **43**, 3419–3421 (2002).
- 18 Mourtas, S., Katakalous, C., Nicolettou, A., Tzavara, C., Gatos, D. & Barlos, K. Resin-bound amino thiols: synthesis and application. *Tetrahedron Lett.* **44**, 179–182 (2003).
- 19 Kamber, K. *et al.* The synthesis of cystine peptides by iodine oxidation of S-trityl-cysteine and S-acetamidomethyl-cysteine peptides. *Helvetica Chimica Acta* **63**, 899–915 (1980).
- 20 Pearson, D. A., Blanchette, M., Baker, M. L. & Guindon, C. A. Trialkylsilanes as scavengers for the trifluoroacetic acid deblocking of protecting groups in peptide synthesis. *Tetrahedron Lett.* **30**, 2739–2742 (1989).
- 21 Anzai, K. & Curtis, R. W. Chemical studies on malformin-III. Structure of malformin A. *Phytochemistry* **4**, 263–271 (1965).
- 22 Anzai, K. & Curtis, R. W. Chemical studies on malformin-IV. Conformational studies of malformin A. *Phytochemistry* **4**, 713–723 (1965).
- 23 Kim, K. W., Sugawara, F., Yoshida, S., Murofushi, N., Takahashi, N. & Curtis, R. W. Structure of malformin A, a phytotoxic metabolite produced by *Aspergillus niger*. *Biosci. Biotech. Biochem.* **57**, 240–243 (1993).
- 24 Sugawara, F. *et al.* Structure of malformin A₂, reinvestigation of phytotoxic metabolites produced by *Aspergillus niger*. *Tetrahedron Lett.* **31**, 4337–4340 (1990).
- 25 Takeuchi, S., Senn, M., Curtis, R. W. & McLafferty, F. W. Chemical studies on malformin-V. Malformin B₁ and B₂. *Phytochemistry* **6**, 287–292 (1967).
- 26 Kim, K. W. *et al.* Structure of malformin B, a phytotoxic metabolite produced by *Aspergillus niger*. *Tetrahedron Lett.* **32**, 6715–6718 (1991).
- 27 Kim, K. W. *et al.* Structure of malformin B, a phytotoxic metabolite produced by *Aspergillus niger*. *Biosci. Biotech. Biochem.* **57**, 787–791 (1993).
- 28 Otaguro, K. *et al.* Potent antimalarial activities of polyether antibiotic, X-206. *J. Antibiot.* **54**, 658–663 (2001).
- 29 Otaguro, K. *et al.* Selective and potent *in vivo* antitrypanosomal activities of ten microbial metabolites. *J. Antibiot.* **61**, 372–378 (2008).
- 30 Seyberth, T., Voss, S., Brock, R., Wiesmüller, K. & Jung, G. Lipolanthionine peptides act as inhibitors of TLR2-mediated IL-8 secretion synthesis and structure–activity relationships. *J. Med. Chem.* **49**, 1754–1765 (2006).

ORIGINAL ARTICLE

Beauvericin and enniatins H, I and MK1688 are new potent inhibitors of human immunodeficiency virus type-1 integrase

Cha-Gyun Shin¹, Dog-Gn An¹, Hyuk-Hwan Song² and Chan Lee²

Some enniatins (ENs) reportedly exhibit antiretroviral activities *in vivo*. The potential inhibitory activities of cyclic hexadepsipeptides such as beauvericin (BEA) and ENs H, I and MK1688 were investigated *in vitro* against human immunodeficiency virus type-1 (HIV-1) integrase and Moloney murine leukemia virus reverse transcriptase. BEA, EN I and EN MK1688 exhibited strong inhibitory activities against HIV-1 integrase, whereas EN H showed relatively weak activity. None of the examined compounds showed anti-reverse transcriptase activity. BEA was the most effective inhibitor of the tested cyclic hexadepsipeptides in inhibiting HIV-1 integrase. These results indicate the potential of cyclic hexadepsipeptides as a new class of potent inhibitors of HIV-1 integrase.

The Journal of Antibiotics (2009) 62, 687–690; doi:10.1038/ja.2009.102; published online 6 November 2009

Keywords: beauvericin; enniatins; HIV-1; inhibitor; integrase

INTRODUCTION

Human immunodeficiency virus type-1 (HIV-1) is the causative agent of AIDS (acquired immunodeficiency syndrome).¹ An essential process in the retroviral life cycle is integration of the viral DNA into the host genome, which is mediated by the viral enzyme integrase² via two consecutive steps.³ The first step, which is called the 3'-processing reaction, proceeds as integrase removes the terminal dinucleotide from the 3'-end of each strand of the viral cDNA in the cytoplasm of the infected cell. In the second step, known as the strand transfer reaction, the processed 3'-end of the viral DNA attaches to the host-cell DNA in the cell nuclei. Extensive efforts over the past few years have focused on frustrating these reactions, which have resulted in the discovery of a large number of HIV-1 integrase inhibitors.⁴ Various classes of the compounds, including natural products and synthetic compounds, have been suggested. Enniatins (ENs) B, B₁ and A₁ produced by *Fusarium* species reportedly exhibit anti-HIV-1 activity,⁵ but the mechanism for EN inhibition of viral replication remains ambiguous. Our group has recently reported the successful copurification of beauvericin (BEA) and ENs H, I, and MK1688 from culture broth of *Fusarium oxysporum* isolated from soil samples collected in Korea.^{6–8} As ENs B, B₁ and A₁ have been shown to protect human lymphoblastoid cells in HIV-1-induced cell death,⁵ we decided to test the antiviral activity of BEA and these ENs, H, I and MK1688, by studying whether or not they inhibit viral enzymes such as reverse transcriptase and integrase *in vitro*. In our assay, BEA, EN I and EN MK1688 were found to strongly inhibit the 3'-processing activity of HIV-1 integrase.

MATERIALS AND METHODS

Preparation of cyclic hexadepsipeptides

BEA and ENs were produced from the liquid culture of *F. oxysporum* strain FB1501 (KFCC 11363P) in *Fusarium* defined medium (FDM; the medium contained sucrose 25 g, NaNO₃ 4.25 g, NaCl 5 g, MgSO₄·7H₂O 2.5 g, KH₂PO₄ 1.36 g, FeSO₄·7H₂O 0.01 g and ZnSO₄·7H₂O 0.0029 g in 1.0 l tap water) as described previously.⁶ For submerged cultures, 100 ml of medium in a 250 ml Erlenmeyer flask was inoculated with approximately 1×10⁵ spores and the culture was incubated at 25 °C with shaking at 120 r.p.m. BEA and ENs H, I and MK1688 were purified from chloroform in two steps on HPLC. A GROM-Sil pack ODS preparative column (1.0×25 cm²; Herrensberg, Germany) was used for the first purification, in which the mobile phase was CH₃CN–H₂O, 65:35 (in volume), at a flow rate of 4 ml min⁻¹. The compounds were further purified with a Shiseido pack C18 column (0.46×25 cm², Shiseido, Tokyo, Japan). The second HPLC purification was performed over 45 min at a constant flow rate (1 ml min⁻¹) with a CH₃CN–H₂O, 70:30 (in volume).

Analysis and identification of BEA and ENs H, I and MK1688 by HPLC, mass spectrometry and liquid chromatography/tandem mass spectrometry

BEA and ENs were analyzed as described previously⁶ with a reverse-phase column (0.46×25 cm, 5 μm, Shiseido) using HPLC with an LC-305 device, 306 pumps and a 151 UV-visible detector from Gilson (Middleton, WI, USA). They were eluted with CH₃CN:H₂O:phosphoric acid, 70:30:0.01 (in volume), at a constant flow rate (1 ml min⁻¹) for 40 min, and the elution was monitored at 210 nm. The BEA and ENs were identified using an electrospray ionization mass spectrometer (LC-MSD Trap VL, Agilent, Santa Clara, CA, USA). An aliquot of 10 μl of the sample was injected in the analytical column

¹Department of Biotechnology, BET Research Institute, Chung-Ang University, Anseong, Gyeonggi, South Korea and ²Department of Food Science and Technology, BET Research Institute, Chung-Ang University, Anseong, Gyeonggi, South Korea
Correspondence: Dr C Lee, Department of Food Science and Technology, Chung-Ang University, Anseong, Gyeonggi 456-756, South Korea.
E-mail: chanlee@cau.ac.kr

Received 31 August 2009; revised 5 October 2009; accepted 6 October 2009; published online 6 November 2009

(0.5×30 cm², C₁₈, 5 μm, Shiseido) for liquid chromatography analysis, in which the composition of elute was CH₃CN–H₂O, 70:30 (in volume), at a flow rate of the mobile phase of 0.5 ml min⁻¹. During liquid chromatography/mass spectrometry analysis, the liquid chromatography effluent entered the mass spectrometer with a source voltage of 4.5 kV. The heated capillary was maintained at 325 °C, the sheath gas and auxiliary gas were adjusted to 89.7 and 14.6 arbitrary units, respectively, and the capillary voltage was 71.6 V. The mass spectrometer was initially programmed to perform full scans at *m/z*=100–900 for BEA and ENs H, I and MK1688 in order to observe the protonated molecular ion signals of these compounds, as well as possible fragment ions and adducts.

Evaluation of anti-HIV-1 integrase activity

The 3'-processing assays of HIV-1 integrase were performed as described previously.⁹ For the *in vitro* 3'-processing reaction, two 20-mer oligonucleotides the sequences of which resemble those of the end of HIV-1 U5-LTR were synthesized at Takara: K16 (U5-LTR, + strand), 5'-TGTGGAAATCTCTAG CAGT-3'; and K17 (U5-LTR, - strand), 5'-ACTGCTAGAGATTTCCACA-3'. Oligonucleotide K16 (15 pmol) was labeled at the 5'-end using 250 μCi [γ-³²P]-ATP (Amersham, Richmond, VA, USA) and 10 units of T4 polynucleotide kinase (New England Biolabs, Beverly, MA, USA) in a 40 μl reaction buffer (70 mM Tris-HCl (pH 7.6), 10 mM MgCl₂ and 5 mM dithiothreitol) for 60 min at 37 °C. After adding 18 pmol of complementary oligonucleotide K17, the mixture was boiled for 3 min and then cooled slowly. The labeled substrates were separated from unincorporated nucleotide by passage through a Biospin 6 column (Biorad, Hercules, Canada). The standard reaction of the 3'-processing activity contained 0.1 pmol of radiolabeled substrate, 3 pmol of HIV-1 integrase and inhibitors at the stated concentrations, 15 mM Tris-HCl (pH 7.4), 100 mM NaCl, 1 mM MnCl₂, 2 mM 2-mercaptoethanol, 2.5 mM CHAPS, 0.1 mM EDTA, 0.1 mM PMSE, 1% glycerol and 10 mM imidazole in a total volume of 10 μl. The reaction solutions were incubated at 37 °C for 60 min and stopped by the addition of 4 μl of 95% formamide, 20 mM EDTA, 0.05% bromophenol blue and 0.05% xylene cyanol FF. The reaction products were analyzed on a 15% denaturing polyacrylamide gel. Reactions were visualized and quantified by autoradiography of the dried gel (GS525 Molecular Dynamic Phosphoimager (Biorad)). The percentage inhibition was calculated according to the equation $100 \times [1 - (D - C) / (N - C)]$, where C, N and D are the fractions of 20-mer substrate converted to 18-mer (3'-processing product) for DNA alone, DNA plus integrase and integrase plus drug, respectively. The IC₅₀ value was determined by plotting the drug concentration versus the percentage inhibition and determining the concentration that produced 50% inhibition.¹⁰

Evaluation of antireverse transcriptase activity

Reverse transcriptase assays were carried out using Moloney murine leukemia virus (MMLV) reverse transcriptase (New England Biolabs). The standard reaction contained 24 pmol poly A(dT), 48 pmol of [³H]-dTTP, 0.6 units of MMLV reverse transcriptase and inhibitors in 50 μl of 50 mM Tris (pH 8.3), 75 mM KCl, 3 mM MgCl₂ and 10 mM dithiothreitol. The reaction mixtures were incubated at 37 °C for 1 h and then spotted onto a DE81 filter (Whatman, Maidstone, UK), which was washed three times with 2× SSC, twice with 95% ice-cold ethanol, and then dried. Radioactivity was measured in a liquid scintillation counter.

RESULTS AND DISCUSSION

Production of cyclic hexadepsipeptides and their identification

Cyclic peptides have been successfully used as enzyme inhibitors, antifungal and antibacterial agents, immunomodulating substances, and anticancer drugs.^{11–15} BEA and ENs share a common cyclohexadepsipeptide structure as a basic skeleton (Figure 1). They are composed of an alternating sequence of three *N*-methyl-*L*-amino acids and three *D*-α-hydroxyisovaleric acids.^{6,16,17} Mixtures of ENs B, EN B₁ and A previously showed anti-HIV-1 activity by protecting human lymphoblastoid cells against HIV-1-induced cell death with an *in vitro* therapeutic index of approximately 200.⁵ Our group has copurified BEA, and ENs H, I and MK1688 from culture broth of *F. oxysporum*, and the production of these cyclic hexadepsipeptides were further characterized during fermentation (Figure 2). The growth

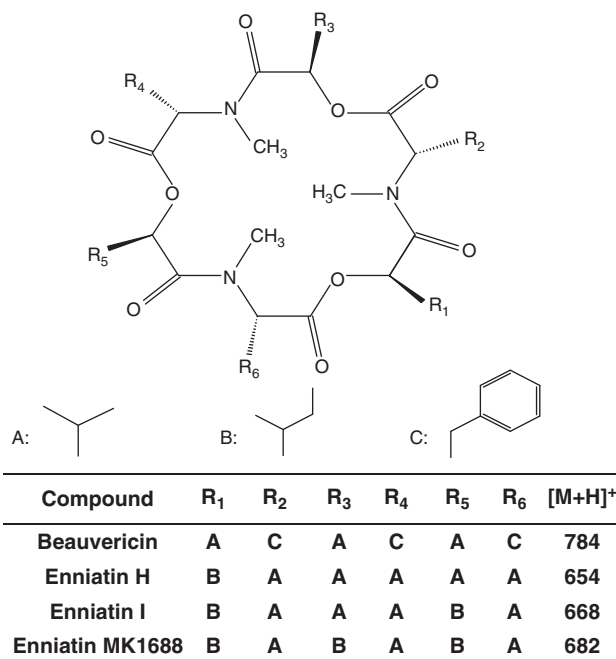


Figure 1 Chemical structures of (A) beauvericin (BEA) and (B) new enniatins (ENs) H (R₁=CH₂CH₃, R₂ and R₃=CH₃), I (R₁ and R₂=CH₂CH₃, R₃=CH₃) and MK1688 (R₁, R₂, and R₃=CH₂CH₃).

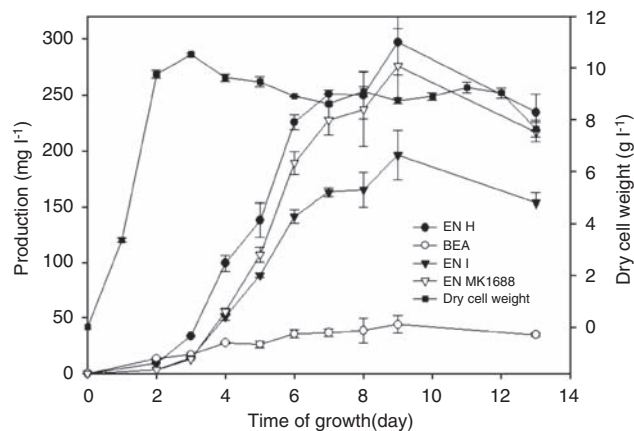


Figure 2 Growth of *Fusarium oxysporum* KFCC11363P and production of BEA and ENs. The levels of BEA and ENs were analyzed from a liquid culture of *F. oxysporum* FB1501 (KFCC 11363P) in FDM.

and production of BEA and ENs H, I and MK1688 by *F. oxysporum* strain KFCC 11363P in FDM are shown in Figure 2. The mycelium weight was maximal at day 3 of cultivation (10 g l⁻¹), and the amounts of BEA and ENs H, I and MK1688 in FDM were maximal at day 9 of cultivation (0.044, 0.29, 0.19 and 0.28 g l⁻¹, respectively). The productions of ENs H, I and MK1688 were first reported from the insect pathogenic fungus *Verticillium hemipterigenum* strain BCC 1449, and their amounts were highest in YES media (yeast extract sucrose; the medium consisted of yeast extract 20 g and sucrose 150 g in 1.0 l tap distilled water): 0.065, 0.004 and 0.0003 g l⁻¹, respectively.¹⁸ These data show that markedly higher amounts of ENs H, I and MK1688 were produced by *F. oxysporum* strain KFCC 11363P than by *V. hemipterigenum*. Moreover, the molecular weights of BEA and

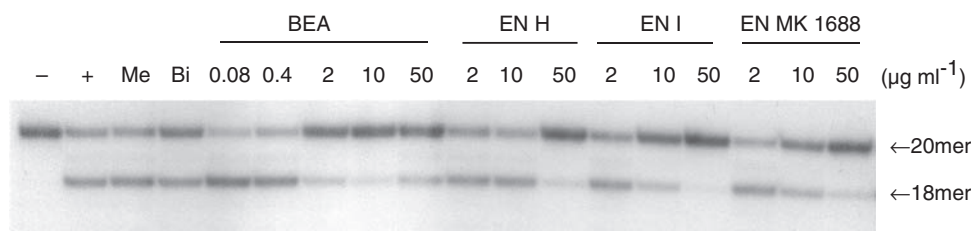


Figure 3 Inhibitory effects of cyclic hexadepsipeptides isolated from *Fusarium oxysporum* KFCC11363p on human immunodeficiency virus type-1 (HIV-1) integrase. Products from the *in vitro* 3'-processing reactions were analyzed on a 15% denaturing polyacrylamide gel, and visualized and quantified by autoradiography of the dried gel. -, no integrase added; +, integrase added; Me, 5% methanol as a final concentration (solvent control); Bi, 5 µg ml⁻¹ baicalein (with a known HIV-1 integrase inhibitor used as inhibitor control).

Table 1 Inhibitory effects of beauvericin and enniatins on human immunodeficiency virus type-1 (HIV-1) IN and Moloney murine leukemia virus (MMLV) RT^a

| Compound | IC ₅₀ (µM) ^b | |
|------------------|------------------------------------|-------------|
| | IN | RT |
| Beauvericin | 1.9 ± 0.4 | 95.6 ± 18.2 |
| Enniatin I | 10.6 ± 1.8 | > 100 |
| Enniatin H | 37.9 ± 2.8 | > 100 |
| Enniatin MK 1688 | 11.8 ± 3.1 | 89.8 ± 15.5 |

Abbreviations: IN, integrase; RT, reverse transcriptase.

^aData are mean ± s.e. values from three independent experiments.

^bInhibitor concentration required to reduce the 3'-processing activity of HIV-1 IN or MMLV RT activity by 50%.

ENs H, I, and MK1688 are 784.5, 654.7, 669.0 and 683.6, respectively, on the basis of molecular ion peaks in *m/z* plots. EN H, BEA, EN I and EN MK1688 could be eluted with retention times of 16.0, 17.6, 20.8 and 27.2 min, respectively, in HPLC chromatograms (data not shown). The following ion products [M+H]⁺ were found in liquid chromatography/tandem mass spectrometry analysis (*m/z* values): BEA: 756.4, 623.4, 523.4, 495.4, 362.4, 280.2 and 262.2; EN H: 626.6, 541.5, 513.6, 441.4, 328.3 and 228.1; EN I: 640.6, 555.5, 527.4, 441.3, 328.4 and 228.2; EN MK1688: 654.4, 569.5, 455.4, 427.2, 342.4 and 228.0.

Evaluation of anti-reverse transcriptase activity

After identifying the cyclic hexadepsipeptides, their inhibitory activities on retroviral enzymes were investigated. Their potentials to inhibit *in vitro* reactions using purified HIV-1 integrase were examined first, with baicalein, a known HIV-1 integrase inhibitor, used as a positive control. BEA and ENs inhibited HIV-1 integrase activity dose-dependently, as shown in Figure 3. BEA strongly inhibited the 3'-processing activity of HIV-1 integrase (IC₅₀, 1.9 ± 0.4 µM, mean ± s.e.) (Table 1), followed by ENs I and MK1688 (IC₅₀, 10.6 ± 1.8 and 11.8 ± 3.1 µM, respectively), and then by EN H (IC₅₀, 37.9 ± 2.8 µM). The inhibitory activities of these cyclic hexadepsipeptides against the viral enzyme were tested in MMLV reverse transcriptase. In contrast to their strong inhibition of HIV-1 integrase, BEA and ENs did not exert any inhibitory effects on reverse transcriptase, as indicated by their IC₅₀ values being around 100 µM or more (Table 1). The relative inhibitory potencies of BEA, EN I and EN MK1688 on HIV-1 integrase were comparable to those of baicalein (IC₅₀, 1.2 µM) and robinetin (IC₅₀, 5.9 ± 1.9 µM), which are strong HIV-1 integrase inhibitors.¹⁹ Lutzke *et al.*²⁰ reported a hexapeptide inhibitor of HIV-1 integrase, the sequence of which is HCKFWW, and suggested that it

acts at or near the catalytic site of integrase. Owing to their structural characteristics, cyclic hexadepsipeptides could inhibit the oligomerization of the enzyme that is essential for catalytic activity.²¹

As there is no known human counterpart of HIV-1 integrase, it is an attractive target for antiviral drug design. To date, several classes of compounds have been identified as being active against HIV-1 integrase. Even though raltegravir and elvitegravir have been shown to be promising in clinical trials, and the first has been recently made available for clinical practice,²² more extensive screening of various biological sources is necessary to identify a clinically effective inhibitor. To our knowledge, this is the first report of cyclic hexadepsipeptides that can inhibit HIV-1 integrase. We surmise that cyclic hexadepsipeptides represent a new class of potent inhibitors of HIV-1 integrase.

ACKNOWLEDGEMENTS

We are grateful to Se-Young Choi for performing the phosphoimage analyses of the 3'-processing assays of HIV-1 integrase. This research was supported by the Basic Science Research Program through the National Research Foundation of Korea (NRF) funded by the Ministry of Education, Science and Technology (No. 2009-0059098).

- Barr-Sinoussi, F. *et al.* Isolation of a T-lymphotropic retrovirus from a patient at risk for acquired immune deficiency syndrome (AIDS). *Science* **220**, 868–870 (1983).
- Asante-Appiah, E. & Skalka, A. M. Molecular mechanisms in retrovirus DNA integration. *Antiviral Res.* **36**, 139–156 (1997).
- Brown, P. O., Coffin, J. M., Hughes, S. H. & Varmus, H. E. *Retroviruses* 161–162 (Cold Spring Harbor Lab Press, New York, 1997).
- Pommier, Y., Johnson, A. A. & Marchand, C. Integrase inhibitors to treat HIV/AIDS. *Nat. Rev.* **4**, 236–248 (2005).
- McKee, T. C. *et al.* Isolation and characterization of new anti-HIV and cytotoxic leads from plants, marine, and microbial organisms. *J. Nat. Prod.* **60**, 431–438 (1997).
- Song, H. H., Ahn, J. H., Lim, Y. H. & Lee, C. Analysis of beauvericin and unusual enniatins co-produced by *Fusarium oxysporum* FB1501 (KFCC 11363P). *J. Microbiol. Biotechnol.* **16**, 1111–1119 (2006).
- Lee, H. S. *et al.* Cytotoxicities of enniatins H, I, and MK1688 from *Fusarium oxysporum* KFCC 11363P. *Toxicol.* **51**, 1178–1185 (2008).
- Song, H. H., Lee, H. S., Jeong, J. H., Park, H. S. & Lee, C. Diversity in beauvericin and enniatins H, I, and MK1688 by *Fusarium oxysporum* isolated from potato. *Int. J. Food Microbiol.* **122**, 296–301 (2008).
- Kim, H. J., Woo, E. R., Shin, C. G. & Park, H. A new flavonol glycoside gallate ester from *Acer okamotoannum* and its inhibitory activity against human immunodeficiency virus-1 integrase. *J. Nat. Prod.* **61**, 145–148 (1998).
- Mazumder, A. *et al.* Probing interactions between viral DNA and human immunodeficiency virus type I integrase using dinucleotides. *Mol. Pharmacol.* **51**, 567–575 (1997).
- Faulkner, D. J. Marine natural products. *Nat. Prod. Rep.* **5**, 613–663 (1998).
- Rosen, M. K. & Schreiber, S. L. Natural products as probes in the study of cellular functions: investigation of immunophilins. *Angew. Chem.* **104**, 413–430 (1992).
- Breithaupt, H. The new antibiotics. *Nat. Biotech.* **17**, 1165–1169 (1999).
- Davies, J. S. in *Cyclic Polymers* (ed Semlyen, J.A.) 85–124 (Kluwer Academic Publishers, The Netherlands, 2000).

- 15 Kohil, R. M., Walsh, C. T. & Burkart, M. D. Biomimetic synthesis and optimization of cyclic peptide antibiotics. *Nature* **418**, 658–661 (2002).
- 16 Hamill, R. L., Higgins, C. E., Boaz, H. E. & Gorman, M. The structure of beauvericin, a new depsipeptide antibiotic toxic to *Artemia salina*. *Tetrahedron Lett.* **49**, 4255–4258 (1969).
- 17 Sagakuchi, M. *et al.* in *Proceedings of First Asian Conference of Plant Pathology* 269–279 (Kuala Lumpur, Malaysia, 2000).
- 18 Nilanonta, C. *et al.* Unusual enniatins produced by the insect pathogenic fungus *Verticillium hemipterigenum*: isolation and studies on precursor-directed biosynthesis. *Tetrahedron* **59**, 1015–1020 (2003).
- 19 Fesen, M. R. *et al.* Inhibition of HIV-1 integrase by flavones, caffeic acid phenethyl ester (CAPE) and related compounds. *Biochem. Pharmacol.* **48**, 595–608 (1994).
- 20 Lutzke, R. A. P., Eppens, N. A., Weber, P. A. & Houghten, R. A. Identification of a hexapeptide inhibitor of the human immunodeficiency virus integrase protein by using a combinatorial chemical library. *Proc. Natl Acad. Sci. USA* **92**, 11456–11460 (1995).
- 21 Maroun, R. G. *et al.* Peptide inhibitors of HIV-1 integrase dissociate the enzyme oligomers. *Biochemistry* **40**, 13840–13848 (2001).
- 22 Ceccherini-Silberstein, F. *et al.* Characterization and structural analysis of HIV-1 integrase conservation. *AIDS Rev.* **11**, 17–29 (2009).

ORIGINAL ARTICLE

The vacuole-targeting fungicidal activity of amphotericin B against the pathogenic fungus *Candida albicans* and its enhancement by allicin

Hasibagan Borjihan¹, Akira Ogita^{1,2}, Ken-ichi Fujita¹, Eiji Hirasawa¹ and Toshio Tanaka¹

In this study, the vacuole disruptive activity was evaluated as a cause of amphotericin B (AmB) lethality against the pathogenic fungus *Candida albicans* in terms of its enhancement by allicin, an allyl-sulfur compound from garlic. Vacuole disruption was observed in parallel to AmB-induced cell death when the antibiotic was used at a lethal concentration and at a non-lethal concentration in combination with allicin. Allicin did not enhance AmB-induced cell death and the accompanying vacuole disruption when the cells were incubated with exogenous ergosterol for its enrichment in the vacuole. The vacuoles isolated from intact cells could be directly disrupted by the action of AmB to the same extent in the absence and presence of allicin, whereas the organelles isolated from ergosterol-enriched cells were resistant to its direct disruptive action. AmB was similarly incorporated into the fungal cytoplasm in cells with or without ergosterol enrichment, supporting the fact that AmB-induced vacuole disruption depends on its direct disruptive action on the organelle. In agreement with these findings, allicin was found to inhibit ergosterol transport from the plasma membrane to the cytoplasm, which is considered to be a cellular protective response to AmB-induced vacuole disruption in *S. cerevisiae*. Our study suggests that AmB lethality against *C. albicans* depends at least in part on its vacuole disruptive activity under the physiological condition permissive for invasive growth of the fungus.

The Journal of Antibiotics (2009) 62, 691–697; doi:10.1038/ja.2009.103; published online 30 October 2009

Keywords: amphotericin B; allicin; *Candida albicans*; vacuole

INTRODUCTION

Candida albicans is a ubiquitous fungus, which is normally found on the skin, and also in the mouth, throat, stomach, rectum and vagina; this fungus causes candidiasis as a result of its proliferation in any of these mammalian organs.¹ Medical treatment for candidiasis includes chemotherapy using amphotericin B (AmB; Figure 1), a typical polyene macrolide antibiotic that is derived from the actinomycete *Streptomyces nodosus*.^{2,3} AmB binds to ergosterol in the fungal plasma membrane and induces lethal damage by altering plasma membrane permeability.⁴ However, the AmB-induced lethal damage cannot be simply explained by the disturbance in plasma membrane ion transfer function because the leakage of K⁺ results in various secondary effects, including the inhibition of protein synthesis.⁵ Moreover, the involvement of additional cytotoxic effects in AmB lethality is supported by the fact that the leakage of K⁺ is not necessarily accompanied by the loss of cell viability in *C. albicans*.⁶ Oxidative stress induction is considered to be another AmB-induced toxic event in the cells of this pathogenic fungus.^{2,7} In our recent study, we observed vacuole membrane fragmentation in *Saccharomyces cerevisiae* cells on incuba-

tion with AmB in distilled water, in which the organelle actively functions for cellular ion homeostasis and osmoregulation.⁸ In addition to the alteration in plasma membrane permeability in *S. cerevisiae*, AmB lethality could be attributed, at least in part, to its direct disruptive action on vacuoles.

Allicin (diallyl thiosulfinate) (Figure 1) exerts various therapeutic effects that could be applicable for protection against the proliferation of pathogenic microbes as well as malignant tumor cells.^{9,10} This allyl-sulfur compound is also of clinical interest because of its beneficial effects on neutral lipid metabolism and its inhibitory effect on platelet aggregation.^{11,12} We recently reported its enhancement effect on the fungicidal activities of AmB and polymyxin B (PMB), which is a bactericidal antibiotic, against various fungal strains.^{8,13,14} Allicin selectively enhanced the vacuole disruptive activity but not the plasma membrane-targeting activity of these antibiotics against *S. cerevisiae*. The enhancement effect of allicin on AmB lethality could be elucidated by its inhibitory effect on ergosterol transport from the plasma membrane to the vacuole membrane that occurs as a cellular response to protect against the direct disruptive action of the antibiotic on the

¹Department of Biology and Geosciences, Graduate School of Science, Osaka City University, 3-3-138 Sugimoto, Sumiyoshi-ku, Osaka, Japan and ²Research Center for Urban Health and Sports, Osaka City University, 3-3-138 Sugimoto, Sumiyoshi-ku, Osaka, Japan

Correspondence: Professor T Tanaka, Department of Biology and Geosciences, Graduate School of Science, Osaka City University, 3-3-138 Sugimoto, Sumiyoshi-ku, Osaka, 558-8585, Japan.

E-mail: tanakato@sci.osaka-cu.ac.jp

Received 6 July 2009; revised 1 October 2009; accepted 8 October 2009; published online 30 October 2009

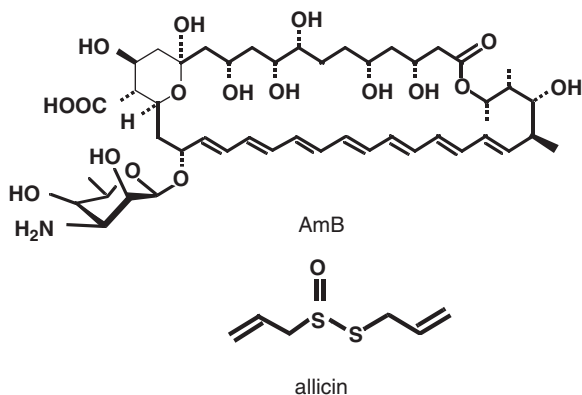


Figure 1 Structures of AmB and allicin.

organelle.¹⁵ In a recent study, it was proposed that allicin could be used to enhance AmB lethality against *C. albicans* on the basis of the *in vivo* experiment conducted using a murine model of candidiasis.¹⁶ They also proposed that plasma membrane phospholipid peroxidation, which is slightly provoked by the action of AmB alone and is markedly enhanced by the combined actions of AmB and allicin, is the most promising effect of allicin as an AmB enhancer. However, because their *in vitro* experiment, as in the case of our study, was conducted in distilled water or mineral salt medium at 30 °C, further studies are required to determine whether the enhancement effect of allicin indeed depends on such a cell surface oxidative event *in vivo*.

In this study, we attempted to examine the enhancement effect of allicin on the fungicidal activity of AmB against *C. albicans* cells in RPMI 1640 medium at 37 °C. We focused our attention on vacuole disruption as well as oxidative stress induction during the course of cell death caused by the combined actions of AmB and allicin. We also examined the mechanism underlying the enhancement effect of allicin on one of these toxic events in *C. albicans* cells by using methods described in our previous experiments with *S. cerevisiae*.

MATERIALS AND METHODS

Measurement of cell growth and viability

C. albicans NBRC 1061 (formerly *C. albicans* IFO 1061) was used in the following experiments to examine the effects of AmB and allicin on cell growth, cell viability and other physiological properties.⁸ The fungal cells were pre-cultivated in YPD medium containing 1% yeast extract (Difco Laboratories, Detroit, MI, USA), 2% Bacto-peptone (Difco Laboratories) and 2% glucose at 30 °C with vigorous shaking. Unless otherwise stated, cells from the overnight culture in YPD medium were collected by centrifugation, washed twice with RPMI 1640 medium with L-glutamine¹⁷ (RPMI 1640 medium) and suspended in the medium to obtain a final cell density of 1×10^7 cells ml⁻¹. Cells were then incubated in the absence and presence of each compound with vigorous shaking at 37 °C. Viable cell number was determined by counting colony forming units after 24-h incubation on YPD agar plate at 30 °C.⁸

Vacuole staining

Vacuoles were visualized by staining with the fluorescent probe FM4-64 as follows.⁸ Cells from the overnight culture in YPD medium were suspended in a freshly prepared medium to obtain a cell density of 1×10^7 cells ml⁻¹. After incubation with 5 μM FM4-64 at 30 °C for 30 min, the cells were collected by centrifugation, washed twice with RPMI 1640 medium and suspended in the medium at a final cell density of 1×10^7 cells ml⁻¹. The cells were incubated in the absence and presence of each compound with vigorous shaking at 37 °C for 60 min, and were then observed under a phase-contrast microscope and a fluorescence microscope with excitation at 520–550 nm and emission at 580 nm.

Vacuole isolation

The vacuoles were isolated from *C. albicans* cells by using previously described methods^{18–20} with slight modifications¹⁵ as follows. Cells from the overnight culture in YPD medium were collected by centrifugation and suspended in spheroplasting buffer (50 mM Tris-HCl, pH 7.5; 1 M sorbitol; 10 mM sodium azide) with 0.5% 2-mercaptoethanol to obtain a cell density of 1×10^9 cells ml⁻¹. After the addition of Yeast Lytic Enzyme at 6 mg ml⁻¹, the cells were converted to spheroplasts by incubation at 30 °C for 60 min. The spheroplasts were then collected by centrifugation, washed with vacuole isolation buffer (10 mM sodium citrate, pH 6.8; 0.6 M sorbitol) and carefully suspended in the buffer at a final density of 5×10^9 cells ml⁻¹. All the subsequent procedures were carried out on ice. The spheroplasts were homogenized with 20 strokes of a Dounce homogenizer. The homogenate (15 ml) was transferred into a centrifugation tube and was gently overlaid first with 10 ml of vacuole isolation buffer containing 7% Ficoll and next with 10 ml of the buffer containing 8% Ficoll. After centrifugation (3000 g) at 4 °C for 30 min, the vacuoles at the 7–0% Ficoll interface were collected.

Assay of reactive oxygen species production

The production of reactive oxygen species (ROS) such as O₂⁻ and H₂O₂ was determined by our previously described method based on the intracellular deacylation and oxidation of 2',7'-dichlorodihydrofluorescein diacetate (DCFH-DA) to the corresponding fluorescent compound.²¹ Isoprenoid farnesol (FOH) was used as a positive control to enhance intracellular ROS production. Cells from the overnight culture in YPD medium were collected by centrifugation, suspended in the medium to obtain a cell density of 1×10^7 cells ml⁻¹ and incubated with 40 μM DCFH-DA at 30 °C for 60 min. The cells were then collected by centrifugation and suspended in an equal volume of RPMI 1640 medium. The cell suspension (1.0 ml) was further incubated in the absence and presence of each compound at 37 °C for 120 min. The cells were collected by centrifugation, washed with phosphate-buffered saline (137 mM NaCl, 8.1 mM Na₂HPO₄·12H₂O, 2.68 mM KCl, 1.47 mM KH₂PO₄, pH 7.4) (PBS) and suspended in 100 μl of PBS. The fluorescence intensities of the cell samples (1×10^7 cells) were measured using the Tecan GENios fluorescence detector (Männedorf, Switzerland) at excitation and emission wavelengths of 480 and 530 nm, respectively. The arbitrary units were derived directly from the fluorescence intensity.

Assay of plasma membrane phospholipid peroxidation

The extent of plasma membrane phospholipid peroxidation was determined using a fluorescence probe, diphenyl-1-pyrenylphosphine (DPPP) and *t*-butyl hydroperoxide (*t*-BOOH) as a positive control as follows.²² Cells from the overnight culture in YPD medium were collected by centrifugation, washed with PBS and suspended in PBS at a final cell density of 3×10^7 cells ml⁻¹. After the addition of DPPP at a concentration of 50 μM and incubation for 10 min in the dark, the cells were collected by centrifugation, washed twice with PBS and finally suspended in RPMI 1640 medium at a final cell density of 1×10^7 cells ml⁻¹. The cell suspension was further incubated in the absence and presence of each compound at 37 °C for 120 min. The fluorescence intensities of the cell samples (1×10^6 cells) were measured using the FP-1520S fluorescence detector (Jasco, Tokyo, Japan) at excitation and emission wavelengths of 351 and 380 nm, respectively. The arbitrary units were derived directly from the fluorescence intensity.

Measurement of AmB content by HPLC

Cells from the overnight culture in YPD medium were collected by centrifugation, washed twice with PBS and suspended in PBS to obtain a final cell density of 1×10^8 cells ml⁻¹. The cell suspension in PBS was incubated with 20 μM AmB in the absence and presence of 120 μM allicin at 37 °C for 60 min. The supernatant obtained after the removal of cells by centrifugation was used as the supernatant fraction. The cell pellets were washed twice with PBS by repeated centrifugation and then suspended in PBS at a cell density of 1×10^8 cells ml⁻¹; the cells were incubated after the addition of Yeast Lytic Enzyme at a final concentration of 6 mg ml⁻¹ and 0.5% 2-mercaptoethanol at 30 °C with gentle agitation for 60 min or longer to ensure complete cell lysis. The supernatant obtained after centrifugation (5000 g, 10 min, 4 °C) of the cell

lysate was used as the cytoplasmic fraction. The pellets were washed twice with PBS by repeated centrifugation, and the final precipitate obtained (plasma membrane phospholipids) was decomposed by repeated vortexing with a mixture of water/methanol/chloroform (30:20:50, v/v) at room temperature. The upper water-soluble layer was used as the plasma membrane fraction.

These fractions were assayed for AmB content by HPLC with a reverse-phase column (4.6 by 250 mm, COSMOSIL 5C₁₈-MS-II, Nacalai Tesque Inc., Kyoto, Japan). The chromatographic solvents were eluted at room temperature with a mobile phase consisting of a mixture of 0.1 M sodium acetate (pH 4.0)/acetonitrile (60:40, v/v) at a flow rate of 1.2 ml min⁻¹. AmB was detected at 405 nm.²³

Detection of ergosterol

The subcellular localization of ergosterol was analyzed by its visualization with filipin III as a selective fluorescent probe according to the previously described method.¹⁵ Cells from the overnight culture in YPD medium were collected by centrifugation, washed twice with RPMI 1640 medium and suspended in the medium to obtain a final cell density of 1×10⁷ cells ml⁻¹. Cells were then incubated in the absence and presence of each compound with vigorous shaking at 37 °C, and fixed with the addition of 3% paraformaldehyde at room temperature for 10 min. The fixed cells were collected by centrifugation, washed with distilled water and incubated in the dark with 50 µg ml⁻¹ filipin III at 30 °C for 15 min. Cells were then observed under a phase-contrast microscope and a fluorescence microscope with excitation at 338 nm and emission at 480 nm.

Preparation of ergosterol-enriched cells

For measurement of cell growth and vacuole staining, cells from the overnight culture in YPD medium were inoculated into a freshly prepared YPD medium containing 240 µM ergosterol at a cell density of 1×10⁷ cells ml⁻¹, and incubated with vigorous shaking at 30 °C for 60 min. For vacuole isolation, cells from the overnight culture in YPD medium were inoculated into a freshly prepared YPD medium containing 500 µM ergosterol at a cell density of 1×10⁹ cells ml⁻¹, and incubated with vigorous shaking at 30 °C for 60 min. For HPLC-analysis of AmB, cells from the overnight culture in YPD medium were inoculated into a freshly prepared YPD medium containing 370 µM ergosterol at a cell density of 1×10⁸ cells ml⁻¹, and incubated with vigorous shaking at 30 °C for 60 min. These ergosterol-enriched cells were treated exactly in the same way as untreated cells in each of the above experiments.

Chemicals

The chemicals were obtained from the following sources: AmB and filipin III, Sigma Aldrich (St Louis, MO, USA); allicin, LKT Laboratories Inc. (St Paul, MN, USA); FM4-64 and DCFH-DA, Molecular Probe (Eugene, OR, USA); DPPP, Dojindo (Kumamoto, Japan); Ficoll 400, Alfa Aesar (Ward Hill, MA, USA); Yeast Lytic Enzyme, ICN Biomedicals (Aurora, OH, USA). The other chemicals used were of analytical reagent grade and purity.

RESULTS

Enhancement effect of allicin on AmB lethality

We first examined whether allicin could enhance AmB lethality against *C. albicans* cells by determining the changes in cell viability. AmB showed a highly lethal effect at 2 µM and even at the non-lethal concentration of 0.25 µM in combination with 120 µM allicin (Figure 2); these lethal concentrations were comparable with the concentration that effectively induced cell death of *S. cerevisiae* in distilled water.⁸

Effects of AmB and allicin, and their combination on ROS production and plasma membrane phospholipid peroxidation

Allicin may not enhance AmB lethality by increasing AmB-induced oxidative stress in *C. albicans* cells in RPMI 1640 medium at 37 °C. As shown in Figure 3a, the level of ROS production was maintained at the control level when the cells were treated with allicin at 120 µM or AmB at the non-lethal concentration of 0.25 µM. We did not observe a

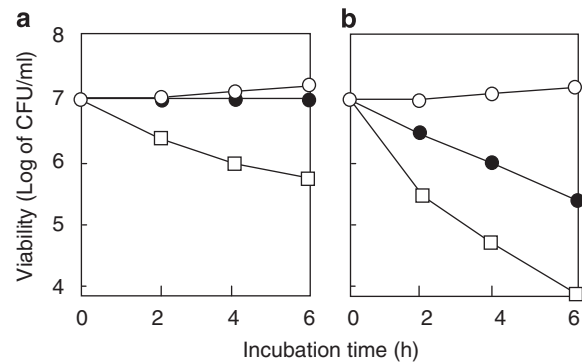


Figure 2 The effects of AmB on the viability of *C. albicans* cells in the absence (a) and presence of allicin (b). For (A), cells (1×10⁷ cells ml⁻¹) were incubated in RPMI 1640 medium containing AmB at 0 µM (○), 0.25 µM (●) and 2 µM (□) at 37 °C. For (b), cells (1×10⁷ cells ml⁻¹) were incubated in RPMI 1640 medium containing 120 µM allicin and AmB at 0 µM (○), 0.25 µM (●) and 2 µM (□) at 37 °C.

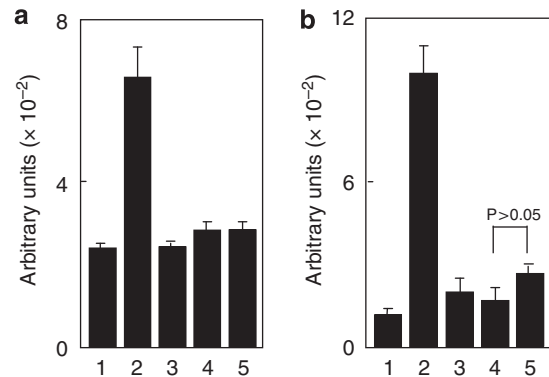


Figure 3 The effects of AmB, allicin and their combination on ROS production (a) and plasma membrane phospholipid peroxidation (b). For (a), cells (1×10⁷ cells ml⁻¹) were incubated in RPMI 1640 medium containing none (1), 25 µM FOH (2), 120 µM allicin (3), 0.25 µM AmB (4) and a combination of 0.25 µM AmB and 120 µM allicin (5) at 37 °C for 120 min. For (b), cells (1×10⁷ cells ml⁻¹) were incubated in RPMI 1640 medium containing none (1), 1 mM t-BOOH (2), 120 µM allicin (3), 0.25 µM AmB (4) and a combination of 0.25 µM AmB and 120 µM allicin (5) at 37 °C for 120 min. Data are expressed as the mean±s.d. of the arbitrary units measured in triplicate assays, and are analyzed by Student's *t*-test. *P*<0.05 is considered statistically significant.

significant difference in the level of ROS production when the cells were simultaneously treated with both AmB and allicin.

Allicin was found to accelerate plasma membrane phospholipid peroxidation in *S. cerevisiae* when the cells were incubated in distilled water at 30 °C.⁸ We therefore examined the relationship between plasma membrane phospholipid peroxidation and the enhancement effect of allicin on AmB lethality against *C. albicans* cells in RPMI 1640 medium at 37 °C. The levels of plasma membrane phospholipid peroxidation were not significantly increased when cells were incubated with either allicin or AmB alone at a non-lethal concentration (0.25 µM) (Figure 3b). Allicin was ineffective in increasing the level of such a cell surface oxidative event that was detected at the control level in AmB-treated cells. These results suggested the involvement of another toxic event in the enhancement effect of allicin on AmB lethality against *C. albicans* cells in RPMI 1640 medium at 37 °C.

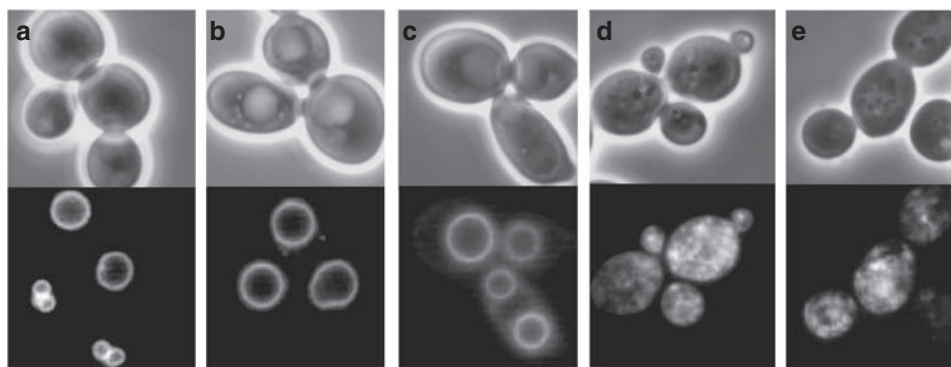


Figure 4 The effects of AmB, allicin and their combination on vacuole morphology in *C. albicans* cells. After treatment with the fluorescent dye FM4-64, cells (1×10^7 cells ml^{-1}) were incubated in RPMI 1640 medium containing none (a), $120 \mu\text{M}$ allicin (b), $0.25 \mu\text{M}$ AmB (c), $2 \mu\text{M}$ AmB (d) and a combination of $0.25 \mu\text{M}$ AmB and $120 \mu\text{M}$ allicin (e) at 37°C for 60 min. Cells were observed under a bright-field microscope (top) and a fluorescence microscope (bottom).

Enhancement effect of allicin on vacuole disruption by AmB

Vacuole disruption was observed when *S. cerevisiae* cells were treated with a lethal concentration of AmB in distilled water in which cells are more susceptible to the lethal action of the antibiotic than in a medium.⁸ We therefore examined whether AmB treatment can trigger vacuole disruption in *C. albicans* cells maintained in RPMI 1640 medium at 37°C . The vacuoles appeared as membrane-enclosed spherical structures in untreated cells although they were smaller in size as compared with those in *S. cerevisiae* cells (Figure 4a). No morphological changes were observed in the organelles of the cells incubated in the medium containing $120 \mu\text{M}$ allicin (Figure 4b). Furthermore, AmB did not exert disruptive effects on the organelles at the non-lethal concentration ($0.25 \mu\text{M}$), but caused serious structural damages when administered at the lethal concentration ($2 \mu\text{M}$) (Figures 4c and d). In combination with allicin, AmB showed a similar vacuole disruptive activity even at non-lethal concentration ($0.25 \mu\text{M}$) in parallel to the enhancement of its lethality (Figures 2b and 4e).

Effects of allicin on AmB-induced cell death and vacuole disruption in ergosterol-enriched cells

Our previous study suggested that allicin inhibits ergosterol transport from the plasma membrane to the vacuole membrane when *S. cerevisiae* cells were treated with AmB in distilled water.¹⁵ Thus, ergosterol transport is considered to be a cellular response to protect the fungal vacuoles against the disruptive action of AmB. As observed in the case of *S. cerevisiae* cells, ergosterol-enriched *C. albicans* cells were completely resistant to the lethal effects of AmB at $2 \mu\text{M}$ or at $0.25 \mu\text{M}$ in combination with $120 \mu\text{M}$ allicin, though the fungal cell growth was inhibited under each of these conditions (Figure 5a). In agreement with the maintenance of cell viability, the vacuoles of ergosterol-enriched cells were observed to be normal spherical structures in the medium containing AmB at the lethal concentration ($2 \mu\text{M}$) and at a non-lethal concentration ($0.25 \mu\text{M}$) in combination with allicin (Figure 5b).

Direct disruption of isolated vacuoles by AmB

We examined whether AmB could directly disrupt the vacuoles isolated from *C. albicans* cells. The vacuoles isolated from intact cells were observed with the swollen spherical structures after incubation with $10 \mu\text{M}$ AmB, whereas the organelles were mostly disrupted into amorphous fragments or particles with increasing concentration of the antibiotic up to $20 \mu\text{M}$ (Figures 6a and c). Allicin did not

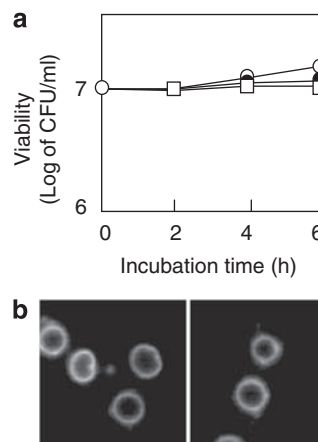


Figure 5 AmB-induced lethality (a) and vacuole disruption (b) in ergosterol-enriched *C. albicans* cells. For (a), ergosterol-enriched cells (1×10^7 cells ml^{-1}) were incubated in RPMI 1640 medium containing none (\circ), $2 \mu\text{M}$ AmB (\bullet), and a combination of $0.25 \mu\text{M}$ AmB and $120 \mu\text{M}$ allicin (\square) at 37°C . For (b), ergosterol-enriched cells (1×10^7 cells ml^{-1}) were incubated in RPMI 1640 medium containing $2 \mu\text{M}$ AmB (left) and a combination of $0.25 \mu\text{M}$ AmB and $120 \mu\text{M}$ allicin (right) at 37°C for 60 min. Cells were observed under a fluorescence microscope.

stimulate or inhibit AmB-induced vacuole disruption, indicating that this compound does not contribute to the direct interaction between the antibiotic and the fungal vacuole (Figures 6b and d). The vacuoles isolated from ergosterol-enriched cells were completely resistant to the disruptive action of $20 \mu\text{M}$ AmB both in the absence and presence of allicin. These findings agreed with our idea that allicin can enhance the fungicidal activity of AmB against *C. albicans* by inhibiting intracellular ergosterol transport, a cellular response to protect against vacuole disruption by AmB, as observed in the case of *S. cerevisiae*.¹⁵

Effect of allicin on cellular uptake of AmB

The enhancement effect of allicin on AmB-induced vacuole disruption also suggests that allicin enhances cellular uptake of the antibiotic into the cytoplasm of *C. albicans* cells via diffusion through the plasma membrane or a transporter-mediated incorporation. Ergosterol-enriched cells are likely to be more resistant to AmB than untreated cells because of its specific binding with ergosterol that may also be

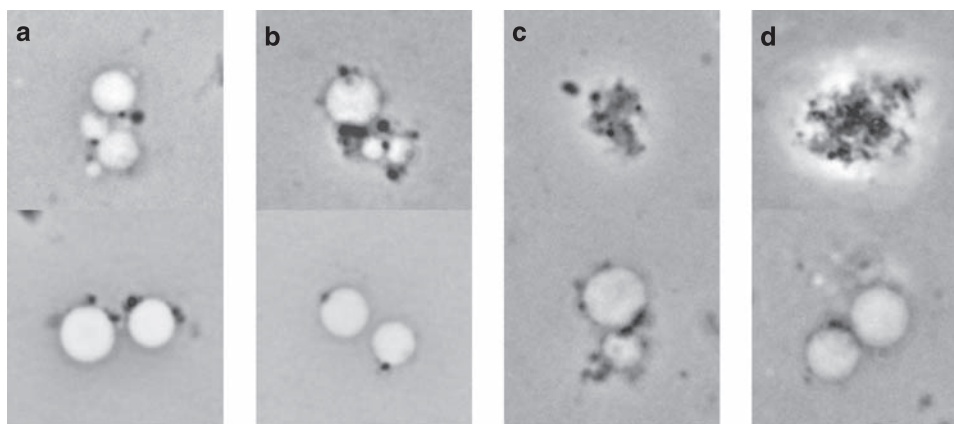


Figure 6 The disruptive effects of AmB, allicin and their combination on isolated vacuoles obtained from *C. albicans* cells. Vacuoles from untreated (top) and ergosterol-enriched cells (bottom) were incubated with 10 μM (a, b) and 20 μM AmB (c, d), respectively, in the absence (a, c) and presence of 120 μM allicin (b, d) at 37 $^{\circ}\text{C}$ for 60 min. Vacuoles were observed under a bright-field microscope.

Table 1 Subcellular localization of AmB in *C. albicans* cells

| Cells | Addition of allicin | AmB content (nmol) ^a in | | |
|---------------------|---------------------|------------------------------------|-----------------|----------------------------|
| | | Supernatant | Plasma membrane | Cytoplasm |
| Untreated | – | 1.0 \pm 0.2 | 16.2 \pm 0.3 | 2.6 \pm 0.3 ^b |
| | + | 0.5 \pm 0.2 | 16.1 \pm 0.6 | 2.4 \pm 0.2 ^b |
| Ergosterol-enriched | – | 0.5 \pm 0.1 | 16.5 \pm 1.1 | 2.3 \pm 0.2 ^b |
| | + | 0.3 \pm 0.1 | 16.7 \pm 1.1 | 2.2 \pm 0.2 ^b |

Data are expressed as the mean \pm s.d. of the AmB content in each fraction measured in triplicate assays. The AmB content of each cytoplasmic fraction is statistically analyzed by Student's *t*-test, in which $P < 0.05$ is considered statistically significant.

^aThe total quantity of AmB initially added to the assay mixture (1.0 ml) was 20 nmol.

^bNo significant difference between each of these values.

enriched in the plasma membrane. We thus examined the effects of allicin on subcellular localization of AmB by measuring its contents in various fractions obtained from untreated and ergosterol-enriched cells. In this experiment, the concentrations of AmB and allicin were increased up to 20 and 240 μM , respectively, with increasing cell density up to 1×10^8 cells ml^{-1} owing to the sensitivity of HPLC analysis. In untreated cells, AmB was mostly absent in the supernatant of the cell suspension when incubated with AmB alone for 60 min, and it was detected in the plasma membrane fraction at a ratio of more than 80% of the initial quantity that was added to the cells (Table 1). This can be explained by the binding of AmB to plasma membrane ergosterol. The remaining antibiotic was quantitatively recovered from the cytoplasmic fraction; this confirmed its penetration across the plasma membrane and into the cytoplasm. Apart from the finding that allicin enhanced AmB-induced vacuole disruption, this compound did not influence the subcellular localization of AmB. AmB penetrated into and across the plasma membrane of ergosterol-enriched cells as effectively as untreated cells, wherein its subcellular localization pattern remained unchanged both in the absence and presence of allicin.

Effect of allicin on subcellular localization of ergosterol

We finally confirmed the role of allicin in its enhancement effect on the fungicidal activity of AmB against *C. albicans* in terms of its effect

on subcellular localization of ergosterol. As shown in Figure 7, ergosterol was more brightly visualized in the plasma membrane than faintly stained cytoplasm of untreated cells, whereas this molecule was predominantly detected in the cytoplasm when cells are treated with AmB at a non-lethal concentration (Figures 7a and b). The intracellular localization of ergosterol was more clearly visualized in cells treated with AmB at a lethal concentration though its mobilization into the cytoplasm failed in protection against the vacuole disruption (Figure 7c). Ergosterol still remained in the plasma membrane when allicin was simultaneously added with AmB to enhance its vacuole-targeting fungicidal activity (Figure 7d).

DISCUSSION

It has been widely accepted that the fungicidal activity of AmB is a result of channel formation across the plasma membrane after the antibiotic selectively binds to ergosterol, thereby enhancing the leakage of intracellular K^+ and other ionic substances.^{2–4} Oxidative stress induction is also considered to be an AmB-induced cytotoxic event although it remains unclear whether this event is caused by auto-oxidation or the ionophoric property of the antibiotic.² We previously reported that allicin enhances the fungicidal activity of Cu^{2+} against *S. cerevisiae* in distilled water where the fungal cells are rendered extremely sensitive to this divalent cation.²⁴ Cu^{2+} -induced toxicity is characterized by intracellular ROS production, plasma membrane peroxidation and subsequent damage due to plasma membrane disruption, but the enhancement effect of allicin on this event was not simply elucidated by the enhancement of oxidative stress induction.²⁵ This also suggested the involvement of a lethal event other than plasma membrane phospholipid peroxidation in the enhancement effect of allicin on AmB lethality against *C. albicans*. On the other hand, An *et al.*¹⁶ attempted to use allicin in AmB-dependent chemotherapy for candidiasis, but insisted that allicin enhances AmB-induced plasma membrane phospholipid peroxidation in *C. albicans* cells. Unlike the case with its invasive growth in mammalian organs, however, the *in vitro* experiment in the above-mentioned study was conducted under a hypoosmotic condition where the metabolic pathways, which are usually not activated under the normal growth condition, may be activated in *C. albicans* cells. This study is thus expected to provide more reliable evidence of AmB lethality as well as its enhancement by allicin against *C. albicans* cells in RPMI 1640 medium at 37 $^{\circ}\text{C}$.

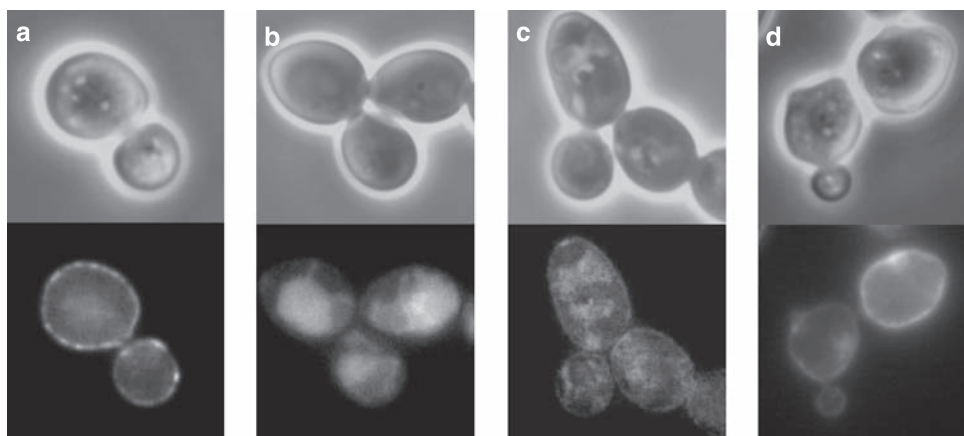


Figure 7 The effect of allicin on subcellular localization of ergosterol in *C. albicans* cells. Cells ($1 \times 10^7 \text{ ml}^{-1}$) were incubated in RPMI 1640 medium containing none (a), $0.25 \mu\text{M}$ AmB (b), $2 \mu\text{M}$ AmB (c) and a combination of $0.25 \mu\text{M}$ AmB and $120 \mu\text{M}$ allicin (d) at 37°C for 60 min. Cells were then fixed with 3% paraformaldehyde, incubated with $50 \mu\text{g ml}^{-1}$ filipin III, and observed under a phase-contrast microscope (top) and a fluorescence microscope (bottom).

Vacuoles are organelles that are involved in osmoregulation, ion homeostasis and cell volume regulation in fungal cells.^{26,27} Various hydrolytic enzymes, including proteases and nucleases, are thought to accumulate in vacuoles; hence, the damage to these organelles is considered to be a critical step in cell death induction.²⁸ In addition, the sudden loss of vacuoles would result in increased sensitivity to osmotic imbalance in the cytoplasm, especially in cells with impaired plasma membrane ion transport. Vacuole disruption was observed in *S. cerevisiae* cells treated with the polyene macrolide antibiotic niphimycin (NM) characterized by a macrocyclic lactone ring containing alkyguanidium.²⁹ A synthetic analog of this side chain could also render *S. cerevisiae* cells sensitive to the lethal effects of AmB, and this effect was indeed accompanied by enhanced vacuole disruption. PMB is a bactericidal antibiotic that can selectively inhibit the growth of Gram-negative bacteria by altering bacterial plasma membrane permeability and is weakly effective against fungal strains such as *S. cerevisiae*.^{13,14} Alternatively, allicin can enhance the fungicidal activity of PMB against *S. cerevisiae* and other fungal strains, including filamentous fungi such as *Aspergillus fumigatus*.¹³ The enhancement of the fungicidal activity of PMB by allicin was accompanied by enhanced vacuole disruption. As deduced from the similarity in the modes of action of AmB, niphimycin and PMB on ion transport through the plasma membrane, the vacuole disruptive activities of these antibiotics are likely to depend on cellular osmotic imbalance because of the leakage of K^+ in addition to their direct disruptive actions on the organelles. To our knowledge, this study is the first of its kind to reveal that enhanced vacuole disruption induced by AmB at a lethal concentration ($2 \mu\text{M}$) and at a non-lethal concentration ($0.25 \mu\text{M}$) in combination with allicin could be lethal against the pathogenic fungus *C. albicans*.

The vacuoles isolated from *C. albicans* cells are subjected to the direct disruptive action of the antibiotic at the lower concentration than is needed for disruption of the organelles from *S. cerevisiae* cells. However, there has been no clear evidence on the cellular uptake of AmB across the plasma membrane and into the cytoplasm. Although the enhancement of AmB-induced vacuole disruption by allicin is independent of this process, we for the first time demonstrated the accumulation of AmB in the cytoplasm of *C. albicans* cells. The AmB resistance of the ergosterol-enriched cells could therefore be attributed to the elevated resistance of the ergosterol-enriched vacuole rather

than an increase in the ergosterol content of the plasma membrane. In spite of such evidence that supports the direct interaction between AmB and the vacuoles, the concentration of AmB required for the direct disruptive action on the organelles ($20 \mu\text{M}$) was apparently higher than the extracellular concentration that resulted in vacuole disruption ($2 \mu\text{M}$). The high AmB concentration for the direct disruptive action may be attributed to the use of concentrated vacuoles in the assay, otherwise this may be elucidated by reduced interaction between AmB and its molecular target possibly in the vacuole membrane under the hypertonic condition used for the maintenance of vacuole architecture. Filipin III, a polyene macrolide antibiotic, is used as a fluorescent probe to determine the subcellular localization of ergosterol in *S. cerevisiae*.¹⁵ This fluorescent probe could visualize ergosterol in the plasma membrane of intact cells and its mobilization into the cytoplasmic compartment in response to AmB treatment. As in the case with *S. cerevisiae*, the enhancement effect of allicin on AmB lethality as well as vacuole disruption (see Figures 2b and 4e) was accompanied by the inhibition of ergosterol transport from the plasma membrane into the cytoplasm of *C. albicans* cells (see Figure 7d). Taking into consideration that ergosterol treatment prevented the enhancement of AmB lethality by allicin, we propose that allicin enhances the vacuole-targeting fungicidal activity of AmB against this pathogenic fungus by inhibiting a mechanism of intracellular ergosterol transport.

ACKNOWLEDGEMENTS

This work was supported in part by a Grant-in-Aid for Scientific Research (C) (No. 20580083) from the Japan Society for the Promotion of Science.

- Dupont, P. F. *Candida albicans*, the opportunist A cellular and molecular perspective. *J. Am. Podiatr. Med. Assoc.* **85**, 104–115 (1995).
- Brajtburg, J., Powderly, W. G., Kobayashi, G. S. & Medoff, G. Amphotericin B: Current understanding of mechanisms of action. *Antimicrob. Agents Chemother.* **34**, 183–188 (1990).
- Ellis, D. Amphotericin B: spectrum and resistance. *J. Antimicrob. Chemother.* **49**, 7–10 (2002).
- Baginski, M., Sternal, K., Czub, J. & Borowski, E. Molecular modelling of membrane activity of amphotericin B, a polyene macrolide antifungal antibiotic. *Acta Biochimica Polonica* **52**, 655–658 (2005).
- Alonso, M. A., Vázquez, D. & Carrasco, L. Compounds affecting membranes that inhibit protein synthesis in yeast. *Antimicrob. Agents Chemother.* **16**, 750–756 (1979).

- 6 Chen, W. C., Chou, D. L. & Feingold, D. S. Dissociation between ion permeability and the lethal action of polyene antibiotics on *Candida albicans*. *Antimicrob. Agents Chemother.* **13**, 914–917 (1978).
- 7 Okamoto, Y., Aoki, S. & Mataga, I. Enhancement of amphotericin B activity against *Candida albicans* by superoxide radical. *Mycopathologia* **158**, 9–15 (2004).
- 8 Ogita, A., Fujita, K., Taniguchi, M. & Tanaka, T. Enhancement of the fungicidal activity of amphotericin B by allicin, an allyl-sulfur compound from garlic, against the yeast *Saccharomyces cerevisiae* as a model system. *Planta Med.* **72**, 1247–1250 (2006).
- 9 Ankri, S. & Mirelman, D. Antimicrobial properties of allicin from garlic. *Microbes Infect.* **1**, 125–119 (1999).
- 10 Oommen, S., Anto, J. R., Srinivas, G. & Karunakaran, D. Allicin (from garlic) induces caspase-mediated apoptosis in cancer cells. *Eur. J. Pharmacol.* **485**, 97–103 (2004).
- 11 Briggs, W. H., Xiao, H., Parkin, K. L., Shen, C. & Goldman, I. L. Differential inhibition of human platelet aggregation by selected *Allium* thiosulfinates. *J. Agric. Food Chem.* **48**, 5731–5735 (2000).
- 12 Gebhardt, R. & Beck, H. Differential inhibitory effects of garlic-derived organosulfur compounds on cholesterol biosynthesis in primary rat hepatocyte cultures. *Lipids*. **31**, 1269–1276 (1996).
- 13 Ogita, A., Nagao, Y., Fujita, K. & Tanaka, T. Amplification of vacuole-targeting fungicidal activity of antibacterial antibiotic polymyxin B by allicin, an allyl sulfur compound from garlic. *J. Antibiot.* **60**, 511–518 (2007).
- 14 Ogita, A., Konishi, Y., Borjhan, B., Fujita, K. & Tanaka, T. Synergistic fungicidal activities of polymyxin B and ionophores, and their dependence on direct disruptive action of polymyxin B on fungal vacuole. *J. Antibiot.* **62**, 81–87 (2009).
- 15 Ogita, A., Fujita, K. & Tanaka, T. Enhancement of the fungicidal activity of amphotericin B by allicin: Effects on intracellular ergosterol trafficking. *Planta Med.* **75**, 222–226 (2009).
- 16 An, M. *et al.* Allicin enhances the oxidative damage effect of amphotericin B against *Candida albicans*. *Int. J. Antimicrob. Agents* **33**, 258–263 (2008).
- 17 Cruz, M. C. *et al.* Calcineurin is essential for survival during membrane stress in *Candida albicans*. *EMBO J* **21**, 546–549 (2002).
- 18 Bryant, N. J. & Stevens, T. H. Vacuole biogenesis in *Saccharomyces cerevisiae*: protein transport pathways to the yeast vacuole. *Microbiol. Mol. Biol. Rev.* **62**, 230–247 (1998).
- 19 Ohsumi, Y. & Anraku, Y. Active transport of basic amino acids driven by a proton motive force in vacuolar membrane vesicles of *Saccharomyces cerevisiae*. *J. Biol. Chem.* **256**, 2079–2082 (1981).
- 20 Tabuchi, M. *et al.* Vacuolar protein sorting in fission yeast: cloning, biosynthesis, transport, and processing of carboxypeptidase Y from *Schizosaccharomyces pombe*. *J. Bacteriol.* **179**, 4179–4189 (1997).
- 21 Machida, K., Tanaka, T., Fujita, K. & Taniguchi, M. Farnesol-induced generation of reactive oxygen species via indirect inhibition of mitochondrial electron transport chain in the yeast *Saccharomyces cerevisiae*. *J. Bacteriol.* **180**, 4460–4465 (1998).
- 22 Takahashi, M., Shibata, M. & Niki, E. Estimation of lipid peroxidation of live cells using a fluorescent probe, iphenyl-1-pyrenylphosphine. *Free Radic. Biol. Med.* **31**, 164–174 (2001).
- 23 Esposito, E., Bortolotti, F., Menegatti, E. & Cortesi, R. Amphiphilic association systems for amphotericin B delivery. *Int. J. Pharm.* **260**, 249–260 (2003).
- 24 Ogita, A. *et al.* Synergistic fungicidal activity of Cu²⁺ and allicin, an allyl sulfur compound from garlic, and its relation to the role of alkyl hydroperoxide reductase 1 as a cell surface defense in *Saccharomyces cerevisiae*. *Toxicology*. **215**, 205–213 (2005).
- 25 Ogita, A., Fujita, K., Taniguchi, M. & Tanaka, T. Dependence of synergistic fungicidal activity of Cu²⁺ and allicin, an allyl sulfur compound from garlic, on selective accumulation of the ion in the plasma membrane fraction via allicin-mediated phospholipid peroxidation. *Planta Med.* **72**, 875–880 (2006).
- 26 Thumm, M. Structure and function of the yeast vacuole and its role in autophagy. *Microsc. Res. Tech.* **51**, 563–572 (2000).
- 27 Wickner, W. Yeast vacuoles and membrane fusion pathways. *EMBO J.* **21**, 1241–1247 (2002).
- 28 Obara, K., Kuriyama, H. & Fukuda, H. Direct evidence of active and rapid nuclear degradation triggered by vacuole rupture during programmed cell death in *Zinnia*. *Plant Physiol.* **125**, 615–626 (2001).
- 29 Ogita, A. *et al.* Synergistic fungicidal activities of amphotericin B and *N*-methyl-*N'*-dodecylguanidine: a constituent of polyol macrolide antibiotic niphimycin. *J. Antibiot.* **60**, 27–35 (2007).

ORIGINAL ARTICLE

Isolation, structure and biological activities of platensimycin B₄ from *Streptomyces platensis*

Chaowei Zhang, John Ondeyka, Ziqiang Guan, Lisa Dietrich, Bruce Burgess, Jun Wang¹ and Sheo B Singh

Platensimycin and platencin are inhibitors of FabF and FabF/H bacterial fatty acid synthesis enzymes, respectively. Discovery of natural congeners provides one of the ways to understand the relationship of chemical structure and biological function. Efforts to discover the natural analogs of platensimycin by chemical screening led to the isolation of platensimycin B₄, a glucoside congener of platensimycin. This analog showed significantly attenuated activity and critically defined the limited binding space around the aromatic ring and established the importance of the free phenolic and carboxyl group for the activity.

The Journal of Antibiotics (2009) 62, 699–702; doi:10.1038/ja.2009.106; published online 13 November 2009

Keywords: antibiotic; FabF inhibitor; FAS II inhibitor; fatty acid synthesis inhibitor; platensimycin B₄; *Streptomyces platensis*

INTRODUCTION

The discovery of platensimycin (1) and platencin (2) (Figure 1) from various strains of *Streptomyces platensis* generated significant excitement within the antibiotic research community.^{1–4} Discovery of these compounds was possible due to the design and introduction of a novel antisense differential sensitivity screening strategy in which FabH/FabF was sensitized.^{3–6} Platensimycin is a selective inhibitor of the FabF acyl-enzyme intermediate and platencin is a balanced dual inhibitor of both FabH and FabF. Both of these compounds showed potent *in vitro* activities in both cell-free and whole-cell assay systems. The *in vitro* activities translated well in an animal model when dosed with intravenous continuous infusion. However, lack of *in vivo* activity was observed under conventional administration due to poor systemic exposure. To improve PK properties and *in vivo* efficacy various approaches were undertaken, including chemical modification of platensimycin at some of the chemically accessible sites.^{7,8} Discovery of congeners is an alternative and complementary approach, which was also simultaneously undertaken to augment structure activity relationship studies. This approach has allowed us the discovery of a number of congeners including platensimide A,⁹ homoplatensimide A,¹⁰ platensimycin B₁–B₃,¹¹ platensimycin A₁¹² and platencin A₁.¹³

Continued searching for additional congeners and related analogs from a large-scale fermentation of *S. platensis* by chemical screening led to the isolation of a new platensimycin glucoside (3a) and its methyl ester (3b) (Figure 1). This compound provided critical information about the scope of substitutions in the aromatic ring and their relationship to the antibacterial activity. The isolation, structure elucidation and biological activity of 3a and 3b are herein described.

RESULTS AND DISCUSSION

Streptomyces platensis MA7327 was fermented in 70 l stirred tanks for 9 days on CLA production medium (consisting of g/l, yellow corn meal, 40, lactose, 40, ambrerex pH 5, antifoaming agent (P2000), 0.8 ml/l; 3% inoculum) and was extracted with MeOH at pH 2.7. The extract was chromatographed on reversed phase Amberchrome resin and eluted with a step gradient of aqueous MeOH. The late-eluting fractions were basified to pH 9, extracted with CH₂Cl₂ and chromatographed on a reversed phase C₈ HPLC to afford 3a (9.2 mg, 0.21 mg/l) and 3b (7.2 mg, 0.17 mg/l) both as amorphous powders.

Platensimycin B₄ (3a) produced parent ions at *m/z* 626 [M+Na] and *m/z* 602 [M-H] in positive and negative ion modes, respectively, suggesting a molecular weight of 603. High resolution electrospray ionization Fourier transformation mass spectrometry analysis showed a protonated molecular ion at *m/z* 604.2372 (M+H) and afforded a molecular formula of C₃₀H₃₇NO₁₂, which differed from platensimycin by C₆H₁₀O₅. The formula was supported by the ¹³C NMR spectrum (Table 1), which showed the presence of 30 resonances and looked similar to platensimycin with the presence of six additional all oxygenated resonances. The IR spectrum showed the presence of the absorption bands for hydroxy group, conjugated ketone, carboxylic acid and aromatic systems. The UV spectrum showed three absorption bands (λ_{\max} 217, 245 and 295 nm), which differed from platensimycin, indicating minor changes in the aromatic moiety. The electrospray ionization MS spectrum showed a fragment ion at *m/z* 273, characteristic of the fragment ion for platensimycin moiety due to the cleavage of the amide bond (Figure 2). The ¹H and ¹³C NMR spectra of 3a were identical to the corresponding spectra of platensimycin, except for the presence of additional resonances corresponding to six

Merck Research Laboratories, Rahway, NJ, USA

¹Current address: Sundia MediTech Company Ltd, Building 8, 388 Jialilue Road, Zhangjiang Hightech Park, Shanghai 201203, China.

Correspondence: Dr SB Singh, Medicinal Chemistry, Merck Research Laboratories, Merck Res Labs, 126 E. Lincoln Ave, Rahway, NJ 07065, USA.

E-mail: sheo_singh@merck.com

Received 17 August 2009; revised 13 October 2009; accepted 15 October 2009; published online 13 November 2009

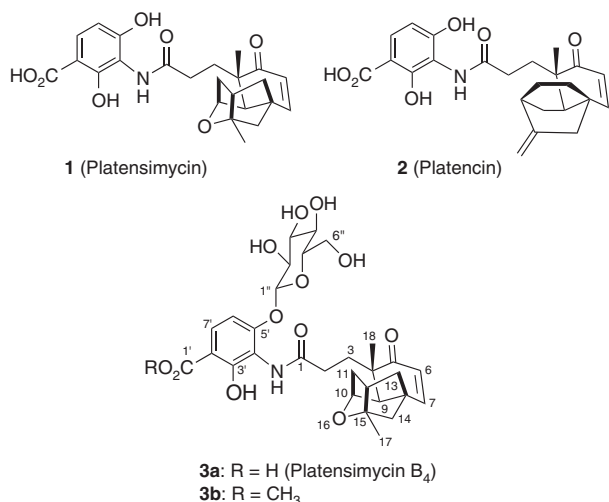


Figure 1 Structures of platensimycin, platencin and platensimycin B₄.

additional carbons and associated protons. The presence of intact platensimycin was confirmed by COSY, total correlation spectroscopy, heteronuclear multiple quantum coherence and heteronuclear multiple bond coherence (HMBC) correlations. The five of the six addition carbons present in the ¹³C NMR spectrum resonated in between δ_C 62.3 and 78.0 p.p.m., and the sixth carbon resonated at δ_C 102.6 p.p.m. The last carbon correlated with a doublet (*J* = 7.4 Hz) appearing at δ_H 4.98 (H-1''), indicative of an anomeric carbon. The double quantum-filtered COSY and total correlation spectroscopy correlations confirmed the presence of a hexose moiety, which was elucidated to a glucoside by HSQC and HMBC correlations. The anomeric proton showed HMBC correlation to C-5'', thus confirming a pyranoside. All protons of the sugar moiety showed large couplings suggesting that all substitutions of the hexose moiety were equatorial, thus confirming the presence of glucoside. The anomeric proton δ_H 4.98 showed an HMBC correlation to the oxygenated aromatic carbon C-5' (δ_C 157.1), thus establishing the glycosidic linkage at C-5'. This was further supported by the NOE enhancements of H-6' on irradiation of the anomeric proton (δ_H 4.98), which also showed NOEs to H-3'' and H-5'', confirming the β-D-glucoside configuration. These NOEs were also confirmed in the methyl ester (3b). In addition, irradiation of H-6' of 3b exhibited NOE to H-1'' further corroborating the glycosidic linkage at C-5'. The mass spectrum of methyl ester 3b showed a molecular weight of 617, which was up by a 14 a.m.u. (CH₂). The ¹H and ¹³C NMR spectrum (Table 1) of 3b was identical to 3a, except for the presence of a methoxy signal assigned for the methyl ester δ_C 52.9 (δ_H 3.92, s). The methoxy singlet (δ_H 3.92) displayed an HMBC correlation to the C-1' carbonyl, thus confirming the methyl ester. On the basis of these data structure 3a, a platensimycin-5'-β-D-glucoside was assigned to platensimycin B₄.

Biological activity

Platensimycin B₄ (3a) and the methyl ester (3b) were evaluated in various *in vitro* cell-free and cell-based assays and the results are summarized below. In the *Staphylococcus aureus* cell-free FASII assay,¹⁴ which measures the inhibitory activity of compounds against fatty acid synthesis, 3a and 3b showed IC₅₀ values of 160 and 40 μg/ml (320- and 80-fold less active than platensimycin), respectively. Similar results were also obtained against saFabH assay, in which 3a and 3b showed IC₅₀ values of 100 and 35 μg/ml, respectively. The two-

three-fold better activity exhibited by the methyl ester was somewhat surprising and is in odds with platensimycin and its methyl ester. Compounds 3a and 3b each showed very poor antibacterial activity minimum detection concentration (defined by minimum concentration of the compound showing differential zone of clearance between antisense plates compared with control plate)⁵ of 1000 μg ml⁻¹ in the most sensitive (antisense two-plate differential sensitivity) assay, which is 25 000-fold worse than platensimycin.¹ As these compounds showed poor activity in all of the assays described above, it was not surprising that they did not show any antibacterial activity against wild-type *S. aureus* and many other bacterial strains at less than 64 μg ml⁻¹. In cell-free FASII assay, 3b and 3a were only 80- and 320-fold less active than platensimycin; however, their antibacterial activity against most sensitive antisense assay was 25 000 poorer than that of platensimycin. This suggested that 5'-glucosylation not only decreases enzyme inhibition activity but may also have blocked the entry to bacterial cells.^{15,16} The loss of activity of platensimycin B₄ could be easily attributed to the loss of water-mediated hydrogen bond of C-5' hydroxy group, as observed in the platensimycin bound X-ray crystal structure (Figure 3).

In summary, we have described the isolation, structure elucidation and biological characterization of platensimycin B₄ and its methyl ester. Platensimycin B₄, a 5'-glucosyl derivative of platensimycin, lost all of the antibacterial activity and has shown significant attenuation of cell-free activity suggesting that the bulky polar groups at C-5' are not tolerated for the biological activities.

METHODS

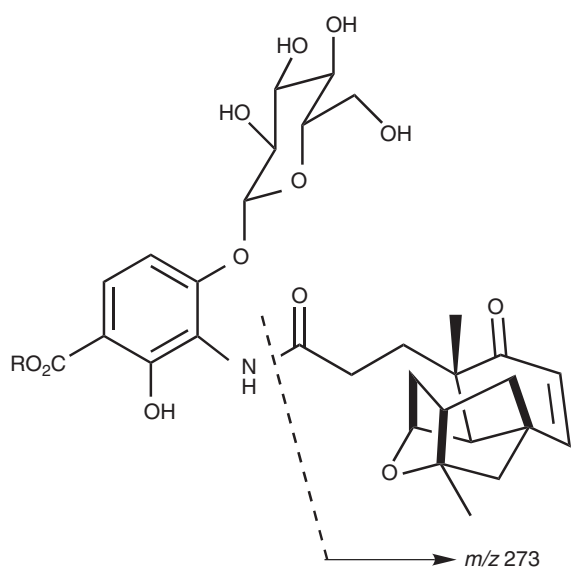
Optical rotations were measured with a Perkin-Elmer 241 polarimeter (Perkin-Elmer, Waltham, MA, USA). UV spectra were recorded on a Beckman DU-70 spectrophotometer (Beckman, Rockville, MD, USA). IR spectra were recorded with a Perkin-Elmer Spectrum One FT-IR spectrophotometer. All NMR spectra were recorded with a Varian Unity 500 (¹H, 500 MHz, ¹³C, 125 MHz) spectrometer (Varian, Palo Alto, CA, USA). The residual protons of solvents were used as internal reference (DMSO-*d*₆ δ_H 2.49, δ_C 39.5; C₅D₅N δ_H 8.74, δ_C 150.35). The COSY, double quantum-filtered COSY, DEPT, total correlation spectroscopy, heteronuclear multiple quantum coherence and HMBC spectra were measured using standard Varian pulse sequences. Electrospray ionization MS data were recorded on an Agilent 1100 MSD (Agilent, Santa Clara, CA, USA) with ESI ionization. High resolution electrospray ionization Fourier transformation mass spectrometry was acquired on a Thermo Finnigan LTQ-FT (Thermo Fisher Scientific, Waltham, MA, USA) with the standard Ion Max API source (without the sweep cone) and ESI probe. Three scan events were used. The ion trap was scanned from 150 to 2000 first in negative ion mode and then in positive ion mode. The FT was scanned from 200 to 2000 in the positive ion mode only. In all cases, the SID was set to 18 V to try to reduce multiple ion clusters. Instrument resolution is set to 100,000 at *m/z* 400. No internal calibration was required; the instrument was calibrated once a week and checked daily to assure accuracy. An Agilent HP1100 instrument was used for analytical HPLC.

Fermentation condition

A 1 ml frozen suspension of *S. platensis* MA7327 (ATCC PTA-5316) was inoculated in 50 ml ATCC-2 seed medium (2% inoculum) in a 250 ml baffled Erlenmeyer flask and incubated at 28 °C at 220 r.p.m. on a shaker for 48 h. The second stage seed was developed by aseptic transfer of 8 ml broth from the stage-1 seed into three 2 l non-baffled Erlenmeyer flasks, containing 500 ml of ATCC-2 medium (consisting of in g per l, starch, 20, dextrose, 10, NZ amine type E, 5, beef extract, 3, peptone, 5, yeast extract, 5, calcium carbonate, 1) each (1.6% inoculum), and cultivated for 48 h at 180 r.p.m. shaker speed at 28 °C. Pooled contents from all three flasks (1500 ml) were transferred into 50 l of 'CLA' production medium in a 70 l fermentation tank. The production batch (43 l volume) was harvested after 9 days at 5 psig pressure, 300 r.p.m. agitation, 7 slpm airflow at 28 °C.

Table 1 ¹H (500 MHz) and ¹³C (125 MHz) NMR assignment of platensimycin B₄ (3a) and methyl ester 3b in CD₃OD

| No. | 3a | | | | 3b | | | |
|-----|----------------|-----------------|--|---------------------|----------------|--|---------------------|--|
| | δ _C | Type | δ _H | HMBC (H → C) | δ _C | δ _H | HMBC (H → C) | |
| 1 | 175.1 | C° | | | 175.0 | | | |
| 2 | 32.3 | CH ₂ | 2.42, m; 2.31, ddd, 14.5, 13.6, 4.1 | | 32.2 | 2.40, m; 2.28, m | | |
| 3 | 32.9 | CH ₂ | 2.26, dd, 14.5, 3.4; 1.86, m | | 32.9 | 2.28, m; 1.86, m | | |
| 4 | 47.8 | C° | | | 47.8 | | | |
| 5 | 205.9 | C° | | | 205.7 | | | |
| 6 | 127.9 | CH | 5.90, d, 10.0 | C-8 | 127.9 | 5.90, d, 10.0 | C-8 | |
| 7 | 156.1 | CH | 6.64, d, 10.0 | C-5, 9, 14 | 156.1 | 6.65, d, 10.0 | C-5, 9, 14 | |
| 8 | 47.3 | C° | | | 47.3 | | | |
| 9 | 47.2 | CH | 2.41, brs | C-8, 10, 11, 13, 18 | 47.2 | 2.41, brs | C-8, 10, 11, 13, 18 | |
| 10 | 77.6 | CH | 4.52, brs | | 77.6 | 4.51, brs | | |
| 11 | 41.5 | CH ₂ | 2.07, d, 11.5 | C-15 | 41.4 | 2.08, d, 11.7 | C-15 | |
| 12 | 46.1 | CH | 2.41, m | | 46.1 | 2.42, m | | |
| 13 | 43.9 | CH ₂ | 1.84, m; 2.05, dd, 11.5, 3.5 | | 43.9 | 1.84, m; 2.06, dd, 11.6, 2.6 | | |
| 14 | 55.8 | CH ₂ | 1.72, d, 11.1; 1.80, dd, 11.8, 3.4 | | 55.8 | 1.73, d, 11.7; 1.80, dd, 11.3, 3.2 | | |
| 15 | 88.7 | C° | | | 88.7 | | | |
| 17 | 23.2 | CH ₃ | 1.41, s | C-12, 14, 15 | 23.2 | 1.42, s | C-12, 14, 15 | |
| 18 | 25.1 | CH ₃ | 1.25, s | C-3, 4, 5, 9 | 25.1 | 1.25, s | C-3, 4, 5, 9 | |
| 1 | 175.6 | C° | | | 171.5 | | | |
| 2 | 114.7 | C° | | | 108.7 | | | |
| 3 | 159.4 | C° | | | 159.2 | | | |
| 4 | 115.5 | C° | | | 115.5 | | | |
| 5 | 157.1 | C° | | | 159.3 | | | |
| 6 | 105.6 | CH | 6.66, d, 9.0 | C-2, 4, 5' | 107.6 | 6.80, d, 9.0 | C-2, 4, 5' | |
| 7 | 130.7 | CH | 7.77, d, 9.0 | C-1, 3, 5' | 130.5 | 7.78, d, 9.0 | C-1, 3, 5' | |
| 8 | — | NH | — | | | | | |
| 9 | — | OMe | — | | 52.9 | 3.92, s | C-1 | |
| 1 | 102.6 | CH | 4.98, d, 7.4 | C-5' | 102.4 | 5.02, d, 7.0 | C-5 | |
| 2 | 78.0 | CH | 3.46, m | | 78.0 | 3.47, m | | |
| 3 | 78.2 | CH | 3.50, t, 9.5 | | 78.3 | 3.47, m | | |
| 4 | 71.1 | CH | 3.43, t, 9.5 | | 71.0 | 3.39, dd, 9.0 | | |
| 5 | 74.7 | CH | 3.46, m | | 74.7 | 3.47, m | | |
| 6 | 62.3 | CH ₂ | 3.72, dd, 12.0, 5.0; 3.87, dd, 12.0, 2.0 | | 62.4 | 3.69, dd, 12.1, 5.5; 3.87, dd, 12.1, 2.0 | | |

**Figure 2** Electrospray ionization MS fragmentation of platensimycin B₄.**Isolation of platensimycin B₄ (3a) and methyl ester (3b)**

The fermentation broth (431) was diluted with 29 l methanol and shaken for 60 h at room temperature. The mixture was then centrifuged in 11 bottles at 5000 r.p.m. for 45 min. The supernatant was diluted to 40% methanol; the pH was adjusted to 2.7 with 2N HCl and concentrated to a volume of 11 l using a 500 kDa ultrafiltration membrane. The filtrate (11 l, aqueous-MeOH ratio 60:40) was charged directly on to a 1.6 l Amberchrome column. The column was eluted with a step gradient of 40–100% aqueous methanol with 10% increments of MeOH. Two 600 ml fractions were collected from each 10% MeOH increments affording 14 fractions (Amberchrome fractions 1–14). Amberchrome fractions 10–12 eluting with 80–90% MeOH were pooled and concentrated under reduced pressure, to remove most of the MeOH, to a volume of 200 ml mostly containing water. Water (300 ml) was added to this extract to produce a final volume of 500 ml, which was basified to pH ~9 by addition of solid sodium bicarbonate. The basic solution was extracted three times with methylene chloride (3 × 450 ml). The methylene chloride extract was dried over anhydrous Na₂SO₄ and filtered. Solid Na₂SO₄ was washed with small amount of MeOH. MeOH and CH₂Cl₂ filtrates were concentrated separately under reduced pressure to give 0.314 g (MeOH fraction) and 1.77 g (CH₂Cl₂ fraction), respectively. The MeOH fraction was chromatographed by reversed-phase HPLC (Zorbax C₈, 21.2 × 250 mm, 40 min gradient of 20–80% aqueous CH₃CN, each containing 0.05% TFA at 10 ml/min). Fraction eluting at 13 min was lyophilized to yield 9.2 mg (0.21 mg/l) of platensimycin B₄ (3a) as an amorphous powder.

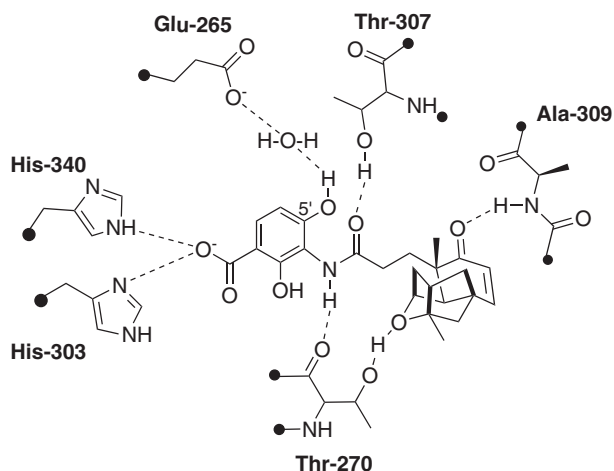


Figure 3 Graphical representation of platensimycin binding with *Escherichia coli* FabF, as observed in the platensimycin bound X-ray crystal structure of ecFabF (C163Q).

The CH₂Cl₂ fraction (1.77 g) was chromatographed on a 11 Sephadex LH-20 (GE Health Care Bio-Sciences AB, Uppsala, Sweden) column and eluted with a step gradient of one column volume each of hexane/CH₂Cl₂ (1:4), acetone:CH₂Cl₂ (1:4) and acetone/CH₂Cl₂ (3:2) at a flow rate 10 ml/min. The column was unpacked and LH20 was washed with MeOH. All fractions were analyzed by silica gel TLC and reversed phase HPLC before pooling. The methanol wash fraction was concentrated to give 224.5 mg residue, which was chromatographed on reversed-phase HPLC (Zorbax C₈, 21.2×250 mm, eluted with 25% aqueous CH₃CN with 0.05% TFA for 40 min followed by a 40 min gradient of 25–100% aqueous CH₃CN at 10 ml/min). Fractions eluting at 37–40 min were pooled and extracted with EtOAc. EtOAc extract was concentrated to furnish 7.2 mg (0.17 mg/l) of the methyl ester **3b** as an amorphous powder. **3a**: [α]_D²³ -28 (c, 0.5, MeOH), UV (MeOH) λ_{max} 217 (ϵ 14 665), 245 (8040), 295 (2815) nm, FTIR (ZnSe) 3284, 2929, 1676 (br, strong), 1440, 1277, 1206, 1138 cm⁻¹ electrospray ionization MS (m/z) 626 [M+Na], 442 [M-glu+H], 273; 602 [M-H]; high resolution electrospray ionization Fourier transformation mass spectrometry (m/z) 604.2372 (calcd for C₃₀H₃₇NO₁₂+H: 604.2316), for ¹H and ¹³C NMR see Table 1. **3b**: [α]_D²³ -56 (c 0.5, MeOH), UV (MeOH) λ_{max} 221 (ϵ 24 830), 250 (13 611), 301 (4405) nm, FTIR (ZnSe) 3320, 2958, 1672 (br, strong), 1503, 1440, 1337, 1279, 1203, 1074 cm⁻¹, electrospray ionization MS (m/z) 640 [M+Na], 600, 456, 273; 730 [M+TFA-H]; 616 [M-H]; high resolution electrospray ionization Fourier transformation mass spectrometry (m/z) 618.2531 (calcd for C₃₁H₃₉NO₁₂+H: 618.2550), for ¹H and ¹³C NMR see Table 1.

FabF_{2p} Assay

Staphylococcus aureus cells (RN450) carrying plasmid S1–1941 bearing antisense to FabF (*fabF* AS-RNA strain) or vector (control strain) were inoculated from a frozen vial source into a tube containing 3 ml of Miller's LB Broth (Invitrogen, Carlsbad, CA, USA) plus 34 µg/ml of chloramphenicol. Tubes were incubated at 37 °C at 220 r.p.m. for 18–20 h and kept at room temperature until use. Miller's LB broth was supplemented with 1.2% Select agar (Invitrogen), 0.2% glucose, 15 µg/ml chloramphenicol and 50 mM of xylose (for the antisense strain only). The OD₆₀₀ (3.0) of the culture was measured and diluted by aforementioned agar media to 1:1000 (OD₆₀₀ 0.003). Aliquots (100 ml) of agar were poured into each 20×20 cm NUNC plates, and well-caster templates placed into the agar and the agar was allowed to solidify for 30 min. Then, 20 µl of test samples were added to the wells and the plates incubated at 37 °C for 18 h and zones of inhibition measured.⁵ Minimum detection concentration values were determined by twofold serial dilution.

FASII Assay

The assay was performed in a phospholipid-coated 96-well flash plate. Briefly, 1.26 µg of the partially purified protein from *S. aureus* containing all the required fatty acid synthesis enzymes was preincubated with a serial dilution of natural products at room temperature for 20 min in 50 µl of buffer containing 100 mM sodium phosphate (pH 7.0), 5 mM EDTA, 1 mM NADPH, 1 mM NADH, 150 µM DTT, 5 mM β-mercaptoethanol, 20 µM *n*-octanoyl-CoA (or lauroyl-CoA), 4% Me₂SO and 5 µM ACP. The reaction was initiated by addition of 10 µl of water-diluted [2-¹⁴C]-malonyl-CoA, giving a final concentration of 4 µM malonyl-CoA with total counts of about 10 000 c.p.m. The reaction was incubated at 37 °C for 90 min. The reaction was terminated by adding 100 µl of 14% perchloric acid. The plates were sealed and incubated at room temperature overnight and counted for 5 min using Packard TopCount NXT scintillation counter (Packard, Meriden, CT, USA). Further details of the assay are described in the study by Kodali *et al.*¹⁴

Antibiotic assay (MIC)

The MIC against each of the strains was determined by twofold dilution as previously described^{5,14} and conducted under National Committee for Clinical Laboratory Standards (NCCLS)—now called the Clinical Laboratory Standards Institute—guidelines.^{5,14} Cells were inoculated at 10⁵ CFU/ml, followed by incubation at 37 °C with a twofold serial dilution of compounds in the growth medium for 20 h. MIC is defined as the lowest concentration of antibiotic inhibiting visible growth.

ACKNOWLEDGEMENTS

We thank S Kodali, A Galgoci, K Young, R Painter, M Motyl and K Dorso for some of the initial biological results.

- 1 Wang, J. *et al.* Platensimycin is a selective FabF inhibitor with potent antibiotic properties. *Nature*. **441**, 358–361 (2006).
- 2 Singh, S. B. *et al.* Isolation, structure, and absolute stereochemistry of platensimycin, a broad spectrum antibiotic discovered using an antisense differential sensitivity strategy. *J. Am. Soc.* **128**, 11916–11920. and 15547 (2006).
- 3 Jayasuriya, H. *et al.* Isolation and structure of platencin: a novel FabH and FabF dual inhibitor with potent broad spectrum antibiotic activity produced by *Streptomyces platensis* MA7339. *Angew. Chem. Int. Ed.* **46**, 4684–4688 (2007).
- 4 Wang, J. *et al.* Platencin is a dual FabF and FabH inhibitor with potent *in vivo* antibiotic properties. *Proc. Natl. Acad. Sci. (USA)* **104**, 7612–7616 (2007).
- 5 Young, K. *et al.* Discovery of FabH/FabF inhibitors from natural products. *Antimicrob. Agents. Chemother.* **50**, 519–526 (2006).
- 6 Singh, S. B., Phillips, J. W. & Wang, J. Highly sensitive target based whole cell antibacterial discovery strategy by antisense RNA silencing. *Curr. Opin. Drug. Disc. Dev.* **10**, 160–166 (2007).
- 7 Singh, S. B., Herath, K. B., Wang, J., Tsou, N. N. & Ball, R. G. Chemistry of platensimycin. *Tetrahedron. Lett.* **48**, 5429–5433 (2007).
- 8 Shen, H. C. *et al.* Synthesis and biological evaluation of platensimycin analogs. *Bioorg. Med. Chem. Lett.* **19**, 1623–1627 (2009).
- 9 Herath, K. B. *et al.* Structure and semisynthesis of platensimide A, produced by *Streptomyces platensis*. *Org. Lett.* **10**, 1699–1702 (2008).
- 10 Jayasuriya, H. *et al.* Structure of homoplatensimide A: a potential key biosynthetic intermediate of platensimycin isolated from *Streptomyces platensis*. *Tetrahedron. Lett.* **49**, 3648–3651 (2008).
- 11 Zhang, C. *et al.* Isolation, structure and fatty acid synthesis inhibitory activities of platensimycin B₁–B₃ from *Streptomyces platensis*. *Chem. Commun. (Camb)* 5034–5036 (2008).
- 12 Singh, S. B. *et al.* Isolation, enzyme-bound structure and antibacterial activity of platensimycin a1 from *Streptomyces platensis*. *Tetrahedron. Lett.* **50**, 5182–5185 (2009).
- 13 Singh, S. B. *et al.* Isolation, enzyme-bound structure and antibacterial activity of platencin A₁ from *Streptomyces platensis*. *Bioorg. Med. Chem. Lett.* **19**, 4756–4759 (2009).
- 14 Kodali, S. *et al.* Determination of selectivity and efficacy of fatty acid synthesis inhibitors. *J. Biol. Chem.* **280**, 1669–1677 (2005).
- 15 Young, K. & Silver, L. L. Leakage of periplasmic enzymes from envA1 strains of *Escherichia coli*. *J. Bacteriol.* **173**, 3609–3614 (1991).
- 16 Markham, P. N. & Neyfakh, A. A. Efflux-mediated drug resistance in Gram-positive bacteria. *Curr. Opin. Microbiol.* **4**, 509–514 (2001).

NOTE

JBIR-25, a novel antioxidative agent from *Hyphomycetes* sp. CR28109

Keiichiro Motohashi¹, Yasuhiro Gyobu², Motoki Takagi¹ and Kazuo Shin-ya³

The Journal of Antibiotics (2009) 62, 703–704; doi:10.1038/ja.2009.96; published online 16 October 2009

Keywords: antioxidative agent; *Hyphomycetes*; JBIR-25; radical scavenging

Active oxygen species cause many diseases such as atherosclerosis, inflammation, ischemia–reperfusion injury, rheumatoid arthritis and central nervous diseases.¹ Further, senility and cancer initiation as well as progression are also believed to involve active oxygen species.² Thus, it is expected that effective antioxidative agents may prevent the onset and development of these diseases. In the course of our screening program of novel antioxidants, we isolated a novel antioxidative agent, designated as JBIR-25 (**1**), from the culture of *Hyphomycetes* sp. CR28109. This paper describes the isolation, structural elucidation and briefly the biological activity of **1** (Figure 1).

Hyphomycetes sp. CR28109 was isolated from a soil sample collected in Ashigara, Kanagawa Prefecture, Japan, and cultured at 25 °C for 14 days in a 500-ml Erlenmeyer flask containing 80 g brown rice and 2 g oatmeal in static culture. The culture was extracted with 80% aq. Me₂CO (100 ml). After concentration *in vacuo*, the aqueous concentrate was extracted with EtOAc (three times). The organic layer was dried over Na₂SO₄ and evaporated to dryness. The residue (0.51 g) was applied to normal-phase medium pressure liquid chromatography (Purif-Pack SI-60, Moritex, Tokyo, Japan) and eluted with a gradient system of *n*-hexane–EtOAc (0–30% EtOAc) and CHCl₃–MeOH (0–50% MeOH), successively. The 5% MeOH elute fraction (25.5 mg) was further purified by the preparative reversed-phase HPLC using a PEGASIL ODS column (Senshu Pak, 20 i.d. × 150 mm, Senshu Scientific, Tokyo, Japan) with 50% MeOH–H₂O containing 0.1% formic acid (flow rate: 10 ml min⁻¹) to yield **1** (13.5 mg, Retention time (Rt), 10.5 min).

Compound **1** was isolated as a colorless oil that gave a [M+H]⁺ ion at *m/z* 477.1504 in the high-resolution electrospray ionization-MS consistent with a molecular formula of C₂₂H₂₄N₂O₁₀ (calculated for C₂₂H₂₅N₂O₁₀, 477.1509), and displayed the UV and IR spectra as follows; UV (MeOH) λ_{max} (ε) 278 (2460) and 219 (13 140); IR (KBr) ν_{max} 3430 and 1720 cm⁻¹.

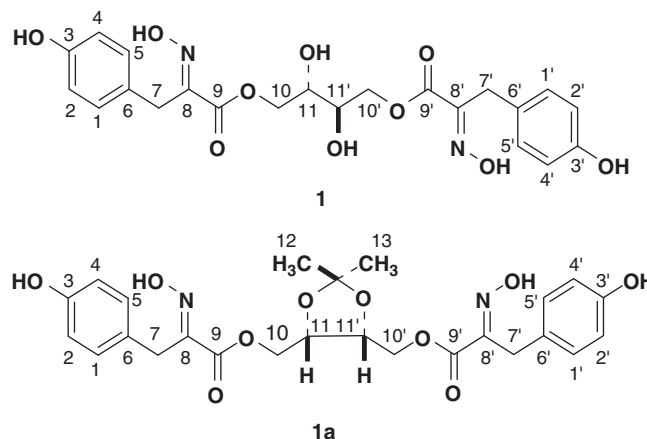


Figure 1 Structures of JBIR-25 (**1**) and 11,11'-acetonide JBIR-25 (**2**).

The ¹H and ¹³C NMR spectral data for **1** are shown in Table 1. The completely symmetrical carbon signals were observed, indicating that **1** is a symmetric compound. The structural information on **1** was further obtained by the series of two-dimensional NMR analyses such as heteronuclear single quantum coherence (HSQC), heteronuclear multiple-bond correlation (HMBC) and double quantum filtered correlation (DQF-COSY) spectra (Figure 2). A ¹H–¹H spin correlation was observed between doublet aromatic protons 1/5-H (δ_H 7.09) and 2/4-H (δ_H 6.65). In the HMBC spectrum, 2/4-H were strongly *m*-coupled to each other and coupled to an aromatic quaternary carbon C-6 (δ_C 127.3). Further, 1/5-H were also strongly *m*-coupled to each other, and coupled to an aromatic carbon C-3 (δ_C 155.8) and a methylene carbon C-7 (δ_C 29.2) in the HMBC spectrum. A singlet

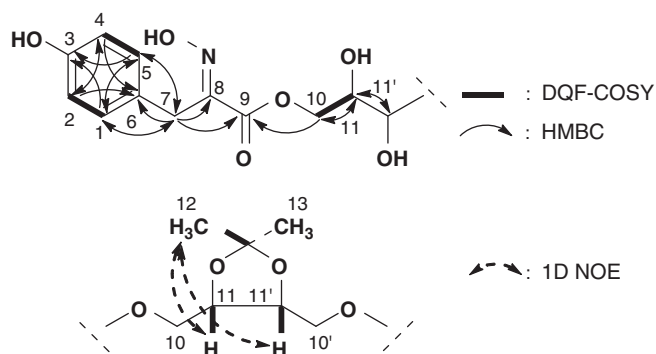
¹Biomedical Information Research Center (BIRC), Japan Biological Informatics Consortium (JBIC), Koto-ku, Tokyo, Japan; ²Bioscience Labs, Meiji Seika Kaisha, Odawara-shi, Kanagawa, Japan and ³Biomedical Information Research Center (BIRC), National Institute of Advanced Industrial Science and Technology (AIST), Koto-ku, Tokyo, Japan
Correspondence: Dr M Takagi, Biomedical Information Research Center (BIRC), Japan Biological Informatics Consortium (JBIC), 2-42 Aomi, Koto-ku, Tokyo 135-0064, Japan.
E-mail: motoki-takagi@aist.go.jp or Dr K Shin-ya, Biomedical Information Research Center (BIRC), National Institute of Advanced Industrial Science and Technology (AIST), 2-42 Aomi, Koto-ku, Tokyo 135-0064, Japan.
E-mail: k-shinya@aist.go.jp

Received 15 June 2009; revised 1 September 2009; accepted 24 September 2009; published online 16 October 2009

Table 1 ^1H and ^{13}C NMR data for **1** and **2**

| No. | 1 | | 2 | |
|---------|-----------------|--|-----------------|--|
| | ^{13}C | ^1H (J in Hz) | ^{13}C | ^1H (J in Hz) |
| 1, 1' | 130.0 | 7.09, d (8.3) | 130.2 | 7.05, d (8.3) |
| 2, 2' | 115.0 | 6.65, d (8.3) | 115.3 | 6.65, d (8.3) |
| 3, 3' | 155.8 | | 157.0 | |
| 4, 4' | 115.0 | 6.65, d (8.3) | 115.3 | 6.65, d (8.3) |
| 5, 5' | 130.0 | 7.09, d (8.3) | 130.2 | 7.05, d (8.3) |
| 6, 6' | 127.3 | | 128.5 | |
| 7, 7' | 29.2 | 3.84, s | 30.3 | 3.81, s |
| 8, 8' | 151.4 | | 152.3 | |
| 9, 9' | 164.2 | | 165.0 | |
| 10, 10' | 66.9 | 4.40, dd (12.2, 4.3), 4.23, dd (12.2, 11.4) | 61.5 | 3.68, dd (11.5, 5.0) 3.61, dd (11.5, 6.5) |
| 11, 11' | 69.5 | 3.76, m | 78.8 | 4.22, m |
| 12 | | | 25.5 | 1.33, s |
| 13 | | | 28.2 | 1.42, s |

^{13}C (125 MHz) and ^1H (500 MHz) NMR spectra were taken on a NMR system 500 NB CL (Varian, Palo Alto, CA, USA) in CD_3OD , and the solvent peak was used as an internal standard (δ_{C} 49.0, δ_{H} 3.30).

**Figure 2** Key correlations in DQF-COSY (bold line) and HMBC (arrow) spectra of **1**, and 1D NOE correlations obtained from **2**.

methylene proton 7-H (δ_{H} 3.84) was long-range coupled to aromatic methine carbons C-1/5 (δ_{C} 130.0) and C-6. Thus, the methylene carbon C-7 was deduced to be substituted at the position of C-6. All the assignments of this disubstituted benzene ring moiety were established by ^1H - ^{13}C long-range couplings, as shown in Figure 2. In addition, the ^1H - ^{13}C long-range couplings from a methylene proton 7-H to an ester carbonyl carbon C-9 (δ_{C} 164.2) and an imino carbon C-8 (δ_{C} 151.4) and from methylene proton 10-H (δ_{H} 4.40, 4.23) to C-9 revealed a 3-(4-hydroxyphenyl)-2-iminopropanoate moiety. A ^1H - ^1H spin coupling in DQF-COSY spectrum was observed between oximethine proton 11-H (δ_{H} 3.76, δ_{C} 69.5) and 10-H. Finally, 11-H was long-range coupled to an oximethine carbon C-11' (δ_{C} 69.5), which is exactly the own carbon signal in the HMBC spectrum, indicating that **1** consisted of a symmetric structure at C-11, as shown in Figure 1. From the molecular formula of **1**, four hydroxyl groups were determined to be substituted at the position of C-3, C-3', C-11 and C-11', and remaining two hydroxyl groups were assigned to oxime functional groups at the imino moieties C-8 and C-8'. The geometries of the C-8 and C-8' at

oxime moieties were elucidated as *E* from the upfield ^{13}C chemical shift of C-7 and C-7' (δ_{C} 29.2) due to the γ -effect of hydroxyl group in the oxime function. The difference in ^{13}C chemical shifts between *E* (δ_{C} 27.5) and *Z* (δ_{C} 35.7) was observed in (*E,Z*)-*N,N'*-bis(3-(3'-bromo-4'-hydroxyphenyl)-2-oximidopropionyl) cystamine³ the positions of which corresponded to C-7 and C-7' in **1**. This result supported the stereochemistry at C-8 and C-8'. The relative configurations of C-11 and C-11' were established by preparation of its five-membered 11,11'-acetonide ring that was subjected to 1D NOE experiment, as shown in Figure 2. Compound **1** (1.0 mg) was dissolved in 0.2 ml of acetone, to which 0.1 ml of 2,2-dimethoxypropane and 0.8 mg of *p*-toluene sulfonate were added, and stirred at room temperature for 2 h to give **2**. The reaction mixture was then concentrated to dryness, and the residue was dissolved with 10 ml of CHCl_3 . The CHCl_3 solution was washed twice with 5 ml of 5% NaHCO_3 solution and then twice with 5 ml of H_2O (pH 7). The organic layer was dried over Na_2SO_4 and concentrated *in vacuo*. The oily residue was purified by an L-column2 ODS column (20 i.d. \times 150 mm; Chemical Evaluation and Research Institute, Tokyo, Japan) with 60% MeOH - H_2O (flow rate: 10 ml min^{-1}) to yield 11,11'-acetonide JBIR-25 (**2**) (0.72 mg; Rt, 10.8 min). The assignments of ^1H and ^{13}C NMR data of **2** were determined by HSQC experiment, as shown in Table 1. The 1D NOE correlation of **2** was observed only between a singlet methyl proton 12-H (δ_{H} 1.33) and oxymethine protons 11-H and/or 11'-H (δ_{H} 4.22). On the basis of this data, the relative configuration of **1** was concluded to be 11*R** and 11'*S**, as shown in Figure 1. Moreover, the optical rotation value of **1** ($[\alpha]_{\text{D}}^{25}$ 0° (*c* 1.0, MeOH)) indicated that **1** is the mixture of enantiomers at the ratio of 1:1. The monomeric structure of **1** was found to be structurally related to phenylpyruvic acid oxime isolated from a marine sponge, *Psammaphysilla purpurea*.⁴ However, the symmetric structure such as that of **1** produced by a fungus is the first example.

We evaluated the 1,1-diphenyl-2-picrylhydrazyl (DPPH) radical scavenging activity of **1**. A 96-well plate was used for the DPPH radical scavenging assay.⁵ Compound **1** and α -tocopherol as a positive control were dissolved in MeOH as the stock solution (1 mM). In total, 90 μl of 200 μM DPPH dissolved in MeOH and 10 μl of sample were mixed in the microplate. After 1 h incubation at room temperature, the absorbance was measured at 540 nm. Compound **1** showed DPPH radical scavenging activity with an IC_{50} value of 79 μM , which was almost the same activity as that of α -tocopherol (IC_{50} =50 μM).

ACKNOWLEDGEMENTS

This work was supported by a grant from the New Energy and Industrial Technology Department Organization (NEDO) of Japan.

- Hammond, B., Kontos, H. A. & Hess, M. L. Oxygen radicals in the adult respiratory distress syndrome, in myocardial ischemia and reperfusion injury, and in cerebral vascular damage. *Can. J. Physiol. Pharmacol.* **63**, 173–187 (1985).
- Finkel, T. Radical medicine: treating ageing to cure disease. *Nat. Rev. Mol. Cell. Biol.* **6**, 971–976 (2005).
- Arabshahi, L. & Schmitz, F. J. Brominated tyrosine metabolites from an unidentified sponge. *J. Org. Chem.* **52**, 3584–3586 (1987).
- Yagi, H., Matsunaga, S. & Fusetani, N. Purpuramines A-1, new bromotyrosine-derived metabolites from the marine sponge *Psammaphysilla purpurea*. *Tetrahedron* **49**, 3749–3754 (1993).
- Izumikawa, M., Nagai, A., Doi, T., Takagi, M. & Shin-ya, K. JBIR-12, a novel antioxidative agent from *Penicillium* sp. NBRC 103941. *J. Antibiot.* **62**, 177–180 (2009).

NOTE

JBIR-54, a new 4-pyridinone derivative isolated from *Penicillium daleae* Zaleski fE50

Akira Mukai¹, Aya Nagai¹, Shigeki Inaba², Motoki Takagi¹ and Kazuo Shin-ya³

The Journal of Antibiotics (2009) 62, 705–706; doi:10.1038/ja.2009.101; published online 23 October 2009

Keywords: JBIR-54; *Penicillium daleae*; pyridinone

Penicillium is a versatile ascomyceteous fungi. It causes opportunistic infections and putrefaction of foods. *Penicillium* species are known to produce more than 900 documented bioactive compounds.¹ Furthermore, important pharmaceutical agents, namely, penicillins and compactin, have been isolated from *Penicillium* spp. We have reported that this fungus also produces valuable secondary metabolites, such as JBIR-12,² JBIR-27³ and JBIR-28.³ Therefore, we further screened for novel secondary metabolites from culture broths of *Penicillium* species. In this paper, we report the fermentation, isolation and structural determination of a new secondary metabolite, JBIR-54 (**1**), in addition to the taxonomy of the producing microorganism.

The *Penicillium daleae* Zaleski fE50 strain that produced **1** was isolated by the sodium dodecyl sulfate-yeast extract method⁴ from a soil sample collected in Fukui Prefecture, Japan. The soil was treated with a solution containing 6% bacto-yeast extract (BD Biosciences, San Jose, CA, USA) and 0.05% sodium dodecyl sulfate at 40 °C for 20 min. The solution was diluted with water, plated on potato dextrose agar plates, and incubated at 27 °C for a few weeks. Individual fungal colonies that appeared on the plate were transferred to potato dextrose agar slants and individual strains were maintained. The fE50 strain was identified by sequence analysis of the ribosomal DNA ITS region, and its microscopic features were observed by using a Zeiss Axioplan 2 imaging system (Carl Zeiss, Oberkochen, Germany). Sequence and morphological analysis revealed that the fE50 strain was 99.8% similar to the *P. daleae* strain NRRL 922. Thus, the strain was identified as *P. daleae* Zaleski.

The seed medium was potato dextrose broth (24 g l⁻¹ potato dextrose; BD Biosciences). The production medium containing 3 g brown rice (Hitomebore, Miyagi, Japan), 6 mg bacto-yeast extract (BD Biosciences), 3 mg sodium tartrate, 3 mg KH₂PO₄ and 9 ml H₂O was dispensed in 100-ml Erlenmeyer flasks. The fE50 strain was cultivated

in 50-ml test tubes containing 15 ml of seed medium. The test tubes were shaken on a reciprocal shaker (355 r.p.m.) at 27 °C for 3 days. Aliquots (1 ml) of the culture were transferred to 100-ml Erlenmeyer flasks containing the production medium and incubated in static culture at 27 °C for 14 days.

The culture of fE50 strain (100-ml Erlenmeyer flasks × 20) was extracted with 80% aqueous Me₂CO. The extract was evaporated *in vacuo*, and the residual aqueous concentrate was extracted with EtOAc (100 ml × 3). After drying over Na₂SO₄, the organic layer was evaporated to dryness. The dried residue (20.4 mg) was applied to a normal-phase medium-pressure liquid chromatography column (Purif-Pack SI-60; Moritex, Tokyo, Japan) and eluted with a chloroform–MeOH gradient (0–50% MeOH). The main fraction (0.98 mg) was finally separated by preparative HPLC using an L-column2 ODS (20 i.d. × 150 mm; Chemical Evaluation Research Institute, Tokyo, Japan) with 55% aqueous MeOH (flow rate, 10 ml min⁻¹, UV detection: 254 nm) to obtain the new compound **1** (0.48 mg; retention time, 14 min).

Compound **1** was obtained as a white powder ($[\alpha]_D^{25} = -22.2$; $c = 0.1$ in MeOH; UV (MeOH) $\lambda_{\max}(\epsilon)$: 223 (15 000), 316 nm (9800), and its IR spectrum showed the characteristic absorptions of the carbonyl group (ν_{\max} , 1669 cm⁻¹). The HR electron spray ionization-MS of **1** produced the (M+H)⁺ ion at m/z 236.1669 consistent with the molecular formula of C₁₄H₂₂NO₂ (calculated value for C₁₄H₂₂NO₂, 236.1651).

The structure of **1** was elucidated by a series of NMR techniques, such as constant time heteronuclear multibond correlation (CT-HMBC)⁵ and double-quantum filtered (DQF)-COSY. The direct C–H connectivity was established by heteronuclear single quantum coherence (see Table 1). In the DQF spectrum, the sequence from a methyl proton 1-H₃ (δ_H 1.01) to an olefinic proton 6-H (δ_H 5.66)

¹Biomedical Information Research Center (BIRC), Japan Biological Informatics Consortium (JBIC), Tokyo, Japan; ²NITE Biotechnology Development Center (NBDC), Department of Biotechnology, National Institute of Technology and Evaluation (NITE), Chiba, Japan and ³Biomedical Information Research Center (BIRC), National Institute of Advanced Industrial Science and Technology (AIST), Tokyo, Japan

Correspondence: Dr M Takagi, Biomedical Information Research Center (BIRC), Japan Biological Informatics Consortium (JBIC), 2-42 Aomi, Koto-ku, Tokyo 135-0064, Japan. E-mail: motoki-takagi@aist.go.jp or Dr K Shin-ya, Biomedical Information Research Center (BIRC), National Institute of Advanced Industrial Science and Technology (AIST), 2-42 Aomi, Koto-ku, Tokyo 135-0064, Japan.

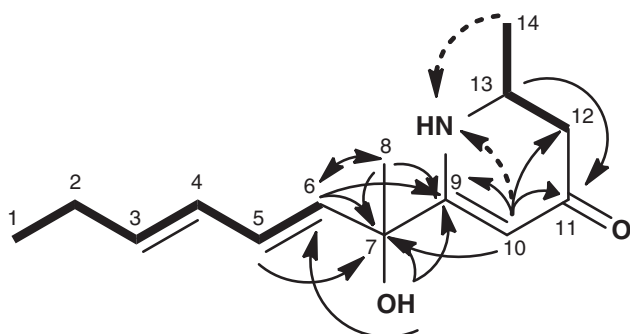
E-mail: k-shinya@aist.go.jp

Received 5 August 2009; revised 29 September 2009; accepted 1 October 2009; published online 23 October 2009

Table 1 ^1H - and ^{13}C -NMR data of JBIR-54 (**1**)

| Position | δ_{C} | δ_{H} (J in Hz) |
|----------|---------------------|--------------------------------------|
| 1 | 13.6 | 1.01, t (7.5, 7.5) |
| 2 | 26.0 | 2.12, m |
| 3 | 139.2 | 5.81, m |
| 4 | 128.1 | 6.01, dd (10, 15) |
| 5 | 130.5 | 6.28, dd (10, 15) |
| 6 | 133.3 | 5.66, d (15) |
| 7 | 73.4 | |
| 7-OH | | 1.90 |
| 8 | 28.1 | 1.54, s |
| 9 | 168.6 | |
| 10 | 95.4 | 4.97, s |
| 11 | 193.2 | |
| 12 | 43.3 | 2.26, dd (6, 12) 2.35, dd (6, 12) |
| 13 | 49.0 | 3.76, m |
| 14 | 20.5 | 1.33, d (6.5) |
| 14-NH | | 5.79 |

The ^{13}C (125 Hz) and ^1H (500 Hz) NMR spectra were obtained using a Varian NMR system 500 NB CL (Palo Alto, CA, USA) in CDCl_3 , and the solvent peak was used as an internal standard (δ_{C} 77.0 p.p.m.; δ_{H} 7.26 p.p.m.).

**Figure 1** Structure of **1**, and ^1H - ^1H (bold lines), main ^1H - ^{13}C (solid arrows) and ^1H - ^{15}N (dotted arrow) correlations in 2D NMR.

through a methylene proton 2- H_2 (δ_{H} 2.12), an olefinic proton 3- H (δ_{H} 5.81), an olefinic proton 4- H (δ_{H} 6.01) and an olefinic proton 5- H (δ_{H} 6.28) was observed as shown in Figure 1. Another spin coupling system was detected from the methylene proton 12- H_2 (δ_{H} 2.26, 2.35) to the methyl proton 14- H_3 (δ_{H} 1.33) through the methine proton 13- H (δ_{H} 3.76). A 2,3-dihydropyridin-4-one moiety was identified by the following correlation. Long-range couplings from the olefinic proton 10- H (δ_{H} 4.97) to the carbonyl carbon C-11 (δ_{C} 193.2) and

methylene carbon C-12 (δ_{C} 43.3), as well as from the methine proton 13- H to C-11 were observed by CT-HMBC. Moreover, ^1H - ^{15}N long-range couplings from 10- H and 14- H_3 to an amine nitrogen atom 9-NH were observed. On the basis of the ^{13}C chemical shift at C-13 (δ_{C} 49.0), this nitrogen atom was confirmed to be substituted at the C-13 position. Thus, these members form a cyclic structure, which is 2-methyl-2,3-dihydropyridin-4-one (Figure 1). The long-range couplings from the methyl proton 8- H_3 (δ_{H} 1.54) to the olefinic carbon C-6, quaternary carbon C-7 (δ_{C} 73.4) and olefinic quaternary carbon C-9 (δ_{C} 168.6), which in turn is long-range coupled from the olefinic proton 10- H , as well as from the hydroxyl proton 7-OH (δ_{H} 1.90) to the olefinic carbon C-6 (δ_{C} 133.3), quaternary carbon C-7 and olefinic quaternary carbon C-9 revealed that the side chain moiety was substituted at the C-9 position. The coupling constants between 3- H and 4- H ($J=15\text{ Hz}$), and 5- H and 6- H ($J=15\text{ Hz}$) indicated that the configurations at C-3 and C-5 are *trans*. Thus, the structure of **1** was determined as shown in Figure 1. Streptazone D, a derivative of **1**, is a known secondary metabolite of *Streptomyces* sp.⁶ To the best of our knowledge, this is first report of streptazone D analogs from fungi.

The 2-pyridinone analogs are reported to be non-nucleoside reverse-transcriptase inhibitors that can be used as anti-HIV agents.⁷ The antimicrobial activities of 2- and 4-pyridinone analogs have also been studied.^{8,9} Therefore, we attempted to investigate the cytotoxic and antimicrobial activities of **1**. The results showed that **1** did not exhibit cytotoxic activity against several cancer cell lines or antibacterial activity against *Micrococcus luteus* and *Escherichia coli*.

ACKNOWLEDGEMENTS

This work was supported by a grant from the New Energy and Industrial Technology Department Organization (NEDO) of Japan.

- Bérdy, J. Bioactive microbial metabolites. *J. Antibiot.* **58**, 1–26 (2005).
- Izumikawa, M., Nagai, A., Doi, T., Takagi, M. & Shin-Ya, K. JBIR-12, a novel antioxidative agent from *Penicillium* sp. NBRC 103941. *J. Antibiot.* **62**, 177–180 (2009).
- Motohashi, K. et al. New sesquiterpenes, JBIR-27 and -28, isolated from a tunicate-derived fungus, *Penicillium* sp. SS080624SCf1. *J. Antibiot.* **62**, 247–250 (2009).
- Hayakawa, M. & Nonomura, H. A new method for the intensive isolation of actinomycetes from soil. *Actinomycetologica* **3**, 95–104 (1989).
- Furihata, K. & Seto, H. Constant time HMBC (CT-HMBC), a new HMBC technique useful for improving separation of cross peaks. *Tetrahedron Lett.* **39**, 7337–7340 (1998).
- Puder, C., Krastel, P. & Zeeck, A. Streptazones A, B₁, B₂, C, and D: new piperidine alkaloids from *streptomyces*. *J. Nat. Prod.* **63**, 1258–1260 (2000).
- Tucker, T. J., Lumma, W. C. & Culberson, J. C. Development of nonnucleoside HIV reverse transcriptase inhibitors. *Methods Enzymol.* **275**, 440–472 (1996).
- Eliopoulos, G. M. et al. *In vitro* activity of a-86719.1, a novel 2-pyridinone antimicrobial agent. *Antimicrob. Agents Chemother.* **39**, 850–853 (1995).
- Erol, D. D. & Yulug, N. Synthesis and antimicrobial investigation of thiazolinoalkyl-4(1*H*)-pyridones. *Eur. J. Med. Chem.* **29**, 893–897 (1994).

NOTE

Enzymatic activity of a glycosyltransferase KanM2 encoded in the kanamycin biosynthetic gene cluster

Fumitaka Kudo¹, Hilda Sucipto² and Tadashi Eguchi²

The Journal of Antibiotics (2009) 62, 707–710; doi:10.1038/ja.2009.107; published online 13 November 2009

Keywords: aminoglycoside antibiotics; biosynthesis; glycosyltransferase; kanamycin; paromamine

Kanamycin, discovered by Umezawa in 1957, is the most well-known 2-deoxystreptamine (2DOS)-containing aminoglycoside antibiotic.¹ Three structurally related kanamycins were identified from the producer *Streptomyces kanamyceticus* (Figure 1). Extensive biosynthetic studies of this class of aminoglycoside antibiotics, especially butirosin and neomycin, clarified that a unique aminocyclitol, 2DOS, is biosynthesized from D-glucose 6-phosphate by three crucial enzymes, 2-deoxy-scyllo-inosose (2DOI) synthase, L-glutamine (Gln):2DOI aminotransferase and 2-deoxy-scyllo-inosamine dehydrogenase.^{2,3} After the 2DOS formation, uridine 5'-diphospho-N-acetylglucosamine (UDP-GlcNAc):2DOS N-acetylglucosaminyltransferase catalyzes the glycosylation of 2DOS to give N-acetylparomamine, which is then deacetylated by N-acetylparomamine deacetylase to yield paromamine.⁴ Paromamine is believed to be a branching biosynthetic intermediate, which is converted to either 4,6-disubstituted 2DOS aminoglycosides, such as kanamycin and gentamicin, or 4,5-disubstituted 2DOS aminoglycosides, such as neomycin and butirosin. Therefore, the regio-specificities and substrate specificities of glycosyltransferases that recognize paromamine as a glycosyl acceptor determine the core structures of aminoglycoside antibiotics.

The biosynthetic gene cluster for kanamycin, comprising 24 open reading frames, was identified in 2004.⁵ Two other research groups also deposited independently identical kanamycin biosynthetic genes by different symbols in the public DNA databases simultaneously.^{6,7} To prevent confusion, herein we use the *btr* gene-based names, which were used systematically by the Piepersberg group and also in our recent review.^{8,9} The entire kanamycin biosynthetic gene cluster was expressed in *Streptomyces venezuelae* and the resultant recombinant strain was reported to produce kanamycin A, which indicates that the *kan* genes are responsible for the biosynthesis of kanamycins.¹⁰ The *kanC*, *kanS1*, *kanE*, *kanM1* and *kanN* genes expressing *Streptomyces lividans* reportedly produce paromamine, confirming that these genes, respectively, encode 2DOI synthase, Gln:2DOI aminotransferase,

2-deoxy-scyllo-inosamine dehydrogenase, UDP-GlcNAc:2DOS N-acetylglucosaminyltransferase and N-acetylparomamine deacetylase (Figure 1).¹¹ Among these, the *kanC* gene was expressed in *Escherichia coli* and the recombinant KanC protein was confirmed to be 2DOI synthase.⁶ Recombinant KanM1 protein was also reported to have weak glycosyltransferase activity with 2DOS as a glycosyl acceptor, and TDP-glucose or GDP-mannose as a glycosyl donor.¹² However, this KanM1 activity is contradictory to the presumed enzymatic function as suggested by the above-mentioned heterologous expression of UDP-GlcNAc:2DOS N-acetylglucosaminyltransferase in *S. lividans*. Detailed enzymatic analysis is thus necessary to elucidate the substrate specificity of KanM1 on using a pure enzyme.

In this study, we heterologously expressed another glycosyltransferase gene, *kanM2*, in the *kan* gene cluster and investigated its enzymatic activities, which were expected to be catalysis of the glycosylation of a pseudo-disaccharide, paromamine, to yield a pseudo-trisaccharide. To obtain soluble KanM2 protein expressed in *E. coli*, a low expression temperature (15 °C) was critically important after addition of isopropyl β-D-thiogalactoside (final concentration 0.5 mM). The cell-free extract of the KanM2-expressing *E. coli* was treated with 2 mM of paromamine as a glycosyl acceptor, and 2 mM of UDP-Glc or UDP-GlcNAc as a glycosyl donor. After incubation at 28 °C for 18 h, the enzymatic reactions were quenched by addition of ethanol. The resulting mixture was treated with 2,4-dinitrofluorobenzene to convert aminoglycosides into N-dinitrophenyl derivatives, which show UV-Vis absorption at 350 nm. Consequently, only a reaction mixture of paromamine and UDP-Glc gave a new peak with 40% conversion from the substrate paromamine in HPLC traces (Figures 2a and b). Liquid chromatography–electrospray ionization–MS analysis (negative mode) of the sample showed the new peak with *m/z* 982.4, which corresponded to [M-H]⁻ for the derivative of glucosylated paromamine (Figure 2c).

Next, we attempted to isolate the KanM2 reaction product from paromamine and UDP-Glc, and determine the chemical structure.

¹Department of Chemistry, Tokyo Institute of Technology, Tokyo, Japan and ²Department of Chemistry and Materials Science, Tokyo Institute of Technology, Tokyo, Japan
Correspondence: Professor T Eguchi, Department of Chemistry and Materials Science, Tokyo Institute of Technology, 2-12-2 O-okayama, Meguro-ku, Tokyo 151-8551, Japan.
E-mail: eguchi@cms.titech.ac.jp

Received 17 August 2009; revised and accepted 20 October; published online 13 November 2009

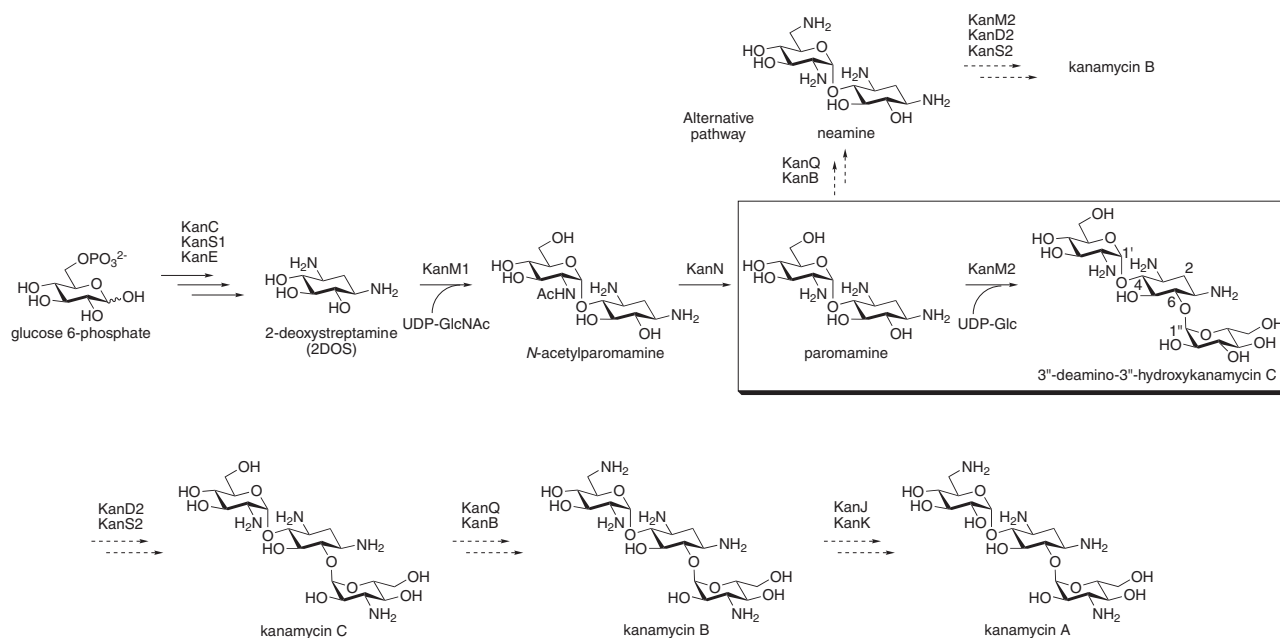


Figure 1 Proposed biosynthetic pathway for kanamycin.

Ammonium sulfate fractionation between 10 and 40% saturation was effective in recovering most of the enzymatic activity from the cell-free extract of KanM2-expressing *E. coli*, although its activity was significantly decreased after a standard dialysis probably because of the instability of the enzyme. We then used the 10–40% $(\text{NH}_4)_2\text{SO}_4$ fractionated solution just after the fractionation, paromamine (3 mM, 10 mg), and UDP-Glc (4.7 mM, 29 mg) in 50 mM HEPES buffer (pH 8.0) containing 1 mM MgCl_2 and 10% glycerol (total 10 ml) at 28 °C for 24 h for a large-scale enzymatic reaction. To ensure maximum consumption of the starting material, the reaction mixture was further treated under identical enzymatic conditions using freshly prepared enzyme solution (0.25 μl) and UDP-Glc (5–10 mg) nine times. Consequently, 84% of paromamine was converted to the new glycosylated product, which was obtained as the sulfate form of aminoglycoside (7.9 mg) by ion exchange chromatography. HR-FAB-MS (positive mode, glycerol) of the compound gave an m/z of 486.2307, which corresponds to the calculated mass for $\text{C}_{18}\text{H}_{36}\text{O}_{12}\text{N}_3$ (486.2299), $[\text{M}+\text{H}]^+$ of glucosylated paromamine.¹ H-NMR analysis of the product showed two anomeric protons and a methylene of the 2DOS moiety, although the other signals were very complex for assignment (see Supplementary information). Spectra of the compound obtained by total correlation spectroscopy (TOCSY) indicated that the signals for H-1 and H-3 of 2DOS at 3.3 p.p.m., those for H-6 at 3.6 p.p.m., and those for H-4 and H-5 at 3.7 p.p.m. are correlated with the signals for H-2ax and H-2eq at 1.7 and 2.3 p.p.m., respectively (data not shown). The use of ^1H - ^1H -COSY, heteronuclear multiple quantum coherence and heteronuclear multiple bond coherence facilitated assignment of ^{13}C chemical shifts for C1'', C1', C-2', C-1 or C-3, C-4, C-5 and C-6. Consequently, a glycosidic linkage between C1'' and C-6 was confirmed in addition to the C1'-O-C4 bond of the paromamine moiety. Therefore, the KanM2 reaction product from paromamine and UDP-Glc appeared to be 3''-deamino-3''-hydroxykanamycin C.

Presumably, 3''-deamino-3''-hydroxykanamycin C is a biosynthetic intermediate leading to kanamycin B and kanamycin A (Figure 1).

A disruptant mutant of the *kanQ* gene homolog encoding a FAD-dependent dehydrogenase in the tobramycin and apramycin producer *Streptomyces tenebrarius* accumulated 3'-deoxy-carbamoylkanamycin C.¹³ This accumulation suggests that the KanM2 homologous protein, TobM2, in tobramycin biosynthesis recognizes paromamine as a substrate to produce 3''-deamino-3''-hydroxykanamycin C, which would be dehydrogenated and transaminated to give kanamycin C. An $\text{NAD}^+/\text{NADP}^+$ -dependent dehydrogenase, KanD2, and an aminotransferase, KanS2, are presumably responsible for this transformation based on bioinformatic analysis of the gene clusters for 2DOS-containing aminoglycoside antibiotics.⁹ Alternatively, this set of enzymes might be responsible for the formation of NDP-3-amino-3-deoxyglucose (kanosamine), which is another possible glycosyl donor in the KanM2 reaction, to afford kanamycin C.¹¹ KanS2 is a protein that is homologous to KanS1 (37% identity/51% positive), which is involved in the double transamination in 2DOS biosynthesis. The difference in substrate specificity of these aminotransferases is an interesting issue to be resolved.

A FAD-dependent dehydrogenase, KanQ, and an aminotransferase, KanB, remaining in the *kan* gene cluster are apparently responsible for the transamination at C-6. The substrate specificity of this set of enzymes is also interesting because the homologous enzymes were reported to recognize mainly the glucosamine moiety and are responsible for the transaminations at C-6 in neomycin biosynthesis.^{14,15} Thus, these enzymes might convert paromamine to neamine, which could be glycosylated by KanM2 to yield kanamycin B. Thus, the substrate specificity of KanM2 is a key determinant for the production of kanamycin analogs in the producer strain.

Finally, kanamycin B is converted to the end product kanamycin A. A feeding experiment of D - ^{14}C glucosamine into the kanamycin producer revealed that the labeled glucosamine was incorporated only into the 6-amino-6-deoxy-glucose moiety of kanamycin A,^{16,17} which suggests that the deamination reaction at C-2 of the glucosamine moiety in kanamycin B is involved in the biosynthesis of

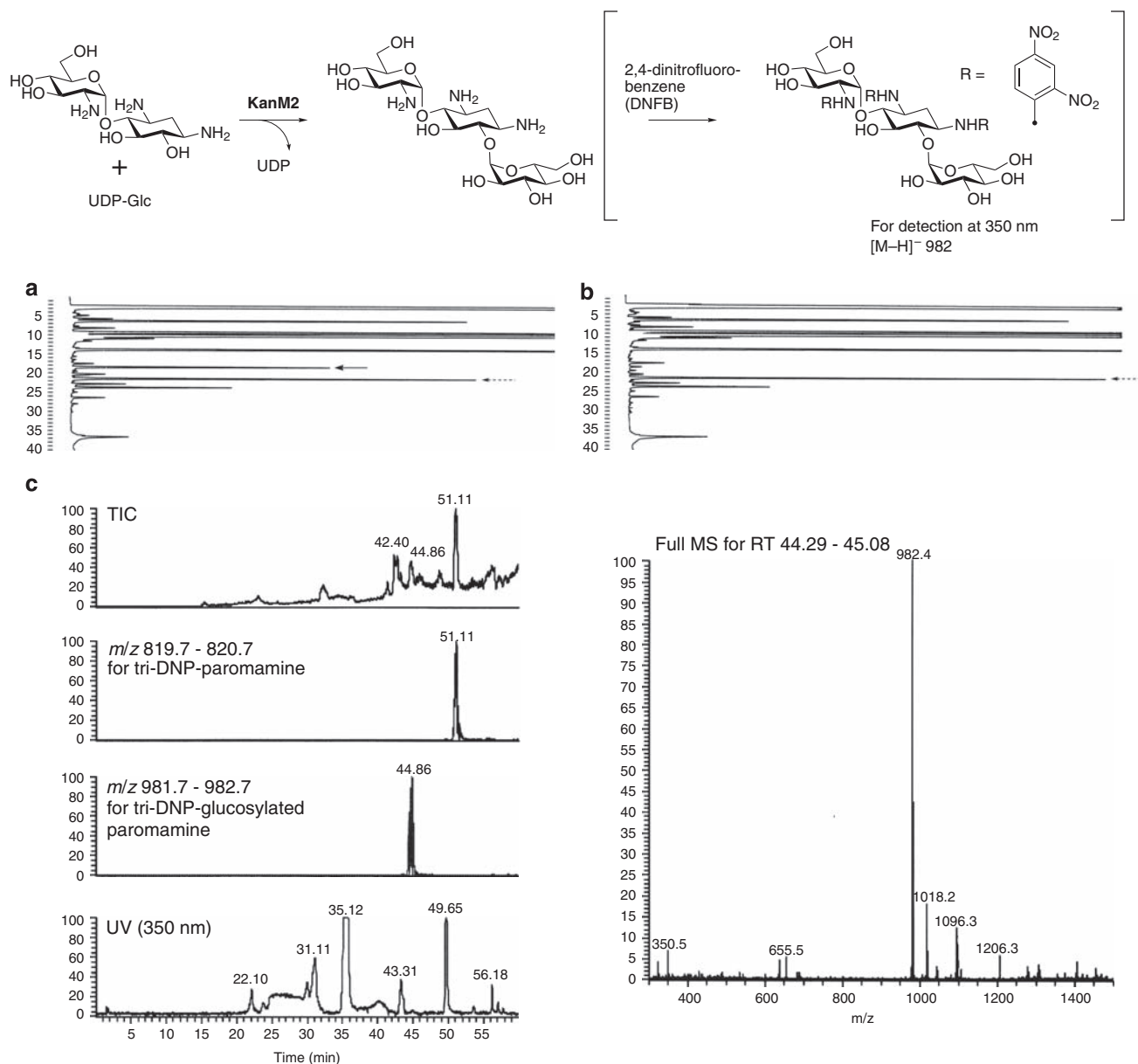


Figure 2 KanM2 reaction of paromamine with UDP-Glc. After the enzymatic reactions, aminoglycoside compounds were converted to the dinitrophenyl derivatives (350 nm) for detection by HPLC (refer the Supplementary information for details). (a) KanM2's reaction with paromamine and UDP-Glc; (b) KanM2's reaction with paromamine (without addition of UDP-Glc); (c) liquid chromatography–electrospray ionization–MS (LC–ESI–MS) analysis (negative mode) of the same solution in (a). The solid arrow indicates the KanM2 reaction product and the broken arrow denotes the paromamine that remained in the enzymatic solution. Several unidentified peaks were observed in the HPLC traces, which might have been derived from impurities in the cell-free extract (CFE) of the KanM2-expressing *E. coli*.

kanamycin A. Two unassigned hypothetical proteins, KanJ (a putative phytanoyl-CoA dioxygenase family protein) and KanK (a putative NAD-dependent protein), are apparently responsible for this unprecedented deamination reaction, which is presumably accomplished through either transamination/dehydrogenation or oxidation (and subsequent hydrolysis of an imine intermediate)/dehydrogenation chemistry.

In conclusion, we clarified that KanM2 catalyzes the glucosylation of paromamine with UDP-Glc to yield 3''-deamino-3''-hydroxykanamycin C. This result strongly supports the proposed stepwise biosynthetic pathway via paromamine as an intermediate (Figure 1).

However, a detailed biochemical analysis of KanM2 including substrate specificity remains to be done. The amino acid sequences of KanM2 and KanM1 show 33% identity and 54% positivity with each other. It is therefore interesting to investigate how these glycosyltransferases distinguish glycosyl acceptors 2DOS or paromamine, and glycosyl donors UDP-GlcNAc or UDP-Glc. In addition, understanding such biochemical properties of glycosyltransferases will provide important information to engineer proteins for glycodiversification in order to create diverse structural glycosides using enzymes.¹⁸ Purification of KanM1 and KanM2 for detailed biochemical studies is currently in progress.

ACKNOWLEDGEMENTS

This work was supported in part by KAKENHI 21710224 (FK).

- 1 Umezawa, H. *et al.* Production and isolation of a new antibiotic: kanamycin. *J. Antibiot.* **10**, 181–188 (1957).
- 2 Kudo, F., Yamamoto, Y., Yokoyama, K., Eguchi, T. & Kakinuma, K. Biosynthesis of 2-deoxystreptamine by three crucial enzymes in *Streptomyces fradiae* NBRC 12773. *J. Antibiot.* **58**, 766–774 (2005).
- 3 Kudo, F. & Eguchi, T. Biosynthetic enzymes for the aminoglycosides butirosin and neomycin. *Methods Enzymol.* **459**, 493–519 (2009).
- 4 Yokoyama, K., Yamamoto, Y., Kudo, F. & Eguchi, T. Involvement of two distinct N-acetylglucosaminyltransferases and a dual-function deacetylase in neomycin biosynthesis. *ChemBiochem* **9**, 865–869 (2008).
- 5 Yanai, K. & Murakami, T. The kanamycin biosynthetic gene cluster from *Streptomyces kanamyceticus*. *J. Antibiot.* **57**, 351–354 (2004).
- 6 Kharel, M. K. *et al.* A gene cluster for biosynthesis of kanamycin from *Streptomyces kanamyceticus*: comparison with gentamicin biosynthetic gene cluster. *Arch. Biochem. Biophys.* **429**, 204–214 (2004).
- 7 Piepersberg, W. Cloning and sequencing of the kanamycin biosynthetic gene cluster from *Streptomyces kanamyceticus* DSM 40500 Accession No. AJ628422 (2006).
- 8 Piepersberg, W., Aboshanab, K. M., Schmidt-Beissner, H. & Wehmeier, U. F. in *Aminoglycoside Antibiotics. The Biochemistry and Genetics of Aminoglycoside Producers* (ed Arya, D. P.) 15–118 (John Wiley & Sons, Inc., Hoboken, NJ, 2007).
- 9 Kudo, F. & Eguchi, T. Biosynthetic genes for aminoglycoside antibiotics. *J. Antibiot.* **62**, 471–481 (2009).
- 10 Thapa, L. P. *et al.* Heterologous expression of the kanamycin biosynthetic gene cluster (pSKC2) in *Streptomyces venezuelae* YJ003. *Appl. Microbiol. Biotechnol* **76**, 1357–1364 (2007).
- 11 Nepal, K. K., Oh, T. J. & Sohng, J. K. Heterologous production of paromamine in *Streptomyces lividans* TK24 using kanamycin biosynthetic genes from *Streptomyces kanamyceticus* ATCC12853. *Mol. Cells* **27**, 601–608 (2009).
- 12 Park, S. H. *et al.* Expanding substrate specificity of GT-B fold glycosyltransferase via domain swapping and high-throughput screening. *Biotechnol. Bioeng.* **102**, 988–994 (2009).
- 13 Yu, Y., Hou, X., Ni, X. & Xia, H. Biosynthesis of 3'-deoxy-carbamoylkanamycin C in a *Streptomyces tenebrarius* mutant strain by *tacB* gene disruption. *J. Antibiot.* **61**, 63–69 (2008).
- 14 Huang, F. *et al.* Elaboration of neosamine rings in the biosynthesis of neomycin and butirosin. *ChemBiochem* **8**, 283–288 (2007).
- 15 Kudo, F., Kawashima, T., Yokoyama, K. & Eguchi, T. Enzymatic preparation of neomycin C from ribostamycin. *J. Antibiot.* **62**, 643–646 (2009).
- 16 Kojima, M., Yamada, Y. & Umezawa, H. Biosynthesis of kanamycins. I. Incorporation of glucose-14C or glucosamine glucosam14C into kanamycins and kanamycin-related compounds. *Agric. Biol. Chem* **32**, 467–473 (1968).
- 17 Rinehart, K. L. Jr & Stroshane, R. M. Biosynthesis of aminocyclitol antibiotics. *J. Antibiot.* **29**, 319–353 (1976).
- 18 Thibodeaux, C. J., Melançon, C. E. III & Liu, H. W. Natural-product sugar biosynthesis and enzymatic glycodiversification. *Angew Chem. Int. Ed.* **47**, 9814–9859 (2008).

Supplementary Information accompanies the paper on The Journal of Antibiotics website (<http://www.nature.com/ja>)

Author Index for Volume 62

| | | | | | |
|------------------------|----------|----------------|-----------------------|--------------------|---------------|
| Adachi, K | 519 | Chung, I-S | 43 | Guan, Y | 315 |
| Afzal, A | 319 | Collado, J | 265 | Guan, Z | 699 |
| Alagumaruthanayagam, A | 377 | Comanducci, A | 109 | Gullo, V | 401 |
| Alarco, A-M | 565 | Conte, MP | 109 | Guo, H-F | 639 |
| Ali, A | 319 | Cui, X | 647 | Guo, S-L | 309 |
| Alihodzic, S | 133 | Czyryca, PG | 539 | Guo, W-Q | 309 |
| Al-Zereini, W | 453 | Dairi, T | 347 | Guo, Z | 201 |
| Amano, S-i | 397 | Demain, AL | 5 | Gyobu, Y | 703 |
| An, D-G | 687 | Dezeny, G | 265 | Haber, VE | 133 |
| An, M-M | 605 | Dezhenkova, LG | 37, 117 | Hahn, DR | 191 |
| Ando, K | 365 | Dietrich, L | 699 | Ham, J | 621 |
| Anke, H | 453 | Doi, T | 177 | Han, L | 647 |
| Anke, T | 119 | Dong, L-J | 605 | Haque, A | 319 |
| Aouidate, M | 565 | Dong, Y | 527 | Harada, K-i | 181, 613 |
| Arima, S | 69 | Dorso, K | 55 | Harigaya, Y | 69, 289 |
| Asami, Y | 105, 339 | Eguchi, T | 471, 507, 643, 707 | Härtner, T | 465 |
| Asker, D | 397 | Endo, A | 277 | Hashimoto, J | 247, 625 |
| Aumelas, A | 295 | Endo, S | 153 | Hashimoto, Seiichi | 625 |
| Bai, H | 483 | Fajdetic, A | 133 | Hashimoto, Seiji | 27 |
| Balzarini, J | 37, 117 | Falardeau, P | 565 | Hattori, N | 469 |
| Bando, T | 339 | Farnet, CM | 565 | Hayakawa, Y | 123, 271, 531 |
| Banskota, AH | 565 | Fedorenko, V | 461 | Hayashi, K-i | 259 |
| Bashir, S | 319 | Fiedler, H-P | 75, 99, 445, 465, 513 | Hayashi-Nishino, M | 251 |
| Basilio, A | 55, 265 | Floss, HG | 405 | He, J | 527 |
| Bechthold, A | 461 | Fujie, A | 89, 95 | Heim, D | 191 |
| Bednarek, E | 581 | Fujii, T | 89, 95 | Helaly, S | 445 |
| Beil, W | 99, 513 | Fujita, K-i | 81, 145, 691 | Helmke, E | 453 |
| Benedit, G | 167 | Fujiwara, T | 393 | Herczegh, P | 113 |
| Bensaci, M | 539 | Fukai, T | 613 | Hino, M | 89, 95 |
| Beppu, T | 397 | Fukuda, I | 221 | Hirasawa, E | 691 |
| Bills, G | 265 | Fukuda, N | 339 | Hirose, T | 277, 495, 681 |
| Bocian, W | 581 | Fukuda, T | 69 | Hohmann, C | 75, 99 |
| Boll, R | 461 | Fukushima, K | 217 | Horbal, L | 461 |
| Borjihan, B | 81 | Funabashi, M | 325 | Horinouchi, S | 371 |
| Borjihan, H | 691 | Furihata, K | 397 | Horváth, P | 113 |
| Brown, R | 75, 99 | Furukawa, C | 365 | Hoshino, Y | 613 |
| Bruntner, C | 75, 99 | Furukawa, Y | 559 | Hosobuchi, M | 325 |
| Bujdosó, S | 113 | Gao, P | 315 | Hosoe, T | 217 |
| Bukhman, VM | 37, 117 | Genilloud, O | 55 | Hosokawa, S | 469 |
| Bull, AT | 99 | Gerwick, BC | 191 | Hosono, K | 571 |
| Burgess, B | 699 | Gilbert, JR | 191 | Hsu, L-Y | 675 |
| Byrne, K | 55, 265 | Goldman, ML | 265 | Huang, L | 201 |
| Calle, F de la | 167 | Goodfellow, M | 75, 99 | Huang, X | 647 |
| Cha, J-H | 43 | Gouda, H | 495 | Huber, J | 265 |
| Chae, J-C | 163 | Gourdeau, H | 565 | Huo, C | 527 |
| Chan, T-M | 401 | Graupner, PR | 191 | Hwang, J-H | 283, 393 |
| Chang, C-WT | 539 | Gray, J | 191 | Iba, S | 425 |
| Chapin, E | 191 | Grond, S | 439 | Ibrahim, A | 565 |
| Chen, Z-J | 587 | Gu, Q-Q | 225 | Iebba, V | 109 |
| Choi, EJ | 621 | Gu, Y | 527 | Iftikhar, T | 319 |
| Choi, SU | 335 | Gualtieri, M | 295 | Iguchi, K | 277, 495 |
| Choo, S-J | 333 | | | Ikeda, D | 63, 243 |
| Chu, M | 401 | | | Ikeda, M | 489 |

| | | | | | |
|----------------|------------------|---------------|---------------|------------------|--------------------|
| Imhoff, JF | 75, 99, 445, 513 | Kobayashi, K | 195 | Matsuhama, M | 51 |
| Imoto, M | 425 | Kojima, S | 365 | Matsuo, Y | 519 |
| Inaba, Shigeki | 159, 247, 705 | Kojima, Y | 681 | McAlpine, JB | 565 |
| Inaba, Susumu | 507 | Komaki, H | 247, 601 | Mellon, C | 565 |
| Inokoshi, J | 51 | Konishi, Y | 81 | Merrell, DS | 43 |
| Inoue, H | 63 | Koseki, T | 533 | Mikami, Y | 613 |
| Inukai, M | 153 | Koshino, H | 105 | Minami, E | 153 |
| Irran, E | 99 | Kozerski, L | 581 | Mishima, S | 385 |
| Ishida, O | 153 | Kozone, I | 123, 159, 593 | Miyakawa, T | 533 |
| Ishiyama, A | 303, 681 | Kozuma, S | 545 | Miyakoshi, S | 153 |
| Isono, F | 153 | Krämer, M | 75, 99 | Miyanaga, A | 371 |
| Isshiki, K | 283 | Kudo, F | 471, 643, 707 | Mizoue, K | 507 |
| Istuk, ZM | 133 | Kumagai, H | 63 | Mohsin, M | 319 |
| Itabashi, T | 217 | Kuzuyama, T | 385 | Momose, I | 243 |
| Ito, A | 221 | Kwa, AL | 675 | Mori, M | 105 |
| Iwatsuki, M | 303 | Kwon, HC | 171, 621 | Morita, K | 397 |
| Izumikawa, M | 177 | | | Motegi, A | 507 |
| | | Laatsch, H | 453 | Motohashi, K | 247, 625, 703 |
| Jang, Y-W | 163 | Laiple, KJ | 465 | Motyl, M | 55, 265 |
| Jayasuriya, H | 265 | Lam, KS | 213 | Mukai, A | 601, 613, 705 |
| Jeon, NB | 631 | Lanen, SGV | 325 | Murakami, R | 123, 153 |
| Ji, Z | 201, 233 | Lang, L | 647 | Muramatsu, Y | 153 |
| Jiang, N | 483 | Laudy, AE | 575 | Murayama, T | 533 |
| Jones, AL | 75, 99 | Lazarevski, G | 133 | Mutak, S | 133 |
| Joo, YM | 43 | Lee, C | 687 | | |
| Jung, J-Y | 635 | Lee, HS | 43 | Nachtigall, J | 445, 513 |
| | | Lee, I-K | 163, 631, 635 | Nagai, A | 159, 177, 247, 705 |
| Kai, H | 89 | Lee, KJ | 163 | Nagai, H | 393 |
| Kajiura, T | 123 | Lee, KR | 335 | Nagai, Kazuo | 507 |
| Kamei, Y | 259 | Lee, W | 675 | Nagai, Kenichiro | 681 |
| Kanai, M | 425 | Leng, Y | 239 | Nagamitsu, T | 69, 289 |
| Kanamoto, A | 393 | Li, J | 647 | Nagase, H | 339 |
| Kanasaki, R | 95 | Li, M | 647 | Nagatsuka, S-y | 271, 531 |
| Kang, H-W | 631 | Li, Y | 647 | Nagayasu, A | 69 |
| Kardos, S | 113 | Li, Y-H | 639 | Nakajima, H | 95 |
| Kataoka, T | 507, 655 | Li, Y-Y | 129 | Nakano, H | 17 |
| Kato, A | 89, 95 | Li, Z-R | 639 | Nakao, Y | 597 |
| Kato, H | 181 | Liang, J-H | 605 | Namatame, M | 303, 681 |
| Kato, T | 63, 283 | Liermann, JC | 119 | Nara, F | 359 |
| Kautz, D | 119 | Lim, T-P | 675 | Nicholson, G | 75, 99, 513 |
| Kawada, M | 63, 243 | Litke, A | 539 | Nishihara, A | 303 |
| Kawai, K-i | 217 | Liu, J-K | 129, 239 | Nishihara, Y | 489 |
| Kawamoto, K | 51 | Loebenberg, D | 401 | Nishimura, Y | 407 |
| Kawasaki, H | 221 | Longhi, C | 109 | Nishino, K | 251 |
| Kawasaki, T | 271, 531 | Lu, X | 527 | Nishiyama, M | 385 |
| Kawashima, T | 643 | Luo, D-Q | 129 | Nitto, A | 533 |
| Kawęcki, R | 581 | | | Nogami, S | 159 |
| Ke, A | 527 | Ma, Y | 527 | Noguchi, Y | 495 |
| Kéki, S | 113 | Maeda, S | 283 | Nonaka, Kenichi | 195, 303, 431 |
| Keller, K | 539 | Maeda, S | 489 | Nonaka, Koichi | 325 |
| Khan, ST | 247 | Magae, J | 365 | Nozaki, H | 259 |
| Kikuchi, N | 397 | Marazzato, M | 109 | Nukina, M | 519 |
| Kim, KH | 335 | Marumoto, K | 69 | Numata, A | 353 |
| Kim, SY | 43 | Maruyama, A | 365 | | |
| Kim, W-G | 333 | Masuda, K | 153 | Ochi, K | 669 |
| Kim, Young-Hee | 333 | Masuda, N | 325 | Ochiai, A | 283 |
| Kim, Young-Ho | 635 | Masuda, S | 571 | Ogawa, Y | 545 |
| Kim, Y-S | 163 | Masuma, R | 195, 303, 431 | Ogihara, J | 571 |
| Kimura, K-i | 533 | Matsuda, D | 195 | Ogihara, S | 289 |
| Kimura, M | 597 | Matsuda, S | 519 | Ogita, A | 81, 145, 691 |
| Kinoshita, Y | 303 | Matsufuji, H | 397 | Ogita, M | 145 |

| | | | | | |
|----------------------|--|---------------------|---|---------------------|-------------------------------|
| Oh, B-T | 163 | Schulz, D | 513 | Tan, T-T | 675 |
| Ohdake, T | 571 | Seganti, L | 109 | Tan, T-Y | 675 |
| Ohnuki, T | 359, 545, 551, 559 | Sekiyama, Y | 105 | Tanaka, H | 625 |
| Ohshiro, T | 69 | Senda, Y | 251 | Tanaka, R | 353 |
| Ohtawa, M | 289 | Seo, G-S | 631 | Tanaka, Toshiaki | 495 |
| Ohya, Y | 159 | Seok, S-J | 333 | Tanaka, Toshio | 81, 145, 691 |
| Okada, R | 425 | Seto, H | 123 | Tanaka, Y | 669 |
| Okunishi, J | 489 | Sharpless, KB | 277 | Tang, H-L | 129 |
| Ômura, S | 1, 17, 51, 69, 195, 207, 277, 289, 303, 431, 435, 495, 681 | Shen, L | 201 | Tao, P-z | 639 |
| Ondeyka, JG | 55, 699 | Shen, Y | 239 | Tariq, A | 319 |
| Ono, Y | 359, 545 | Shi, Q | 527 | Tashiro, E | 425 |
| Opatz, T | 119 | Shi, Y-L | 129 | Tatsuta, K | 469 |
| Osada, H | 105, 221 | Shibata, T | 325 | Tavcar, B | 133 |
| Otoguro, K | 303, 681 | Shigetate, H | 353 | Terada, R | 259 |
| Ozaki, T | 385 | Shimada, J | 3 | Terracciano, J | 401 |
| Padovan, J | 133 | Shimanuki, K | 533 | Teruya, T | 105 |
| Palej, I | 133 | Shimizu, H | 365 | Tevyashova, AN | 37, 117 |
| Paljetak, HC | 133 | Shin, C-G | 687 | Thaler, J-O | 295 |
| Park, J-S | 171 | Shindo, M | 597 | Thorn, A | 439 |
| Park, KM | 335 | Shinozaki, J | 123 | Tokuyama, S | 669 |
| Park, S-M | 163 | Shin-ya, K | 123, 159, 177, 247, 283, 393, 593, 601, 625, 703, 705 | Tomoda, H | 51, 69, 195, 207, 431, 435 |
| Patel, M | 401 | Shiomi, K | 277, 289, 303, 495 | Tsueng, G | 213 |
| Pavankumar, AR | 377 | Shiono, Y | 533 | Tsuji, K | 181 |
| Pérez, M | 167 | Shizuri, Y | 519 | Tsuji, E | 89, 95 |
| Pintér, G | 113 | Shtil, AA | 37, 117 | Tsujiuchi, G | 243 |
| Pirae, M | 565 | Simizu, S | 105 | Tsuruga, M | 365 |
| Poralla, K | 513 | Singh, SB | 55, 265, 699 | Uchida, R | 69 |
| Preobrazhenskaya, MN | 37, 117 | Sitkowski, J | 581 | Uchida, Y | 597 |
| Rajnisz, A | 575 | Solecka, J | 575, 581 | Ueda, J-Y | 159, 283, 593 |
| Rebets, Y | 461 | Someno, T | 63, 243 | Ueda, K | 397 |
| Ren, X | 527 | Song, D | 315 | Ueno, C | 89, 95 |
| Riedlinger, J | 513 | Song, H-H | 687 | Ueno, M | 89, 95 |
| Rodríguez, P | 167 | Sørensen, D | 565 | Ui, H | 277 |
| Rozgonyi, F | 113 | Stach, JEM | 99 | Uramoto, M | 221 |
| Ryoo, I-J | 333 | Stimac, V | 133 | Usui, T | 105, 507 |
| Saeed, MA | 319 | Sucipto, H | 707 | Usuki, Y | 145 |
| Saitoh, H | 221 | Sueyoshi, M | 259 | Vasanthamallika, TK | 377 |
| Sakaida, Y | 153 | Sugawara, A | 277, 495 | Vicente, F | 55, 265 |
| Sakamoto, K | 625 | Sugiyama, H | 339 | Vikineswary, S | 445 |
| Sakuda, S | 397 | Sugiyama, K | 289 | Vollmar, D | 439 |
| Sakurai, F | 271 | Sunazuka, T | 277, 495, 681 | Wachi, H | 217 |
| Salazar, O | 55 | Süssmuth, RD | 75, 99, 445, 513 | Wakana, D | 217 |
| Sanchez, S | 5 | Suzuki, Takashi | 153 | Wang, C | 483 |
| Sánchez-Sancho, F | 167 | Suzuki, Toshihiro | 545 | Wang, F | 239 |
| Sankaran, K | 377 | Suzuki, Tsukasa | 339 | Wang, H | 483 |
| Sarwar, Y | 319 | Sztaricskai, F | 113 | Wang, Ji-dong | 229, 483, 501, 587 |
| Sasaki, I | 597 | Takagi, M | 123, 159, 177, 247, 283, 393, 593, 601, 625, 703, 705 | Wang, Jun | 699 |
| Sasamura, H | 89 | Takagi, Y | 51 | Wang, Ming | 587 |
| Sasikala, S | 675 | Takahashi, Takashi | 625 | Wang, Mingan | 233 |
| Sato, B | 89, 95 | Takahashi, Teruyuki | 339 | Wang, R | 605 |
| Schippa, S | 109 | Takahashi, Y | 303 | Wang, S-q | 639 |
| Schleissner, C | 167 | Takakura, K | 95 | Wang, W-L | 225 |
| Schneider, K | 75, 99, 445, 513 | Takatsu, T | 153, 359, 545, 551, 559 | Wang, X-J | 229, 309, 501, 587 |
| Schuberth, I | 439 | Takemoto, JY | 539 | Wang, X | 339 |
| Schöffler, A | 119 | Tamaki, M | 597 | Wang, Y-Y | 605 |
| Schuhmann, I | 453 | Tamura, K | 397 | Wang, Z | 647 |
| | | Tan, GYA | 445 | Watanabe, M | 159 |

| | | | | | |
|---------------|--------------------|---------------|---------------|----------------|----------|
| Watanabe, T | 339 | Yang, HO | 171, 621 | Zbarsky, VB | 37, 117 |
| Watanabe, T | 277 | Yang, L-M | 129 | Zhang, C | 55, 699 |
| Weber, T | 465 | Yang, S-W | 401 | Zhang, Hua | 527 |
| Wei, S | 233 | Yang, X-H | 587 | Zhang, Hui | 483 |
| Wohlleben, W | 465 | Yano, T | 545, 551, 559 | Zhang, Ji | 229, 501 |
| Wrigley, SK | 649 | Yao, CBF-F | 453 | Zhang, Jianjun | 539 |
| Wu, W | 201, 233 | Yao, G-W | 605 | Zhang, Jiwen | 201, 233 |
| | | Yasuhide, M | 353 | Zhang, L | 239 |
| Xi, D | 309 | Yazawa, K | 613 | Zhang, T | 639 |
| Xiang, W-S | 229, 309, 501, 587 | Yi, H | 639 | Zhang, Y-P | 225 |
| Xiao, C | 315 | Ying, L | 483 | Zhao, J | 647 |
| Xie, H | 225 | Yokoyama, K | 643 | Zhao, L-Y | 129 |
| Xin, Z-H | 225 | Yonesu, K | 359 | Zheng, C-J | 333 |
| Xu, G-H | 333 | Yoo, I-D | 333 | Zheng, D | 647 |
| | | Yoo, Y-J | 43 | Zheng, Y-T | 129 |
| Yada, C | 325 | Yoshida, J | 533 | Zheng, Z | 527 |
| Yaguchi, T | 217 | Yoshida, M | 221, 283 | Zhou, Y | 483 |
| Yamada, H | 303 | Yoshida, S | 469 | Zhu, D-Y | 605 |
| Yamada, T | 353 | Yoshihara, S | 469 | Zhu, H-J | 129, 239 |
| Yamagishi, Y | 89, 95 | Yu, SH | 163 | Zhu, W-M | 225 |
| Yamaguchi, A | 251 | Yun, B-S | 163, 631, 635 | Zinecker, H | 445 |
| Yamamoto, T | 277, 495 | | | Zink, DL | 55, 265 |
| Yamanouchi, M | 625 | Zazopoulos, E | 565 | Zsuga, M | 113 |
| Yamazaki, H | 195, 207, 431, 435 | Zbarsky, EN | 37, 117 | Zúñiga, P | 167 |

Substance Index for Volume 62

| | | | |
|---|--|--|----------------------------------|
| A-33853 | 99 | Bingchamide A, B | 501 |
| A-500359A | 325 | Bleomycin | 5 |
| A-500359B | 325 | BMS-345541; 4-(2'-aminoethyl)amino-1,8-dimethylimidazo(1,2-a)quinoxaline | 655 |
| Actinomycin D | 315 | Butein | 655 |
| Adriamycin | 425 | Butirosin | 471, 643, 707 |
| Alamethicin I | 303 | Butyrolactone II | 119 |
| Albidopyrone | 75, 445 | Bravomicin | 565 |
| Albucidin | 191 | | |
| Albucidin, acetylated | 191 | Caboxamycin | 99 |
| Aldgamycin E, F, G, I | 171 | Calicheamicins | 5 |
| Allantofuranone | 119 | Camptothecin | 425 |
| Amidepsine A, B, C, D | 51, 69 | Caspofungin | 5 |
| Amidepsine E | 69 | Catathelasmol A, B, C, D, E | 239 |
| Amikacin | 319, 377, 539 | Cefixime | 319 |
| 2-((Aminocarbonyl)amino)-5-(4-fluorophenyl)-3-thiophenecarboxamide | 655 | Cefoperazone | 319 |
| 2-Amino-6-(2-(cyclopropylmethoxy)-6-hydroxyphenyl)-4-piperadin-4-yl nicotinonitrile | 655 | Cefradine | 319 |
| Aminoglycosides | 5 | Ceftazidime | 377, 675 |
| Ammocidin A, B, C, D | 123 | Celastrol | 655 |
| Amphotericin B | 5, 27, 81, 171, 217, 649, 691 | Cephalosporins | 5 |
| Ampicillin | 171, 201, 251, 319, 325, 377, 539, 675 | Cephalothin | 315 |
| Anisomycin | 655 | Cephotaxime | 377 |
| Antimycin A | 75, 145 | Ceramidastin | 63 |
| Anthracyclines | 5 | Chaetomugilin A, B, C, D, G, H | 353 |
| Aplysamine 4 | 393 | Chalcomycin | 171 |
| Aquastatin A | 359 | Chloramphenicol | 319 |
| Argadin | 277, 495 | Ciprofloxacin | 5, 109, 113, 319, 431 |
| Argifin | 277, 495 | Citrinin | 225 |
| Arsenite | 655 | Clarithromycin | 43, 133, 605, 649 |
| Artemisolide | 655 | Clarithromycin derivatives, 3-O-(3-aryl-propenyl)- | 605 |
| AS1720807 | 89 | Clavulanic acid | 5 |
| Asochlorin | 571 | Clindamycin | 259 |
| Asochlorin, 4-O-carboxymethyl- | 365 | Cloxacillin | 251 |
| Asochlorin, 4-O-methyl- | 365 | Colistin A, B | 181 |
| Ascotricin A, B | 359 | CP-44161 | 89, 95 |
| Astaxanthin | 397 | CRP-2504-1 | 445 |
| Astaxanthin dirhamnoside | 397 | 1-(2-Cyano-3,12-dioxooleana-1,9-dien-28-oyl)imidazole | 655 |
| Atpenin A4, A5 | 243, 289 | 2-Cyano-3,12-dioxooleana-1,9-dien-28-oic acid methyl ester | 655 |
| Atpenin B, (±)- | 289 | Cycloepoxydon | 655 |
| Auranofin | 655 | Cyclo(-Lys ^{1,1'} -Orn ^{2,2'} -Lys ^{3,3'} -D-Phe ^{4,4'} -Pro ^{5,5'} -) ₂ | 597 |
| Aureobasidin A | 545 | Cyclo(-Orn ^{1,1'} -Orn ^{2,2'} -Orn ^{3,3'} -D-Phe ^{4,4'} -Pro ^{5,5'} -) ₂ | 597 |
| Avermectins | 5 | Cycloheximide | 99, 105, 167, 201, 445, 639, 655 |
| Avilamycin A | 461 | Cycloheximide, acetoxy | 655 |
| 1-Azasugar | 407 | Cycloheximide derivatives; 4-[2'-(3''(R),5''(S))-3'',5''-dimethyl-2''-hydroxyl-cyclohexylidene)ethyl]piperidine-2,6-dione | 639 |
| Bacitracin | 5, 325 | Cycloheximide derivatives; 4-[2'-(3''(R),5''(S))-3'',5''-dimethyl-2''-oxocyclohexylidene)ethyl]piperidine-2,6-dione | 639 |
| Bacitracin A | 5, 181, 325 | Cycloheximide derivatives; 4-[2'-(3''(S),5''(S))-3'',5''-dimethyl-2''-oxocyclohexylidene)ethyl]piperidine-2,6-dione | 639 |
| Bafilomycin A1 | 425 | | |
| BE 51068 | 445 | | |
| Beauvericin | 687 | | |
| Benzophomopsin A | 533 | | |
| Berberine | 655 | | |
| Bialaphos | 5 | | |

| | | | |
|---|---|--|-----|
| Cycloheximide derivatives; <i>N</i> -methyl-4-[2'-(3''(<i>R</i>), 5''(<i>S</i>))-3'',5''-dimethyl-2''-oxocyclohexylidene]ethyl]piperidine-2,6-dione | 639 | Erythromycin A, 4''- <i>O</i> -[3-(3-quinolinyloxy)propanoyl]-6- <i>O</i> -methyl-8a-aza-8a-homo- | 133 |
| Cycloheximide derivatives; <i>N</i> -propyl-4-[2'-(3''(<i>R</i>), 5''(<i>S</i>))-3'',5''-dimethyl-2''-oxo-cyclohexylidene)-ethyl]piperidine-2,6-dione | 639 | Erythromycin A, 4''- <i>O</i> -[3-(4-aminophenyl)propanoyl]-8a-aza-8a-homo- | 133 |
| Cyclonienin A, B | 635 | Erythromycin A, 4''- <i>O</i> -[3-(4-aminophenyl)propanoyl]-8a-aza-8a-homo- | 133 |
| Cycloserine D | 315 | Erythromycin A, 4''- <i>O</i> -[3-(4-nitrophenyl)-2-propenoyl]-6- <i>O</i> -methyl-8a-aza-8a-homo- | 133 |
| Cyclosporin A | 5 | Erythromycin A, 4''- <i>O</i> -[3-(4-nitrophenyl)-2-propenoyl]-8a-aza-8a-homo- | 133 |
| Diemenensin A, B | 445 | Erythromycin A, 4''- <i>O</i> -[3-(4-quinolinyloxy)-2-propenoyl]-6- <i>O</i> -methyl-8a-aza-8a-homo- | 133 |
| Doramectin | 5 | Erythromycin A, 4''- <i>O</i> -[4-(3-quinolinyloxy)-3-butenoyl]-6- <i>O</i> -methyl-8a-aza-8a-homo- | 133 |
| Echinosporamycin | 565 | Erythromycin A, 4''- <i>O</i> -[4-(3-quinolinyloxy)butanoyl]-6- <i>O</i> -methyl-8a-aza-8a-homo- | 133 |
| Enniatin H, I, MK1688 | 687 | Erythromycin A, 4''- <i>O</i> -[5-(3-quinolinyloxy)-3-pentenoyl]-6- <i>O</i> -methyl-8a-aza-8a-homo- | 133 |
| Epigallocatechin gallate, (-)- | 153 | Erythromycin A, 4''- <i>O</i> -[5-(3-quinolinyloxy)-4-pentenoyl]-6- <i>O</i> -methyl-8a-aza-8a-homo- | 133 |
| Epothilone A 3- α -D-arabinofuranoside | 483 | Erythromycin A, 4''- <i>O</i> -[5-(3-quinolinyloxy)-4-pentenoyl]-8a-aza-8a-homo- | 133 |
| Epothilone A 3- α -D-arabinofuranoside, 8-demethyl | 483 | Erythromycin A, 4''- <i>O</i> -[5-(3-quinolinyloxy)pentanoyl]-6- <i>O</i> -methyl-8a-aza-8a-homo- | 133 |
| Epothilone B | 483 | Erythromycin A, 9- <i>O</i> -(2-chlorobenzyl)oxime | 605 |
| Epothilone B 3- α -D-arabinofuranoside | 483 | Erythromycin A, 9- <i>O</i> -(2-chlorobenzyl)oxime 11,12-carbonate, 2'- <i>O</i> -Ac-3- <i>O</i> -allyl-6- <i>O</i> -methyl- | 605 |
| Epothilone C ₉ 3- α -D-arabinofuranoside | 483 | Erythromycin A, 9- <i>O</i> -(2-chlorobenzyl)oxime 11,12-carbonate, 2'- <i>O</i> -Ac-3-OH-6- <i>O</i> -methyl- | 605 |
| Epothilone D 3- α -D-arabinofuranoside | 483 | Erythromycin A, 9- <i>O</i> -(2-chlorobenzyl)oxime 11,12-carbonate, 3- <i>O</i> -[3-(1'-phenyl)- <i>Z</i> -1-propenyl]-6- <i>O</i> -methyl- | 605 |
| Epothilones | 5 | Erythromycin A, 9- <i>O</i> -(2-chlorobenzyl)oxime 11,12-carbonate, 3- <i>O</i> -[3-(3'-pyridyl)- <i>Z</i> -1-propenyl]-6- <i>O</i> -methyl- | 605 |
| (2 <i>R</i> ,3 <i>R</i> ,4 <i>S</i>)-2,3-Epoxy-4-hydroxy-5-hydroxymethyl-6-(1 <i>E</i>)-propenyl-cyclohex-5-en-1-one | 655 | Erythromycin A, 9- <i>O</i> -(2-chlorobenzyl)oxime 11,12-carbonate, 3- <i>O</i> -[3-(3'-quinolyl)- <i>Z</i> -1-propenyl]-6- <i>O</i> -methyl- | 605 |
| Epoxyquinol A, B | 655 | Erythromycin A, 9- <i>O</i> -(2-chlorobenzyl)oxime 11,12-carbonate, 3- <i>O</i> -[3-(4'-isoquinolyl)- <i>Z</i> -1-propenyl]-6- <i>O</i> -methyl- | 605 |
| Epoxyquinone A monomer | 655 | Erythromycin A, 9- <i>O</i> -(2-chlorobenzyl)oxime 11,12-carbonate, 3- <i>O</i> -[3-(5'-indolyl)- <i>E</i> -2-propenyl]-6- <i>O</i> -methyl- | 605 |
| Eremoxylarin A, B | 533 | Erythromycin A, 9- <i>O</i> -(2-chlorobenzyl)oxime 11,12-carbonate, 3- <i>O</i> -[3-(5'-isoquinolyl)- <i>Z</i> -1-propenyl]-6- <i>O</i> -methyl- | 605 |
| Ergosta-6,9,22-triene-3 β -ol, (22 <i>E</i> ,24 <i>R</i>)-5 α ,8 α -epidioxy- | 335 | Erythromycin A, 9- <i>O</i> -(2-chlorobenzyl)oxime 11,12-carbonate, 3- <i>O</i> -allyl-6- <i>O</i> -methyl- | 605 |
| Ergosta-6,22-dien-3 β -ol, (22 <i>E</i> ,24 <i>R</i>)-5 α ,8 α -epidioxy- | 335 | Erythromycin A, 9- <i>O</i> -(2-chlorobenzyl)oxime, 2',4''- <i>O</i> -bis(trimethylsilyl)-6- <i>O</i> -methyl- | 605 |
| Ergosta-7-en-3 β -ol, (24 <i>S</i>)- | 335 | Erythromycin A, 9- <i>O</i> -(2-chlorobenzyl)oxime, 2,4''- <i>O</i> -bis(trimethylsilyl)- | 605 |
| Ergosta-9(14),22-diene-3 β ,7 α -diol, (22 <i>E</i> ,24 <i>R</i>)-5 α ,6 α -epoxy- | 335 | Erythromycin A, 9- <i>O</i> -(2-chlorobenzyl)oxime, 2'- <i>O</i> -Ac-3-OH-6- <i>O</i> -methyl- | 605 |
| Erythromycin | 5, 109, 133, 251, 259, 431, 461, 605, 675 | Erythromycin A, 9- <i>O</i> -(2-chlorobenzyl)oxime, 3- <i>O</i> -[3-(3'-pyridyl)- <i>Z</i> -1-propenyl]-6- <i>O</i> -methyl- | 605 |
| Erythromycin A, 4''- <i>O</i> -(3-pyridinyl)acetyl-6- <i>O</i> -methyl-8a-aza-8a-homo- | 133 | | |
| Erythromycin A, 4''- <i>O</i> -(3-quinolinyloxy)carbonyl-6- <i>O</i> -methyl-8a-aza-8a-homo- | 133 | | |
| Erythromycin A, 4''- <i>O</i> -[(4-nitrophenyl)acetyl]-6- <i>O</i> -ethyl-8a-aza-8a-homo- | 133 | | |
| Erythromycin A, 4''- <i>O</i> -[(4-nitrophenyl)acetyl]-6- <i>O</i> -methyl-8a-aza-8a-homo- | 133 | | |
| Erythromycin A, 4''- <i>O</i> -[(4-nitrophenyl)acetyl]-8a-aza-8a-homo- | 133 | | |
| Erythromycin A, 4''- <i>O</i> -[3-(1,2,3,4-tetrahydro-3-quinolinyloxy)propanoyl]-6- <i>O</i> -methyl-8a-aza-8a-homo- | 133 | | |
| Erythromycin A, 4''- <i>O</i> -[3-(1,2,3,4-tetrahydro-3-quinolinyloxy)propanoyl]-8a-aza-8a-homo- | 133 | | |
| Erythromycin A, 4''- <i>O</i> -[3-(3-quinolinyloxy)-2-propenoyl]-6- <i>O</i> -allyl-8a-aza-8a-homo- | 133 | | |
| Erythromycin A, 4''- <i>O</i> -[3-(3-quinolinyloxy)-2-propenoyl]-6- <i>O</i> -ethyl-8a-aza-8a-homo- | 133 | | |
| Erythromycin A, 4''- <i>O</i> -[3-(3-quinolinyloxy)-2-propenoyl]-6- <i>O</i> -methyl-8a-aza-8a-homo- | 133 | | |
| Erythromycin A, 4''- <i>O</i> -[3-(3-quinolinyloxy)-2-propenoyl]-8a-aza-8a-homo- | 133 | | |

| | | | |
|--|-------------------------|---|---------------------------------------|
| Erythromycin A, 9- <i>O</i> -(2-chlorobenzyl)oxime, | 605 | JBIR-54 | 705 |
| 3- <i>O</i> -[3-(3'-quinolyl)- <i>Z</i> -1-propenyl]-6- <i>O</i> -methyl- | | Jesterone dimer | 655 |
| Erythromycin A, 9- <i>O</i> -(2-chlorobenzyl)oxime, | 605 | JS-1 | 575, 581 |
| 3- <i>O</i> -[3-(4'-isoquinolyl)- <i>Z</i> -1-propenyl]-6- <i>O</i> -methyl- | | | |
| Erythromycin A, 9- <i>O</i> -(2-chlorobenzyl)oxime, | 605 | Kanamycin | 43, 153, 251, 325, 377, 471, 703, 707 |
| 3- <i>O</i> -[3-(5'-pyrimidyl)- <i>Z</i> -1-propenyl]-6- <i>O</i> -methyl- | | Kerriamycin B | 221 |
| Erythromycin A, 9- <i>O</i> -(2-chlorobenzyl)oxime, | 605 | Khafrefungin | 545, 551, 559 |
| 3- <i>O</i> -allyl-6- <i>O</i> -methyl- | | Kirromycin | 465 |
| Erythromycin A, 9- <i>O</i> -(2-chlorobenzyl)oxime, | 605 | KS-501 | 359 |
| 3- <i>O</i> -OH-6- <i>O</i> -methyl- | | KS-505 | 347 |
| Erythromycin A 11,12-cyclic carbonate | 315 | | |
| Erythromycin A 11,12-cyclic carbonate, | 133 | β-lactam antibiotics | 5 |
| 4''- <i>O</i> -[3-(3-quinolinyl)-2-propenoyl]- | | Lactoferricin B | 109 |
| 6- <i>O</i> -methyl-8a-aza-8a-homo- | | Lehualide A, B, C, D | 445 |
| Etoposide | 425 | Leptomycin B | 425 |
| | | Leucinostatin A, B | 303, 343 |
| F-11334A1 | 153 | Levofloxacin | 315 |
| F01-1358A | 527 | Lincomycin | 315 |
| F01-1358B | 527 | Lincosamides | 5 |
| FD-891 | 507 | Lipstatin | 5 |
| FK506 | 5 | Lividomycin B | 471, 643 |
| FK46324 | 27 | LL-Z1272α | 571 |
| Flavonoid | 259 | LL-Z1272α epoxide | 571 |
| Flavonoid, prenylated | 385 | Lovastatin | 5 |
| Fortimicin | 471 | | |
| FR131535 | 27 | Macroleptotin | 335 |
| FR901379 | 27 | Macrolides | 5 |
| Fredericamycin A | 75 | Malfilanol A, B | 217 |
| | | Malformin A1, A2 | 105 |
| Gambogic acid | 655 | Malformin C | 105, 681 |
| Gentamicin | 5, 109, 319, 325, 377, | Malformin C, derivatives | 681 |
| | 471, 539, 643, 675, 707 | Manumycin A | 655 |
| Glabramycin A, B, C | 265 | Menaquinone | 347 |
| Gombapyrone A, B, C, D | 445 | Meropenem | 675 |
| | | Metronidazole | 43 |
| Haplofungin A | 545, 551, 559 | Mevinolin | 5 |
| Haplofungin B, C, D, E, F, G, H | 545, 551 | Micafungin | 5, 27 |
| Helenalin | 655 | Milbemycin A ₃ , A ₄ | 309 |
| Helicobasidin, deoxy- | 333 | Milbemycin, β-class | 229, 587 |
| Helicobasidin, isodeoxy- | 333 | Milbemycin A, B, seco- | 229, 501 |
| Hispidin | 631 | Milbemycin, β ₁₃ , β ₁₄ , α ₂₈ , α ₂₉ , α ₃₀ | 229 |
| Hitachimycin | 513 | Mikamycin A, B | 181 |
| HM-242 | 498 | Mithramycin | 5 |
| | | Mitomycin C | 5 |
| IMD-0354; <i>N</i> -(3,5-bis-trifluoromethyl-phenyl)- | 655 | Mitosanes | 5 |
| 5-chloro-2-hydroxybenzamide | | ML120B; <i>N</i> -(6-chloro-7-methoxy-9 <i>H</i> -β-carbolin- | 655 |
| 1- <i>N</i> -Iminosugar | 407 | 8-yl)-2-methylnicotinamide | |
| Inostamycin | 425 | MK-0991 | 5 |
| Istamycin | 471 | Monacolin K | 5 |
| Ivermectin | 5 | Monensin | 5 |
| | | Multiplolide A, B | 163 |
| JBIR-12 | 177, 705 | Mycophenolic acid | 225, 527 |
| JBIR-12, (7,8,13)- <i>O</i> -trimethyl | 177 | | |
| JBIR-16 | 601 | Nafcillin | 251 |
| JBIR-17 | 283 | Nalidixic acid | 5, 55, 167, 319, 377, 445 |
| JBIR-19, -20 | 159 | Nanchangmycin | 309 |
| JBIR-25 | 703 | NBRI23477 A, B | 243 |
| JBIR-25, 11,11'-acetone | 703 | Neomycin | 325, 471, 707 |
| JBIR-27, -28 | 247, 705 | Neomycin B, C | 643 |
| JBIR-44 | 393 | Neomycin C, 6'''-deamino-6'''-hydroxy- | 643 |
| JBIR-52 | 593 | Neomycin derivatives, 5''-modified | 539 |

| | | | |
|---|-------------|---|------------------------|
| Nidulalin A | 469 | Olivomycin I, 2'-(carboxymethoxime), amide | 37 |
| Nigericin | 89 | Olivomycin I, 2'-(carboxymethoxime), ethanolamide | 37 |
| Nitro derivatives; (4'-Hydroxy-3',5'-dinitrophenyl)-2-chloropropionic acid methyl ester | 453 | Olivomycin I, 2'-(carboxymethoxime), <i>tert</i> -butylamide | 37 |
| Nitro derivatives; 2,6-Dimethoxy-1,4-benzoquinone | 453 | Ouabain | 655 |
| Nitro derivatives; 2,6-Dinitro-4-(2'-nitroethyl)phenol | 453 | Oxacillin | 251 |
| Nitro derivatives; 2-Chloro-3-(4'-hydroxy-3'-nitrophenyl)propionic acid methyl ester | 453 | Paclitaxel | 5 |
| Nitro derivatives; 2-Hydroxy-3-(4'-hydroxy-3'-nitrophenyl)-propionic acid methyl ester | 453 | Panepoxydone | 655 |
| Nitro derivatives; 2-Methoxy-3,5-dinitrophenol | 453 | Paromomycin | 471, 643 |
| Nitro derivatives; 2-Methoxy-4,5-dinitrophenol | 453 | Parthenolide | 655 |
| Nitro derivatives; 2-Methoxy-4,6-dinitrophenol | 453 | PAX 1, 2, 3, 4, 5 | 295 |
| Nitro derivatives; 2-Nitro-4-(2'-nitroethyl)phenol | 453 | PD116740 | 167 |
| Nitro derivatives; 3-(4'-Hydroxy-3',5'-dinitrophenyl)-propionic acid methyl ester | 453 | Penicillins | 5 |
| Nitro derivatives; 3',5'-Dinitro-genistein | 453 | Pennicitrinone A, D | 225 |
| Nitro derivatives; 3'-Indolyethyl-methyl ether | 453 | Pentacecilde A, B, C | 195, 207 |
| Nitro derivatives; 3-Methoxy-4,5-dinitrophenol | 453 | Pentostatin | 5 |
| Nitro derivatives; 3'-Nitro-daidzein | 453 | Peperomin B, 2,6-didehydro- | 655 |
| Nitro derivatives; 3'-Nitrogenistein | 453 | Peperomin E | 655 |
| Nitro derivatives; 3'-Nitrotyrosol | 453 | Pepsatin | 1 |
| Nitro derivatives; 4'-Hydroxy-3',5'-dinitrophenylacetic acid | 453 | PF-184; 8-(2-(3,4-bis(hydroxymethyl)-3,4-dimethylpyrrolidin-1-yl)-5-chloroisonicotinamido)-1-(4-fluorophenyl)-4,5-dihydro-1 <i>H</i> -benzo-[g]indazole-3-carboxamide | 655 |
| Nitro derivatives; 4'-Hydroxy-3',5'-dinitrophenylacetic acid methyl ester | 453 | PHA-408; 8-(5-chloro-2-(4-methylpiperazin-1-yl)isonicotinamido)-1-(4-fluorophenyl)-4,5-dihydro-1 <i>H</i> -benzo[g]indazole-3-carboxamide | 655 |
| Nitro derivatives; 4'-Hydroxy-3',5'-dinitrophenylethylchloride | 453 | Phellinin A1, A2 | 631, 635 |
| Nitro derivatives; 4'-Hydroxy-3',5'-dinitrophenylpropionic acid | 453 | Phenazine-carboxamide, 6-hydroxymethyl-1- | 621 |
| Nitro derivatives; 4'-Hydroxy-3'-nitrobenzoic acid | 453 | Phenazinedimethanol, 1,6- | 621 |
| Nitro derivatives; 4'-Hydroxy-3'-nitrophenylacetic acid | 453 | Phenylpropanoids, prenylated | 385 |
| Nitro derivatives; 4'-Hydroxy-3'-nitrophenylacetic acid methyl ester | 453 | Phomenone | 247 |
| Nitro derivatives; 4'-Hydroxy-3'-nitrophenylpropionic acid | 453 | Piceamycin | 513 |
| Nitro derivatives; Dinitrotyrosol | 453 | Piceamycin, <i>N</i> -acetylcysteine adduct | 513 |
| Nitro derivatives; <i>N</i> -Acetyl-3',5'-dinitrotyramine | 453 | Platensimycin | 55, 265, 649, 699 |
| Nitro derivatives; <i>N</i> -Acetyl-3'-nitrotyramine | 453 | Platensimycin B ₄ | 699 |
| Nitro derivatives; Pyriculamide | 453 | Platensimycin B ₄ , methyl ester | 699 |
| Nocardithiocin | 613 | Pleofungin A | 545 |
| Norfloracin | 5, 109, 113 | Pleurotin | 153 |
| NPI-0047 | 213 | Plicamycin | 5 |
| NPI-0052 | 213 | PM070747 | 167 |
| NPI-2065 | 213 | Pneumocandin | 5 |
| NW-G01 | 201 | Pogopyrone B | 75, 81 |
| Odoroside A | 655 | Polymyxin | 295 |
| Okilactomycin | 55, 265 | Polymyxin B | 81, 295, 575, 675, 691 |
| Okilactomycin A, B, C, D | 55 | Polymyxin B1, B2 | 181 |
| Oleandrin | 655 | Posaconazole | 5 |
| Oligomycin | 425 | Pravastatin | 1, 5 |
| Olivomycin I | 37 | Prodiginine, butyl- <i>meta</i> -cycloheptyl- | 271 |
| Olivomycin I, 2'-(carboxymethoxime), 2-amino-2-methylpropane-1,3-diol amide | 37 | Prodiginine, undecyl- | 271 |
| Olivomycin I, 2'-(carboxymethoxime) | 37 | Prodigiosin | 271 |
| Olivomycin I, 2'-(carboxymethoxime), 2-adamantylamide | 37 | Prodigiosin R1 | 271, 531 |
| | | Prodigiosin R2 | 531 |
| | | Prostaglandin J ₂ | 655 |
| | | Prostaglandin J ₂ , 15-deoxy- $\Delta^{12,14}$ - | 655 |
| | | PS-1145; <i>N</i> -(6-chloro-9 <i>H</i> - β -carbolin-8-yl)nicotinamide | 655 |
| | | Quinolones | 5 |
| | | Quinolonecarboxylic acid derivatives | 113 |
| | | Quinazolinamine, 4-methyl-2- | 439 |
| | | Quinomycin, dehydroxymethylepoxy- | 655 |

| | | | |
|---|---|--|------------------|
| Rapamycin | 1, 5, 367 | Thailandolide A, B | 195, 207 |
| Resorcinol, bis-5-alkyl- | 371 | Thapsigargin | 425 |
| Rhodamine 123 | 145 | Thiopeptin B | 181 |
| Rhodamine 6G | 251 | Tigecycline | 671, 675 |
| Ribostamycin | 643 | TLN-05220, -05223 | 565 |
| Rifampicin | 5, 315, 613, 675 | Tobramycin | 5, 471, 539, 707 |
| Rifamycin S | 519 | Trichostatic acid | 283 |
| Roselipin 1A, 1B, 2A, 2B | 51 | Trichostatin A | 283 |
| Roseophilin | 271, 531 | Tsushimycin | 303 |
| Roseophilin, dechloro- | 531 | TT-1-4, -1-11 | 445 |
| Rubratoxin A | 63 | Tunicamycin | 425 |
| Rustmicin | 545, 551, 559 | | |
| | | UK-1 | 99 |
| Saliniketals A | 519 | | |
| Salinisporamycin | 519, 537 | Vancomycin | 295, 539, 565 |
| Salinomycin | 81 | Vanillin derivatives; 2,4,6- Trihydroxybenzaldehyde | 625 |
| Sannanine | 647 | Vanillin derivatives; 2,4-Dihydroxybenzaldehyde | 625 |
| Sansalvamide A | 501 | Vanillin derivatives; 2-Hydroxy- 4,6-dimethoxybenzaldehyde | 625 |
| Sargachromenol | 259 | Vanillin derivatives; 4,6-Bis(benzyloxy)- 2-hydroxybenzaldehyde | 625 |
| Sargafuran | 259 | Vanillin derivatives; 4-Hydroxy-3,5- dimethoxyacetophenone | 625 |
| Sargaquinoic acid | 259 | Vanillin derivatives; 4-Hydroxy-3- methoxyacetophenone | 625 |
| SC-514; 4-Amino-2,3'-bithiophene- 5-carboxamide | 655 | Vanillin derivatives; 5-Bromosalicylaldehyde | 625 |
| Sch 1385568 | 401 | Vanillin derivatives; 5-Chlorosalicylaldehyde | 625 |
| Siastatin B | 407 | Vanillin derivatives; 5-Nitrosalicylaldehyde | 625 |
| Sirolimus | 5 | Vanillin derivatives; 3-hydroxy-4- methoxybenzaldehyde | 625 |
| Sisomicin | 471 | Vanillin derivatives; 4-hydroxy-3-methoxybenzoic acid | 625 |
| Spinosyn | 5 | Vanillin derivatives; 4-hydroxy-3- methoxybenzaldehyde | 625 |
| Sporogen-AO1 | 247 | Vellatretetraol | 129 |
| SRC2; (11S)-2 α -bromo-3-oxoeudesmano- 13,6 α -lactone | 655 | Vinblastine | 425 |
| ST906 | 229, 501 | | |
| Staurosporine | 1, 17, 105, 519, 655 | WAP-8294A2 | 181 |
| Staurosporine analogs | 17 | WF-3681 | 119 |
| Streptomycin | 5, 37, 89, 95, 105, 119, 129, 145, 217, 233, 243, 247, 287, 303, 309, 315, 319, 325, 339, 359, 431, 471, 507, 625, 669 | Wortmannin | 425 |
| Streptothricin | 325 | | |
| Streptothricin D acid | 233 | Xanthohumol | 51, 655 |
| Streptothricin D acid, 12-carbamoyl- | 233 | Xanthoradone A, B | 431, 435 |
| Streptothricin D acid, <i>N</i> -acetyl- | 233 | Xanthoviridicatin D, E, F | 435 |
| Streptothricin E acid, 12-carbamoyl- | 233 | Xenofuranone A, B | 119 |
| Streptothricin F acid | 233 | Xylarenal A, B | 163 |
| Streptozotocin | 5 | Xylariamide A | 163 |
| Suramin | 303 | Xylarinic acid A, B | 163 |
| | | Xylarinol A | 163, 533 |
| Tacrolimus | 5 | Xylarinol B | 163 |
| TAN-1085 | 167 | Xyloketal A, B, C, D, E | 163 |
| Tautomycin | 105 | | |
| Taxol | 5, 425 | Zeaenol, 5Z-7-oxo- | 655 |
| Telithromycin | 5 | | |
| Tetracyclin | 315, 319 | | |
| Tetracyclines | 5 | | |